July 16, 2019

Dear Dr. Rupert Holzinger,

Thank you for providing us the opportunity to revise and improve our manuscript entitled "High contributions of fossil sources to more volatile organic carbon" by Ni et al. We are also grateful for the valuable comments and suggestions by the two reviewers.

The comments on the main text and supplement are addressed accordingly. Detailed responses to each of the reviewer's comments are provided in blue. Attached please also find the marked-up manuscript to track the changes in the revised manuscript.

Sincerely,

Dr. Haiyan Ni
Centre for Isotope Research (CIO)
Energy and Sustainability Research Institute Groningen (ESRIG)
University of Groningen
Nijenborgh 6, 9747 AG Groningen, the Netherlands
Email: h.ni@rug.nl

Response to reviewer #2:

General comments

In this manuscript, the authors report their results of an extensive measurement and analysis effort to assess the contribution of fossil sources to a fraction of particulate organic carbon, i.e., more volatile organic carbon (mvOC), which they define as the fraction of organic carbon desorbing at 200 °C in a helium stream. The combination of numerous analytical techniques, including ^{14}C analysis and ^{13}C determination with statistical analysis is intriguing. The authors also discuss several aspects of data uncertainty, including e.g. positive sampling artifacts due to the adsorption of volatile organic compounds onto the quartz filters used for sampling and recoveries of mvOC during filter aliquot desorption. They also outline the influence of nuclear bomb tests in the 1960s and 1970s on the measured $^{14}C/^{12}C$ ratios. Further positive points are the detailed presentation of assumptions and estimations going into the calculations, and the extensive supporting information. The scientific methods and assumptions are presented clearly and appear to be valid. In my opinion, the presented, well-written manuscript meets all requirements for publication in ACP.

Response: We thank the reviewer for the nice summary of our manuscript and the positive evaluation of our work. We have carefully addressed the reviewer's comments. Below are point-to-point responses.

Specific comments

However, I am not that familiar with the term 'more volatile' organic carbon and thus I do not know how common it really is and if the title is self-explanatory in its current state.

Response: In this manuscript, mvOC is operationally defined as more volatile fraction of total organic carbon (OC) aerosol that evaporates in helium at 200 °C. The term "more volatile" OC refers to the more volatile OC fraction compared to the total OC. This is clarified several times in the Introduction section, for example:

> "In some recent studies, a thermal desorption approach has been used for analysis of filter samples at lower and higher temperatures as an indicator of volatility (Holzinger et al., 2013; Lopez-Hilfiker et al., 2014, 2015; Timkovsky et al., 2015; Masalaite et al., 2017, 2018). Even though the desorption temperature is not a direct measure of the particle volatility, OC desorbed from the filter at lower temperature tends to be more volatile, whereas the less volatile (i.e., more refractory) OC tends to be desorbed at higher temperatures." (page 3, line 16-20)
>
> "In addition, we operationally define a more volatile OC fraction (mvOC) as the carbon fraction desorbed from the filter samples at 200 °C in helium (He), and investigate sources of mvOC." (page 4, line 11-12)

In the literature, the term "more volatile" (or "less refractory") and "less volatile" (or "more refractory") are usually used, when thermal desorption is used for separation of different fractions of organic aerosol (e.g., Masalaite et al., 2017, 2018; Meusinger et al., 2017), or thermodenuder

(TD) is used for determination of volatility of organic aerosols (e.g., Huffman et al., 2008, 2009; Zhang et al., 2011).

Following the reviewer's concern about the title, we change the title to better reflect the content of the manuscript and to be more specific (changes are underlined):

> "High contributions of fossil sources to more volatile organic aerosol"

Technical comments

1) Please check the manuscript again for the proper introduction of abbreviations before they are used for the first time.

Response: Thank you for this comment. We have checked the abbreviations accordingly and defined abbreviations when first used. The following abbreviations are defined in the revised manuscript:

> "mvOC is isolated by desorbing organic carbon from the filter samples in helium (He) at 200 °C" (page 1, line 15)

> "Secondary OC (SOC) concentrations and sources are modelled based on the ^{14}C-apportioned OC and EC" (page 1, line 22)

> "In this study, wintertime fine particulate matter ($PM_{2.5}$, particles with aerodynamic diameter < 2.5 µm) samples from 6 Chinese megacities are studied." (page 4, line 8-9)

> "filter pieces of 1.5 cm^2 were taken for OC and EC analysis using a carbon analyzer (Model 5L, Sunset Laboratory, Inc., Portland, OR, USA) following the thermal-optical transmittance protocol EUSAAR_2 (European Supersites for Atmospheric Aerosol Research; Cavalli et al., 2010)." (page 4, line 29 to page 5, line 1)

> "Different from EUSAAR_2 protocol, IMPROVE_A (Interagency Monitoring of Protected Visual Environments) protocol defines OC fractions at stepwise temperature of 140 °C, 280 °C, 480 °C, and 580 °C in He." (page 5, line 8-10)

> "we selected the samples carefully to cover periods of low and high total carbon (TC, the sum of OC and EC) and $PM_{2.5}$ concentrations to get samples representative of various pollution conditions that did occur in each city." (page 5, line 14-15)

2) Page 6, Line 12: You have diluted the CO_2 with He, thus it should read "CO_2/He"

mixture, not "CO_2/H_2" mixture

Response: Thank you for your carefully reading. Done. Now it reads:

> "The CO_2/He mixture is directly fed into the Cs sputter ion sources of…" (page 6, line 30)

References:

Huffman, J., Docherty, K., Mohr, C., Cubison, M., Ulbrich, I., Ziemann, P., Onasch, T., and Jimenez, J.: Chemically-resolved volatility measurements of organic aerosol from different sources, Environ. Sci. Technol., 43, 5351-5357, 2009.

Huffman, J. A., Ziemann, P. J., Jayne, J. T., Worsnop, D. R., and Jimenez, J. L.: Development and characterization of a fast-stepping/scanning thermodenuder for chemically-resolved aerosol volatility measurements, Aerosol Sci. Tech., 42, 395-407, 2008.

Masalaite, A., Holzinger, R., Remeikis, V., Roeckmann, T., and Dusek, U.: Characteristics, sources and evolution of fine aerosol (PM_1) at urban, coastal and forest background sites in Lithuania, Atmos. Environ., 148, 62-76, 2017.

Masalaite, A., Holzinger, R., Ceburnis, D., Remeikis, V., Ulevičius, V., Röckmann, T., and Dusek, U.: Sources and atmospheric processing of size segregated aerosol particles revealed by stable carbon isotope ratios and chemical speciation, Environm. Pollut., 240, 286-296, https://doi.org/10.1016/j.envpol.2018.04.073, 2018.

Meusinger, C., Dusek, U., King, S. M., Holzinger, R., Rosenørn, T., Sperlich, P., Julien, M., Remaud, G. S., Bilde, M., Röckmann, T., and Johnson, M. S.: Chemical and isotopic composition of secondary organic aerosol generated by α-pinene ozonolysis, Atmos. Chem. Phys., 17, 6373-6391, https://doi.org/10.5194/acp-17-6373-2017, 2017.

Zhang, Q., Jimenez, J. L., Canagaratna, M. R., Ulbrich, I. M., Ng, N. L., Worsnop, D. R., and Sun, Y.: Understanding atmospheric organic aerosols via factor analysis of aerosol mass spectrometry: a review, Anal. Bioanal. Chem., 401, 3045-3067, 10.1007/s00216-011-5355-y, 2011.

Response to reviewer #3:

General comments

The manuscript describes a novel approach of radiocarbon source apportionment, which investigates the contributions of fossil vs. non-fossil emissions to the more volatile organic carbon (mvOC) fraction that evaporates in helium at 200°C. This approach shows for particulate matter samples from different cities in China that the fossil impact on mvOC is larger than for total OC and secondary OC. This new insight has implications on a better understanding of sources of carbonaceous aerosols, which is currently a hot topic in atmospheric chemistry and physics. Therefore, I recommend accepting the manuscript after minor revisions.

Response: Thank you, Sönke Szidat, for the helpful comments and providing us the opportunity to strengthen our research. We try to address all of them carefully and this is really a big help to improve the manuscript.

Specific comments

Main comments:

1) P4, L1-2, P12, L18-19, P18, L10-11: In previous work (Agrios et al., 2016; https://doi.org/10.1017/RDC.2016.88), we established a continuous-flow coupling of the Sunset OC/EC analyzer with the MICADAS and measured ^{14}C online for low temperature OC steps and even monitored the change of the ^{14}C signal during the temperature ramp. We also found a more fossil signal for the 200°C step than for the following OC steps using higher temperature. We furthermore observed that even a shift from fossil to non-fossil emissions occurred within the 200°C peak for some samples, which indicates that the fossil character of mvOC would probably have been even more pronounced, if Ni et al. had chosen a temperature lower than 200°C.

Response: We regret that we were not aware of the work by Agrios et al. (2016), and thank you for pointing this out. We read Agrios et al. (2016) very carefully and find that the low temperature OC steps including 200°C step were conducted in O_2. However, in this study mvOC is desorbed at 200°C in helium (He). OC extracted in O_2 and He even at the same temperature can be very different in the extracted carbon mass and therefore $F^{14}C$ values. Thus, OC extracted at 200°C in O_2 by Agrios et al. (2016) can not be compared directly to mvOC defined in this study. But Angrios et al. (2016) and this study have the qualitatively similar finding that OC extracted at 200°C is more fossil than that extracted at higher temperature, no matter the extraction occurs in O_2 or He.

However, we do not know if we can extrapolate this conclusion to a temperature lower than 200 °C. Agrios et al. (2016) observed a shift from fossil to non-fossil emissions occurred within the 200°C peak for some samples extracted in O_2, indicating OC extracted at temperature lower than 200°C is more fossil than OC at 200°C. In contrast to Agrios et al. (2016), we extracted mvOC in He and observed higher $F^{14}C$ (i.e., less fossil) for samples with mvOC recovery <1, which probably resulted from lower desorption temperature than 200°C, as discussed in the second paragraph of Sect. 3.1 and shown in Fig. 1b.

We think this citation is very helpful for readers to understand the fossil character of OC extracted at lower temperature, and we add the citation in the revised text.

> "Agrios et al. (2016) had the qualitatively similar finding that $F^{14}C$ of OC extracted in O_2 at 200°C was smaller than $F^{14}C$ of OC extracted in O_2 at higher temperature for samples collected from an urban and rural site in the Switzerland and from the Los Angeles Basin, USA." (page 13, line 10-12)

Furthermore, we avoid using the expression "*the first time* that the source contribution to more volatile fraction of OC" or "*the first* ^{14}C *measurement* of the more volatile fraction of OC". The revised text shows (changes are underlined):

> "In addition, we operationally define a more volatile OC fraction (mvOC) as the carbon fraction desorbed from the filter samples at 200 °C in helium (He), and investigate sources of mvOC. The source contribution to mvOC is measured unambiguously by ^{14}C." (page 4, line 11-14)
>
> "We can unambiguously conclude from ^{14}C measurements of mvOC and OC that mvOC is more fossil than OC in six Chinese cites." (page 13, line 13-14)
>
> "Radiocarbon measurements are conducted for EC and OC of $PM_{2.5}$ samples collected in six Chinese megacities at wintertime. In addition, the sources of mvOC are measured unambiguously using ^{14}C." (page 19, line 4-6)

2) P10, L22-24: Fig. 1b reveals that low recoveries are associated with a bias in $F^{14}C_{(mvOC)}$. Therefore, the correction of sample winter-L should address this bias accordingly by subtraction. A simple increase of the uncertainty is not appropriate.

Response: Fig. 1b shows that for sample winter-H and winter M, low recoveries of mvOC lead to biased high $F^{14}C_{(mvOC)}$ values. But we are not sure if we can generalize this conclusion to other samples. In addition, Agrios et al. (2016) found that for some samples a shift from fossil to non-fossil emissions occurred within the 200°C peak, which indicates that opposite to Fig. 1b, low recovery of mvOC could in principle also result in biased low $F^{14}C_{(mvOC)}$. The findings in Agrios et al. (2016) and Fig. 1b of this study suggest that low recovery of mvOC can lead to either biased higher or lower $F^{14}C_{(mvOC)}$ values.

In this study, the mvOC recovery of sample winter-L is low (0.51), and we could not repeat it due to due to the limited filter material. Instead, we take the measured $F^{14}C_{(mvOC)}$ for sample winter-L but assign a bigger absolute uncertainty of 0.05, due to its low mvOC recovery. This is based on the difference in $F^{14}C_{(mvOC)}$ for winter-H and winter-M with low and high mvOC recoveries which is roughly 0.05 (Fig. 1b), as explained in the Sect. 3.1. The larger uncertainty is assigned for the measured $F^{14}C_{(mvOC)}$ for sample winter-L so that possible effects of its low mvOC recovery are taken into consideration and could be either positive or negative

3) P11, L1-2 and P12, L8-11: In order to identify reasons for differences between cities and individual samples, meteorological data should be shown in the Supplement.

Response: Meteorological data including wind speed, temperature and relative humidity (RH) are added in Supplemental Table S1. There was no precipitation in all cities during all sampling dates, since we only included samples collected on dry days in this study, to eliminate this variable as a potential confounding factor.

TC concentrations in Chongqing were higher than the other southern Chinese cities (Shanghai and Guangzhou) (P11, L1-2 in the original manuscript). Beside high anthropogenic emissions, higher TC concentrations in Chongqing were associate with unfavorable meteorological conditions characterized by high RH and low wind speed, which enhanced both the accumulation of pollutants and the formation of secondary aerosol (Zheng et al., 2015; Tie et al., 2017).

For samples collected in the same city, we found that compared to samples representing low (L) TC concentrations, samples representing high (H) TC concentrations were collected under more stagnant conditions indicated by lower wind speed (Table S1 in the revised manuscript).

4) P13, L16-18: The fact that the correlation between f_{nf}(mvOC) and f_{nf}(OC) is better than the correlation between f_{nf}(mvOC) and f_{bb}(EC) is mainly caused by the comparison of different fractions of the carbonaceous aerosol: in the former case, two OC fractions are compared (i.e. mvOC and OC), whereas in the latter case, OC and EC are compared. EC_{bb} may be transferred into POC_{bb} (see Eq. 8), but one has to take into account that the large variability of r_{bb} contributes to the r^2 value of the correlation between f_{nf}(mvOC) and f_{bb}(EC) in Fig. 5. (The uncertainty of r_{bb} was estimated to be 25%; see P8, L12.) Therefore, the suggestion of the importance of secondary formation of mvOC and/or other non-fossil contribution to mvOC besides primary biomass burning is not valid. This sentence should be removed. Consequently, the corresponding sentence P18, L30 to P19, L2 should also be deleted.

Response: We agree with the reviewer that correlation between f_{nf}(mvOC) and f_{nf}(OC) is better than the correlation between f_{nf}(mvOC) and f_{bb}(EC) is mainly caused by comparison of two OC fractions in the former case. In addition, as the reviewer explained, the very variable r_{bb} (i.e., $POC_{\mathrm{bb}}/EC_{\mathrm{bb}}$ ratio) and the unknown mvOC/EC ratio from primary biomass burning can contribute to better correlation between f_{nf}(mvOC) and f_{nf}(OC) than that between f_{nf}(mvOC) and f_{bb}(EC).

Consequently, we have deleted the following sentence (a strikethrough is used to indicated the deletion of text) as the reviewer suggested:

> "~~This suggests that primary combustion sources including biomass burning and fossil fuel combustion (i.e., EC sources) can not fully explain the variation of~~ ~~f_{nf}~~ ~~(mvOC), and indicates the importance of secondary formation of mvOC and/or other non-fossil contribution to mvOC besides primary biomass burning.~~" (page 14, line 11-13)
>
> "~~This suggests that primary combustion sources including biomass burning and fossil fuel combustion (i.e., EC sources) can not fully explain the variation of fnf(mvOC), and indicates the importance of secondary formation of mvOC and/or other non-fossil contribution to mvOC besides primary biomass burning~~." (page 19, line 26-29)."

5) P15, L1-14: The authors try to draw conclusions from different r^2 values of correlations between mvOC$_{nf}$ with POC$_{bb}$ and with SOC$_{nf}$ (Fig. 7b). However, the statistical difference of both r^2 values was not proven by a proper test (e.g. an F-test). Furthermore, the high uncertainties of POC$_{bb}$ (see my comment to P13, L16-18) and SOC$_{nf}$ (which are indicated in Fig. 6) are also not considered for this discussion. As these important factors were not taken into account, the whole passage (P15, L1-14) should be removed.

Response: To statistically compare the r^2 values of correlations between mvOC$_{nf}$ with POC$_{bb}$ and with SOC$_{nf,}$, we compute their bootstrap r^2 values and then evaluate overlap of the corresponding 95% confidence intervals. The bootstrapped 95% confidence intervals for r^2 of correlations between mvOC$_{nf}$ with POC$_{bb}$ and with SOC$_{nf}$ are (0.21, 0.94) and (0.60, 0.99), respectively. Their 95% confidence intervals are clearly overlapped, therefore there is no significant difference in r^2 values of correlations between mvOC$_{nf}$ with POC$_{bb}$ and with SOC$_{nf}$. We chose the bootstrap method as opposed to a parametric method, due to the few data points in the regression, which made it difficult to determine, if the residuals have a normal distribution, i.e. if a parametric test is applicable.

Furthermore, we agree with the reviewer that the high uncertainties of POC$_{bb}$ and SOC$_{nf}$ that resulted from the uncertain r_{bb} should be considered for this discussion. Consequently, we rewrite the passage (page 15, line 27 to page 16, line 9):

> "Good correlation was found between mvOC$_{nf}$ and SOC$_{nf}$ ($r^2 = 0.87$, bootstrapped 95% confidence interval: (0.21, 0.94); Fig. 7), which is not significantly different from the correlation between mvOC$_{nf}$ and POC$_{bb}$ ($r^2 = 0.71$, bootstrapped 95% confidence interval: (0.60, 0.99)). SOC$_{nf}$ is estimated by subtracting primary OC from biomass burning (POC$_{bb}$) from OC$_{nf}$, where POC$_{bb}$ is estimated by multiplying EC$_{bb}$ with the OC/EC ratio of fresh biomass burning plumes (r_{bb}) (Eq. 7). Due to the large uncertainty in r_{bb}, separation between POC$_{bb}$ and SOC$_{nf}$ is rather uncertain, and the r^2 for a correlation of mvOC$_{nf}$ and SOC$_{nf}$ is therefore affected by r_{bb}. For example, with lower r_{bb} of 3 (mean), the correlation between SOC$_{nf}$ and mvOC$_{nf}$ is stronger ($r^2 = 0.92$) than for our best estimate of r_{bb} (4) ($r^2 = 0.87$). For r_{bb} of 5, it is slightly weaker ($r^2 = 0.76$, Fig S8). OC$_{nf}$, the sum of POC$_{bb}$ and SOC$_{nf}$, is well-constrained by F^{14}C$_{OC}$ and not affected by r_{bb}. mvOC$_{nf}$ correlates strongly with OC$_{nf}$ ($r^2 = 0.91$), suggesting strong impacts on the variability of mvOC$_{nf}$ from non-fossil emissions including the secondary formation from non-fossil sources and primary biomass burning emissions."

Consequently, the corresponding sentences in the Conclusion section are also revised:

> "Good correlation is found between mvOC$_{nf}$ and OC$_{nf}$ ($r^2 = 0.91$). This indicates strong impacts on the variability of mvOC$_{nf}$ from non-fossil emissions, including the secondary formation of OC from non-fossil sources and primary biomass burning." (page 20, line 6-9)

Technical comments:

6) P1, L20: Better use the following phrasing: (range: 7 %–25 %)

Response: Thank you for pointing this out. Done. The revised abstract shows:

> "The average difference in the fossil fractions between mvOC and OC is 13 % (range: 7 %–25 %)," (page 1, line 21)

There are also several occasions in the Results/Conclusion sections, and the revised text shows:

> "mvOC and OC concentrations averaged 3.3 ± 2.2 μg m^{-3} (range: 0.7–7.4 μg m^{-3}) and…" (page 11, line 19)

> "The relative contribution of fossil sources to mvOC is on average 59 % (range: 45 %–78 %)," (page 20, line 5)

7) P2, L4-7: The focus of this sentence should be changed, because a) PAHs are only a minor fraction of OC and b) EC is carcinogenic as well. I suggest characterizing OC and EC very broadly without mentioning health effects or special substance classes.

Response: Thank you for this comment. The revised manuscript shows:

> "Aerosol particles are of importance for atmospheric chemistry and physics, and exert a crucial effect on the climate system, air quality and human health (Fuzzi et al., 2015). The carbonaceous fraction of aerosol comprises a large fraction of the fine aerosol mass (20 %–80 %) (Cao et al., 2007; Tao et al., 2017). Carbonaceous aerosols are often operationally subdivided into organic carbon (OC) and elemental carbon (EC). OC consists of a large variety of organic species that cover a great range of volatilities and are not or weakly light absorbing, while EC is non-volatile, resistant to chemical transformation and strongly light absorbing (Pöschl, 2005)." (page 2, line 2-10)

8) P2, L32: A comma is missing before "can"

Response: The revised manuscript shows:

> "the volatility of different OA components, such as hydrocarbon-like OA (HOA), biomass burning OA (BBOA) and OOA, can be estimated for ambient aerosols." (page 3, line 2-4)

9) P3, L1-3: Examples of high-volatility BBOA components should be given, as these may be relevant for the mvOC fraction.

Response: Following the reviewer's suggestion, we do the literature search of high-volatility BBOA components. To the best of our knowledge, studies on the volatility of BBOA components are very limited. When BBOA is identified and quantified using aerosol mass spectrometry (AMS) technique in combination with positive matrix factorization (PMF), the detection and identification of specific molecular tracers is not possible. This is because the AMS technique utilizes electron impact ionization resulting in extensive fragmentation. However, the volatility distribution for BBOA components can be estimated using the volatility basis set. For example, Paciga et al. (2016) found that the BBOA in an urban background site in Paris contained 50% semi-volatile organic components (SVOCs with effective saturation concentrations *C** of 1–100 μg m^{-3} range) and 30% low volatility organic compounds (LVOCs with *C** of 10^{-3}–0.1 μg m^{-3}).

Recently, high-resolution-time-of-flight chemical ionization mass spectrometer (HRTOF-CIMS) coupled to a Filter Inlet for Gases and AEROsols (FIGAERO) is developed (Lopez-Hilfiker et al., 2014) and used for measurements of ambient biomass burning aerosol (e.g., Gaston et al., 2016). This technique allows the detection and quantification of oxygenated and nitrogen-containing compounds on the molecular level and provides information on volatility by detecting gas-and particle-phase compounds simultaneously. Gaston et al. (2016) applied this technique to BBOA in the northwestern US. They found that levoglucosan (i.e., the biomass burning tracer) is semi-volatile and has the potential to form low volatility products during the chemical aging of ambient biomass burning aerosol.

Regarding the high-volatility BBOA components, the following underlined sentences have been added in the Introduction section:

> "Source and ambient studies indicate that BBOA and HOA are generally more volatile than OOA. Meanwhile, the volatility of BBOA can be quite variable, depending on type of biomass and the combustion conditions, and either higher or lower than that of HOA (e.g., Grieshop et al. 2009c; Huffman et al. 2009a; Paciga et al. 2016; Cao et al., 2018). For example, Huffman et al. (2009b) measured the volatility of primary OA from biomass burning and found that the more volatile BBOA was generally dominated by smoldering combustion, while the less volatile BBOA was more influenced by flaming combustion. Paciga et al. (2016) found that the BBOA was more volatile than HOA in a urban background site in Paris, with 50% semi-volatile organic components (SVOCs with effective saturation concentrations *C** of 1–100 μg m^{-3} range) and 30% low volatility organic compounds (LVOCs with *C** of 10^{-3}–0.1 μg m^{-3}). Gaston et al. (2016) found that levoglucosan (i.e., the biomass burning tracer) was semi-volatile and had the potential to form low volatility products during the chemical aging of ambient biomass burning aerosol, applying high-resolution-time-of-flight chemical ionization mass spectrometer (HRTOF-CIMS) coupled to a Filter Inlet for Gases and AEROsols (FIGAERO) to aerosol in the northwestern US. " (page 3, line 4-15)

10) P4, L10-11: pre-baked

Response: Corrected. The revised manuscript shows:

> "$PM_{2.5}$ samples were collected on pre-baked (780 °C for 3 h) quartz fiber filter…" (page 4, line 22)

11) P5, L29-30: Even though the blank is small compared to the sample amount, a blank correction has to be performed for both mvOC concentrations and their $F^{14}C$ values. If a direct analysis of the $F^{14}C$ of the blank hasn't been performed, a value of 0.50 ± 0.29 should be applied to cover the full $F^{14}C$ range from 0 to 1 based on the assumption that a continuous uniform distribution (i.e. a rectangular distribution) is valid.

Response: Thank you for pointing this out.

(1) blank corrections for mvOC concentrations

The contamination introduced by the combustion processes yields 0.52 ± 0.31 µgC mvOC, which was determined by following exactly the same mvOC isolating procedures with either empty filter boat or with blank filters. Blank corrections for mvOC mass from the isolation procedure were performed in the original manuscript, but we did not state this clearly. In the revised manuscript, we add:

> "The contamination introduced by the combustion process yields 0.72 ± 0.44 µgC EC, 0.85 ± 0.49 µgC OC, 0.52 ± 0.31 µgC mvOC per extraction, respectively. Compared with our sample size of 30–391 µgC EC, 30–445 µgC OC, and 15–121 µgC mvOC, the blanks are ≤7 % of the mvOC sample amount and < 3% of OC and EC sample amount, therefore relatively small compared to our sample sizes. The mvOC concentrations reported in this study are corrected for contamination by subtraction." (page 6, line 7-11)

(2) blank corrections for $F^{14}C_{(mvOC)}$

The ^{14}C values of carbon fractions (i.e., mvOC, OC and EC) can be blank corrected according to the mass balance equation:

$$F^{14}C_S = \frac{F^{14}C_m \times M_m - F^{14}C_b \times M_b}{M_m - M_b} \qquad (S4)$$

where $F^{14}C_S$ is $F^{14}C$ of the aerosol carbon collected on the filter, which is blank corrected, $F^{14}C_m$ and M_m are the measured $F^{14}C$ and the measured mass of the respective carbon fraction (mvOC, OC or EC), and $F^{14}C_b$ and M_b the fraction modern and the mass of the respective carbon fraction of blanks.

Since the directly determined system blank (i.e. the amount of CO_2 measured, when no sample is introduced into the aerosol combustion system) is 0.52 ± 0.31 µgC mvOC per extraction (i.e., M_b for mvOC), it is much too small to be analyzed for $F^{14}C_b$ of mvOC. Therefore, the $F^{14}C_{(mvOC)}$ values in the manuscript were not blank corrected.

To do blank corrections for mvOC, we need to estimate its $F^{14}C_b$.. We assume that $F^{14}C_b$ for mvOC ranges from 0 to 1 with a continuous uniform distribution as the reviewer suggested. To propagate uncertainties, a Monte Carlo simulation with 10,000 individual calculations of $F^{14}C_S$ for mvOC was conducted according to Eq. (S4). For calculation inputs, $F^{14}C_b$ of mvOC. was randomly chosen from a continuous uniform distribution between 0 and 1. $F^{14}C_m$ for mvOC was randomly chosen from a normal distribution symmetric around the measured values with uncertainties as standard deviation (Table S4). The random values for M_m and M_b were taken from a triangular distribution, which has its maximum at the central value and 0 at the upper and lower limits. Then 10,000 different estimations of $F^{14}C_S$ for mvOC were calculated. The derived average represents the best estimate, and the standard deviation represents the combined uncertainties.

Figure S9 shows the $F^{14}C$ of mvOC before and after blank corrections ($F^{14}C_m$ and $F^{14}C_s$, repectively) for the contamination introduced by the isolation procedure.

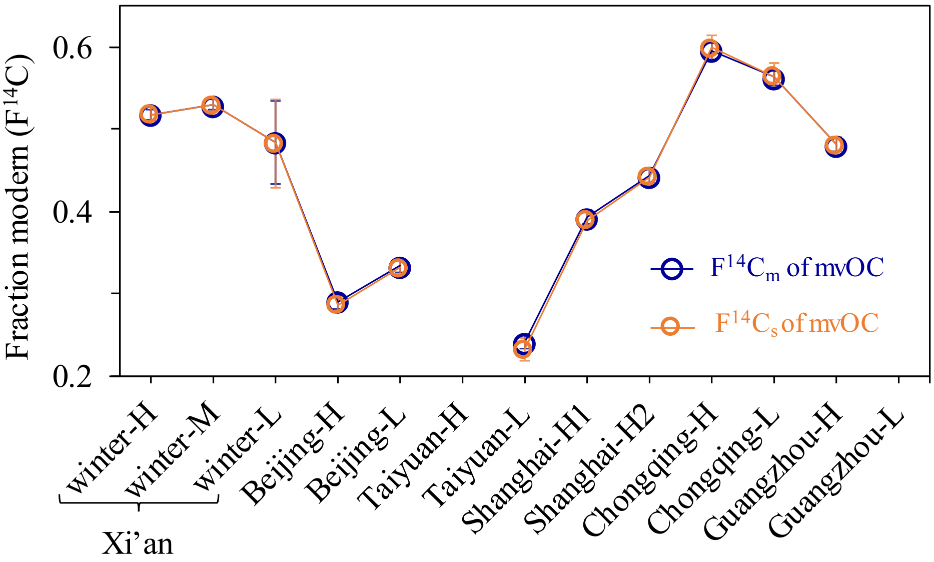

Figure S9. Fraction modern ($F^{14}C$) of mvOC before and after blank corrections ($F^{14}C_m$ and $F^{14}C_s$, respectively) for the contamination introduced by the isolation procedure. Detailed method to do the blank corrections is described in Supplement S3.

As shown in Fig. S9, the differences in $F^{14}C$ values of mvOC before and after blank corrections are really small, with the biggest absolute difference of 0.009 for sample Taiyuan-L. The small correction of $F^{14}C$ for mvOC will not affect any conclusion from this study. If possible, we think it probably acceptable to show the $F^{14}C$ of mvOC before corrections as it was in the original manuscript. Otherwise, we need to recalculated everything, and change nearly all figures and tables. This will not change any conclusion but will lead to inconsistence between the discussion paper and the final one.

For OC and EC, the contamination introduced by the isolation procedure yields 0.72 ± 0.44 µgC EC and 0.85 ± 0.49 µgC OC per extraction, respectively, which are the directly determined system blank (i.e. the amount of CO_2 measured, when no sample is introduced into the aerosol combustion system). The blanks are less than 3% of the sample amount and thus can be neglected, compared with our sample size of 30–391 µgC EC per extraction and 30–445 µgC OC per extraction. Therefore, the blank correction will not introduce large uncertainties to the data. In this study, the contamination is assessed but not used for further data correction for $F^{14}C$ of OC and EC.

To make this clear, we add the detailed calculation of blank correction for $F^{14}C$ of mvOC, OC and EC in supplemental material (Supplement S3). Figure S9 is also added in the revised Supplement. Furthermore, the revised manuscript adds:

> "Compared with our sample size of 30–391 µgC EC, 30–445 µgC OC, and 15–121 µgC mvOC, the blanks are ≤7 % of the mvOC sample amount and < 3% of OC and EC sample amount, therefore relatively small compared to our sample sizes. The mvOC concentrations reported in this study are corrected for contamination by subtraction. OC and EC concentrations are measured following thermal-optical protocols using carbon analyzers (Sect. 2.2), thus are not affect by the isolation procedure using the ACS. For ^{14}C values (Eq. 1), the contamination is assessed but not used for further ^{14}C data correction for mvOC, OC and EC, because the corrections for the small blanks will not introduce large uncertainties to the data, as explained in Supplement S3." (page 6, line 9-15)

12) P6, L7-8: Here, the same applies as for P5, L29-30.

Response: OC and EC concentrations were determined following thermal-optical protocols using carbon analyzers (Sect. 2.2, page 4), which are corrected by the system blank and thus were not affected by the isolation procedure of OC and EC using aerosol combustion system (ACS). To make this clear, we add:

> "OC and EC concentrations are measured following thermal-optical protocols using carbon analyzers (Sect. 2.2), thus are not affect by the isolation procedure using the ACS." (page 6, line 11-13).

(2) blank corrections for $F^{14}C$ of OC and EC

The calculation of of blank correction for $F^{14}C$ of OC and EC is given in response of question 11 and in the Supplement S3. In question 11, the contamination is the directly determined system blank (i.e. the amount of CO_2 measured, when no sample is introduced into the aerosol combustion system). We have explained in the response of question 11 why the contamination is assessed but not further used for $F^{14}C$ data correction. Here, the contamination is determined indirectly by combusting small amounts of standard material, with known $F^{14}C$ values, i.e., the OXII standard ($F^{14}C$ =1.3406) and ^{14}C free standard ($F^{14}C$ = 0). If contamination is introduced into the combustion, the measured $F^{14}C$ values of the standards will deviate from the nominal values and from this deviation the contamination can be estimated. The contamination inferred in this indirect way is below 1.5 µgC per extraction, and this is an estimate for TC blank (TC = OC+ EC). It is also relatively small compared to the size of OC (30–445 µgC) and EC samples (30–391 µgC) in this study and thus will not lead to large uncertainties to the $F^{14}C$ data. The $F^{14}C$ of the contamination can also be indirectly inferred from the standard measurements and varied between 0.2 and 0.6 for standards measured on the system with the last two years. This is broadly within the range of our samples and implies that a correction for $F^{14}C$ will even be considerably smaller than 3%.

The revised text shows:

> "The contamination inferred in this indirect way is below 1.5 µgC per extraction, which is slightly higher than the directly measured contamination of OC and EC separately but in the range of a TC contamination. It is also relatively small compared to the size of OC (30–445 µgC) and EC samples (30–391 µgC) in this study and thus can be neglected (Supplement S3). The $F^{14}C$ (Eq. 1) of the contamination can also be indirectly inferred and varied between 0.2 and 0.6 for standards measured on the ACS with the last two years. This is broadly within the range of our samples and implies that a correction for $F^{14}C$ will even be considerably smaller than 3%." (page 6, line 21-26)

13) P6, L22: "and 1970s" should be deleted.

Response: Done. The revised text shows that:

> "the $F^{14}C$ values of contemporary carbon are higher than 1 due to the nuclear bomb tests that nearly doubled the $^{14}CO_2$ in the atmosphere in the 1960s" (page 7, line 8-9)

14) P7-9, Chapter 2.4: In the explanation of the calculation "can be" should be substituted by "was" several times.

Response: We correct them all in Chapter 2.4. (page 7-9)

15) P7, L26-27: A reference should be shown for the statement that the contributions from plant detritus, bioaerosols and spores to $PM_{2.5}$ are likely small.

Response: We add Song et al. (2006), Hu et al. (2010) and Guo et al. (2012). (page 8, line 14)

The new citations are included in the revised reference list:

Guo, S., Hu, M., Guo, Q., Zhang, X., Zheng, M., Zheng, J., Chang, C. C., Schauer, J. J., and Zhang, R.: Primary sources and secondary formation of organic aerosols in Beijing, China, Environ. Sci. Technol., 46, 9846–9853, 2012.

Hu, D., Bian, Q., Lau, A. K. H., and Yu, J. Z.: Source apportioning of primary and secondary organic carbon in summer $PM_{2.5}$ in Hong Kong using positive matrix factorization of secondary and primary organic tracer data, J. Geophys. Res.-Atmos., 115, 10.1029/2009jd012498, 2010.

Song, Y., Zhang, Y., Xie, S., Zeng, L., Zheng, M., Salmon, L. G., Shao, M., and Slanina, S.: Source apportionment of $PM_{2.5}$ in Beijing by positive matrix factorization, Atmos. Environ., 40, 1526-1537, https://doi.org/10.1016/j.atmosenv.2005.10.039, 2006.

16) P10, L14: "the" was erroneously repeated at the beginning of the line.

Response: Corrected. (page 11, line 6)

17) P10, L20: "Taken together" should be removed.

Response: Done. (page 11, line 12)

18) P13, L7: I suggest to begin the sentence with "As fnf(mvOC) is smaller"

Response: Done. (page 14, line 2)

19) P13, L14: The citation "(Fig. 4b)" should be moved to the end of the sentence in L10.

Response: Done. (page 14, line 5)

20) P15, L19: we conclude (remove "can")

Response: Done. (page 16, line 14)

21) P15, L20-21: In Fig. 7c there are two outlier data points from sample

Response: Done. The revised text shows

> "In Fig. 7c there are two outlier data points from sample…." (page 16, line 16)

22) P15, L30: In other words

Response: We have replaced "In another word" by "In other words" (page 16, line 25)

23) P18, L3: Consequently, our conclusion

Response: We have replaced "That is" with "Consequently". The revised manuscript shows:

> "Consequently, our conclusion that mvOC is more fossil than OC and SOC is still valid…" (page 18, line 28)

24) P18, L30: References to the literature (Masalaite et al., 2017, 2018) and figures (Fig. 5) from the paper should be removed from the Conclusions.

Response: Done. (page 19, line 26)

25) Fig. 2: An uncertainty of the average $F^{14}C_{(mvOC)}$ should be given in line 6 using the standard deviation of the three replicates.

Response: Done, the revised caption of Fig. 2 shows:

> "The dashed line in dark green indicates the expected mvOC loading and the horizontal in solid green the $F^{14}C_{(mvOC)}$ for the combined winter-M (weighted mean ± standard deviation; 0.524 ± 0.028)." (page 29, line 5-6)

26) Fig. 3: The following sentence should be added to the caption: "For details see Tab. S4."

Response: Done. (page 30, line 5)

27) Supplement PS4, second to last line: $OC_{280°C}$ (instead of $OC_{2800°C}$)

Response: Corrected. The revised Supplement shows:

> "The desorption temperature for mvOC is 200 °C, falling within the 140 °C for $OC_{140°C}$ and 280 °C for $OC_{280°C}$. We thus estimated the particulate fraction for mvOC will fall within the X_{p1} for $OC_{140°C}$ and X_{p2} for $OC_{280°C}$." (page S6 in the Supplement)

28) Fig. S5, last line of the caption: The panels (a) and (b) have

Response: Corrected. Now it reads "The panel (a) and (b) have the same *x*-axis." (page S11 in the Supplement)

29) Table S4: Uncertainties are missing for $\delta^{13}C_{EC}$ (last column)

Response: The uncertainties of $\delta^{13}C_{EC}$ have been added in Table S4. (page S19 in the Supplement)

References:

Gaston, C. J., Lopez-Hilfiker, F. D., Whybrew, L. E., Hadley, O., McNair, F., Gao, H., Jaffe, D. A., and Thornton, J. A.: Online molecular characterization of fine particulate matter in Port Angeles, WA: Evidence for a major impact from residential wood smoke, Atmos. Environ., 138, 99-107, https://doi.org/10.1016/j.atmosenv.2016.05.013, 2016.

Lopez-Hilfiker, F. D., Mohr, C., Ehn, M., Rubach, F., Kleist, E., Wildt, J., Mentel, Th. F., Lutz, A., Hallquist, M., Worsnop, D., and Thornton, J. A.: A novel method for online analysis of gas and particle composition: description and evaluation of a Filter Inlet for Gases and AEROsols (FIGAERO), Atmos. Meas. Tech., 7, 983-1001, https://doi.org/10.5194/amt-7-983-2014, 2014.

Paciga, A., Karnezi, E., Kostenidou, E., Hildebrandt, L., Psichoudaki, M., Engelhart, G. J., Lee, B.-H., Crippa, M., Prévôt, A. S. H., Baltensperger, U., and Pandis, S. N.: Volatility of organic aerosol and its components in the megacity of Paris, Atmos. Chem. Phys., 16, 2013-2023, https://doi.org/10.5194/acp-16-2013-2016, 2016.

Tie, X., Huang, R.-J., Cao, J., Zhang, Q., Cheng, Y., Su, H., Chang, D., Pöschl, U., Hoffmann, T., Dusek, U., Li, G., Worsnop, D. R., and O'Dowd, C. D.: Severe Pollution in China Amplified by Atmospheric Moisture, Sci. Rep., 7, 15760, 10.1038/s41598-017-15909-1, 2017.

Zheng, G. J., Duan, F. K., Su, H., Ma, Y. L., Cheng, Y., Zheng, B., Zhang, Q., Huang, T., Kimoto, T., Chang, D., Pöschl, U., Cheng, Y. F., and He, K. B.: Exploring the severe winter haze in Beijing: the impact of synoptic weather, regional transport and heterogeneous reactions, Atmos. Chem. Phys., 15, 2969-2983, https://doi.org/10.5194/acp-15-2969-2015, 2015.

High contributions of fossil sources to more volatile organic ~~carbon~~ aerosol

Haiyan Ni[1,2,3], Ru-Jin Huang[2*], Junji Cao[2], Wenting Dai[2], Jiamao Zhou[2], Haoyue Deng[1], Anita Aerts-Bijma[1], Harro A. J. Meijer[1], Ulrike Dusek[1]

[1]Centre for Isotope Research (CIO), Energy and Sustainability Research Institute Groningen (ESRIG), University of Groningen, Groningen, 9747 AG, the Netherlands
[2]State Key Laboratory of Loess and Quaternary Geology, Key Laboratory of Aerosol Chemistry and Physics, Institute of Earth Environment, Chinese Academy of Sciences, Xi'an, 710061, China
[3]University of Chinese Academy of Sciences, Beijing, 100049, China

Correspondence to: Ru-Jin Huang (rujin.huang@ieecas.cn)

Abstract. Sources of particulate organic carbon (OC) with different volatility have rarely been investigated despite the significant importance for better understanding of the atmospheric processes of organic aerosols. In this study we develop a radiocarbon (^{14}C) based approach for source apportionment of more volatile OC (mvOC) and apply to ambient aerosol samples collected in winter in six Chinese megacities. mvOC is isolated by desorbing organic carbon from the filter samples in helium (He) at 200 °C in a custom-made aerosol combustion system for ^{14}C analysis. Evaluation of this new isolation method shows that the isolated mvOC amount agrees very well with the OC1 fraction (also desorbed at 200 °C in He) measured by a thermal optical analyzer using the EUSAAR_2 protocol. The mvOC, OC and elemental carbon (EC) of thirteen combined $PM_{2.5}$ samples in six Chinese cities are analyzed for ^{14}C to investigate their sources and formation mechanisms. The relative contribution of fossil sources to mvOC is 59 ± 11 %, consistently larger than the contribution to OC (48 ± 16 %) and smaller than that to EC (73 ± 9 %), despite large differences in fossil contributions in different cities. The average difference in the fossil fractions between mvOC and OC is 13 % (range: 7 %–25 %~~; range~~), similar to that between mvOC and EC (13 %; 4 %–25 %). Secondary OC (SOC) concentrations and sources are modelled based on the ^{14}C-apportioned OC and EC, and compared with concentrations and sources of mvOC. SOC concentrations (15.4 ± 9.0 µg m^{-3}) are consistently higher than those of mvOC (3.3 ± 2.2 µg m^{-3}), indicating that only a fraction of SOC is accounted for by the more volatile carbon fraction desorbed at 200 °C. The fossil fraction in SOC is 43 % (10 %–70 %), lower than that in mvOC (59 %; 45 %–78 %). Correlation between mvOC and SOC from non-fossil sources ($mvOC_{nf}$ vs. SOC_{nf}) and from fossil sources ($mvOC_{fossil}$ vs. SOC_{fossil}) are examined to further explore sources and formation processes of mvOC and SOC.

1 Introduction

Aerosol particles are of importance for atmospheric chemistry and physics, and exert a crucial effect on the climate system, air quality and human health (Fuzzi et al., 2015). The ~~Carbonaceous~~carbonaceous fraction of aerosol~~s, consisting of organic carbon (OC) and elemental carbon (EC),~~ comprises a large fraction of the fine aerosol mass (20 %–80 %) (Cao et al., 2007; Tao et al., 2017). Carbonaceous aerosols are often operationally subdivided into organic carbon (OC) and elemental carbon (EC). OC ~~contains~~ consists of a large variety of organic species that cover a great range of volatilities and are not or weakly light absorbing, while EC is non-volatile, resistant to chemical transformation and strongly light absorbing ~~, such as polycyclic aromatic hydrocarbons and other components with potential mutagenic and carcinogenic effects, while EC contains chars, amorphous-like carbon consisting of randomly oriented poly-aromatic layers and carbon nanospheres formed from incomplete combusted carbon-based fuels~~ (Pöschl, 2005). It should be noted that since no clear distinction between OC and EC exists, OC and EC are operationally defined based on the measurement techniques (Petzold et al., 2013). When a thermo-optical method is used to separate and determine OC and EC, EC is described as a thermally refractory carbon continuum and OC is weakly refractory (Pöschl, 2003, 2005; Petzold et al., 2013).

EC is exclusively emitted as primary aerosols from incomplete combustion of biomass (e.g., wood, crop residues, and grass) and fossil fuels (e.g., coal, gasoline, and diesel). OC can be of both primary and secondary origin. Primary OC (POC) is emitted directly from non-fossil (e.g., biomass burning, biogenic emissions, and cooking) and fossil sources. Secondary OC (SOC) is formed in the atmosphere via atmospheric oxidation of volatile organic compounds (VOCs) (Jacobson et al., 2000; Hallquist et al., 2009; Bond et al., 2013). High concentrations of aerosol particles have been observed in many cities, especially in China, where carbonaceous aerosols dominate particle mass concentrations, with SOC responsible for a large fraction of OC (Guo et al., 2014; Huang et al., 2014; Fang et al., 2017). Thus, understanding the sources, formation and transformation of EC, OC and SOC is important for better understanding of air pollution.

For aerosol source apportionment, radiocarbon (^{14}C) analysis of OC and EC has been used to quantify their fossil and non-fossil fractions, based on the fact that emissions from fossil sources are ^{14}C-free due to long-time decay, whereas non-fossil emissions contain the contemporary ^{14}C content (e.g., Szidat et al., 2004, 2006; Dusek et al., 2013, 2017). Earlier ^{14}C measurements of OC and EC found that fossil sources contribute more to EC than OC (Heal, 2014 and references therein). However, direct ^{14}C measurements on SOC are not possible yet, due to the technical and conceptual difficulties in isolating the SOC fraction from filter samples. In positive matrix factorization (PMF) based source apportionment of aerosol mass spectrometer (Jayne et al., 2000) dataset, oxidized organic aerosols (OOA, also referred to as secondary organic aerosol, SOA) can be separated into semi-volatile OOA (SV-OOA) and low-volatility OOA (LV-OOA) based on their volatility (e.g., Huffman et al., 2009a; Wang et al., 2017). Volatility is an important physical property as it determines the partitioning between gas and particulate phases of organic species (Donahue et al., 2006, 2009). Direct measurement of OA volatility is challenging because OA is a mixture of thousands of individual organics spanning a wide range of volatilities (Donahue et al., 2011). Different approaches have been used to estimate the OA volatility. For example, using thermodenuder (TD) coupled with an aerosol mass spectrometer (Burtscher et al., 2001; Wehner et al., 2002), the volatility of different OA components, ~~(~~such as hydrocarbon-like OA (HOA), biomass burning OA (BBOA) ~~or~~ and OOA~~)~~, can be estimated for ambient aerosols. Source and ambient studies indicate that BBOA and HOA are generally more volatile than OOA. Meanwhile, the volatility of BBOA can be quite variable, depending on type of biomass and the combustion conditions, and either higher or lower than that of HOA (e.g., Grieshop et al. 2009c; Huffman et al. 2009a; Paciga et al. 2016; Cao et al., 2018).For example, Huffman et al. (2009b) measured the volatility of primary OA from biomass burning and found that the more volatile BBOA was generally dominated by smoldering combustion, while the less volatile BBOA was more influenced by flaming combustion. Paciga et al. (2016) found that the BBOA was more volatile than HOA in an urban background site in Paris, with 50% semi-volatile organic components (SVOCs with effective saturation concentrations C^* of 1–100 μg m^{-3} range) and 30% low volatility organic compounds (LVOCs with C^* of 10^{-3}–0.1 μg m^{-3}). Gaston et al. (2016) found that levoglucosan (i.e., the biomass burning tracer) was semi-volatile and had the potential to form low volatility products during the chemical aging of ambient biomass burning aerosol, applying high-resolution-time-of-flight chemical ionization mass spectrometer (HRTOF-CIMS) coupled to a Filter Inlet for Gases and AEROsols (FIGAERO) to aerosol in the northwestern US.

In some recent studies, a thermal desorption approach has been used for analysis of filter samples at lower and higher temperatures as an indicator of volatility (Holzinger et al., 2013; Lopez-Hilfiker et al., 2014, 2015; Timkovsky et al., 2015; Masalaite et al., 2017, 2018). Even though the desorption temperature is not a direct measure of the particle volatility, OC desorbed from the filter at lower temperature tends to be more volatile, whereas the less volatile (i.e., more refractory) OC tends to be desorbed at higher temperatures. Vodička et al. (2015) and Masalaite et al. (2017) found that OC in urban samples was desorbed at lower temperatures compared to costal, forest, and rural background samples in Eastern Europe. Both studies suggest that OC is more volatile in urban area close to the emission sources. Keller and Burtscher (2017) found that after aging of biomass burning emissions less OC desorbed at lower temperatures. The reduction in volatility after aging agrees with previous TD aerosol mass spectrometer studies (Grieshop et al., 2009b). Even though the thermal desorption and TD measurements are different methods, results of both methods are usually in qualitative agreement and show similar trends. Earlier studies (e.g., Grieshop et al., 2009c; Chen et al., 2007) show similar trends qualitatively. Ma et al. (2016) made first efforts to link the OC fractions desorbed at different temperatures from filter samples on a thermal-optical analyzer to the volatility basis set, showing that OC fractions desorbed at lower temperatures (e.g., 140 °C, 280 °C) are semi-volatile.

Both POC and SOC can contribute to the OC fraction desorbed at lower temperatures. A number of previous studies have found that at least a part of POC from various sources is semi-volatile, including wood burning, gasoline and diesel vehicle exhausts and cooking (Lipsky and Robinson, 2006; Shrivastava et al., 2006; Robinson et al., 2007; Grieshop et al., 2009b, 2009c; May et al., 2013a, 2013b). Moreover, a significant part of freshly formed SOC is semi-volatile and will contribute to the more volatile OC fraction desorbed at lower temperatures (Holzinger et al., 2010; Salo et al., 2011; Meusinger et al., 2017; Gkatzelis et al., 2018). The relative contributions from fossil and non-fossil sources to OC can be dependent on the volatility. For example, recent studies in wintertime of Lithuania have shown that vehicular sources are associated with OC fractions desorbed at lower temperatures while biomass burning (as a non-fossil source) contributes more strongly to less volatile OC fractions desorbed at higher temperatures (Masalaite et al., 2017, 2018).

Although an increasing number of studies has shown that OC from different emission sources and/or at different aging status may have different volatility, a quantitative study of the sources of OC with different volatility is scarce. In this study, wintertime fine particulate matter ($PM_{2.5}$, particles with aerodynamic diameter < 2.5 μm) samples from 6 Chinese megacities are studied. Sources of carbonaceous aerosols including different carbon fractions such as OC, EC and SOC are estimated by radiocarbon (^{14}C) source apportionment. In addition, we operationally define a more volatile OC fraction (mvOC) as the carbon fraction desorbed from the filter samples at 200 °C in helium (He), and investigate sources of mvOC. ~~To our best knowledge, this is the first time that the~~ The source contribution to ~~the more volatile fraction of OC~~mvOC is measured unambiguously by ^{14}C..

2 Methods

2.1 Sampling

Simultaneous sampling was made during winter 2013/2014 in two northern (Beijing and Taiyuan) and three southern (Chongqing, Guangzhou and Shanghai) Chinese cities (Fig. S1). The samples from Xi'an in northern China were collected during winter 2015/2016. These sites were selected to represent urban-scale concentration and located in the university or research center campus, >100 m from local sources such as main roadways (Table S1). The 24 h integrated $PM_{2.5}$ samples were collected from 10:00 to 10:00 the next day (local standard time, LST). Filter samplers were deployed on roof-tops about 6 to 20 m above ground level. In Xi'an, Beijing, Guangzhou and Shanghai, $PM_{2.5}$ samples were collected on pre-baked ~~pre-backed~~ (780 °C for 3 h) quartz fiber filter (QM/A, Whatman Inc., Clifton, NJ, USA, 20.3 cm × 25.4 cm) using a high-volume sampler (TE-6070 MFC, Tisch Inc., Cleveland, OH, USA) at a flow rate of 1.0 m^3 min^{-1}. In Taiyuan and Chongqing, samples were collected on pre-baked 47-mm Whatman quartz microfiber filters (QM/A) using mini-volume samplers at a flow rate of 5 L min^{-1} (Airmetrics, Oregon, USA). After sampling, all filters were packed in a pre-baked aluminum foils (450 °C for 3 h), sealed in polyethylene bags and stored in a freezer at -18 °C until analysis.

2.2 Determination of carbon fractions by thermal-optical analysis

For the $PM_{2.5}$ samples collected in Xi'an, filter pieces of 1.5 cm^2 were taken for OC and EC analysis using a carbon analyzer (Model 5L, Sunset Laboratory, Inc., Portland, OR, USA) following the thermal-optical transmittance protocol EUSAAR_2

(European Supersites for Atmospheric Aerosol Research; Cavalli et al., 2010). The EUSAAR_2 protocol defines OC1 as the carbon fraction that desorbs in helium (He) at 200 °C for 2 min. OC1 is compared with more volatile OC (mvOC) extracted also in He at 200 °C but for 5 min using our aerosol combustion system (ACS) (Dusek et al., 2014). No charred OC is observed by the transmittance signal in the OC1 stage during the thermo-optical analysis. For PM$_{2.5}$ samples collected in Beijing, Taiyuan, Chongqing, Guangzhou and Shanghai, filter pieces of 0.5 cm^2 were used to measure OC and EC using a Desert Research Institute (DRI) Model 2001 Thermal/Optical Carbon Analyzer (Atmoslytic Inc., Calabasas, CA, USA) following the IMPROVE_A thermal/optical reflectance (TOR) protocol (Chow et al., 2007). OC fractions of EUSAAR_2 protocol are desorbed in He at 200 °C (OC1), 300 °C (OC2), 450 °C (OC3), and 650 °C (OC4) in He. Different from EUSAAR_2 protocol, IMPROVE_A (Interagency Monitoring of Protected Visual Environments) protocol defines OC fractions at stepwise temperature of 140 °C, 280 °C, 480 °C, and 580 °C in He. Details of the carbon fraction measurements were described in our previous work (Cao et al., 2013; Zenker et al., 2017).

2.3 Radiocarbon (^{14}C) measurements of mvOC, OC and EC

2.3.1 Sample selection for ^{14}C analysis

For ^{14}C analysis, we selected the samples carefully to cover periods of low and high total carbon~~TC~~ (TC, the sum of~~=~~ OC ~~+~~ and EC) and PM$_{2.5}$ concentrations to get samples representative of various pollution conditions that did occur in each city. Two or three composite samples from each city representing high (H), medium (M) and low (L) TC concentrations ~~are~~were selected for ^{14}C analysis of EC, OC and mvOC (Fig. S2). Each composite sample consists of 2 to 4 24 h filter pieces with similar TC loadings and air mass backward trajectories (Fig. S2, Table S1).

2.3.2 Extraction of mvOC, OC, EC

Three separate extractions were performed for mvOC, OC and EC on our aerosol combustion system (ACS) (Dusek et al., 2014). The ACS consists of a combustion tube and a purification line. Aerosol filter pieces placed on the filter boat are heated at different temperatures in pure He or O$_2$ and oxidized through the platinum catalyst in the combustion tube. The resulting CO$_2$ is isolated and separated from other gases (e.g., NO$_x$, water vapor) in the purification line. The purification line is equipped with an oven filled with copper grains and silver wire heated at 650 °C to remove NO$_x$ and liberated halogen, a U-type tube cooled with a dry ice-ethanol mixture for water removal and a flask containing phosphorous pentoxide (P$_2$O$_5$) for removal of any trace water. The amount of purified CO$_2$ is manometrically quantified and subsequently stored in flame-sealed glass ampoules.

mvOC is desorbed by heating the filter pieces at 200 °C in He for 5 min. After introducing the filter, the ovens are flushed with He for 10 min. Pilot tests show that the flushing time (10 min, 15 min or 60 min) before heating the filter pieces does not affect the desorbed amount of mvOC (Table S2). OC is combusted by heating filter pieces at 375 °C in pure O$_2$ for 10 min. EC is extracted from a separate filter piece after removing OC completely. First water-soluble OC is removed from the filter through water extraction (Dusek et al., 2014) to minimize the charring of organic materials (Yu et al., 2002; Zhang et al., 2012). Then, by heating the filter pieces at 375 °C in O_2 for 10 minutes, most water-insoluble OC can be removed. Subsequently, the oven temperature is increased to 450 °C for 3 min to remove the most refractory OC that left on the filter. However, during this step some less refractory EC might be lost. Finally, the remaining EC is combusted by heating at 650 °C in O_2 for 5 min (Dusek et al., 2014, 2017; Zenker et al., 2017).

Contamination introduced by the isolation procedure is determined by following exactly the same isolating procedures with either empty filter boat or with pre-heated filters (at 650 °C in O_2 for 10 min). The contamination introduced by the combustion process yields 0.72 ± 0.44 µgC EC, 0.85 ± 0.49 µgC OC, 0.52 ± 0.31 µgC mvOC per extraction, respectively. Compared with our sample size of 30–391 µgC EC, 30–445 µgC OC, and 15–121 µgC mvOC, the blanks are ≤7 % of the mvOC sample amount and < 3% of OC and EC sample amount, ~~and~~ therefore relatively small compared to our sample sizes. The mvOC concentrations reported in this study are corrected for contamination by subtraction. OC and EC concentrations are measured following thermal-optical protocols using carbon analyzers (Sect. 2.2), thus are not affect by the isolation procedure using the ACS. For ^{14}C values (Eq. 1), the contamination is assessed but not used for further ^{14}C data correction for mvOC, OC and EC, because the corrections for the small blanks will not introduce large uncertainties to the data, as explained in Supplement S3.

Two standards with known $^{14}C/^{12}C$ ratios are combusted using the ACS as quality control for the combustion process: an oxalic acid standard and anthracite. Small amounts of solid standard materials are directly put on the filter boat of the combustion tube and heated in O_2 at 650 °C for 10 min. In the further ^{14}C analysis, the CO_2 derived from combustion of the standards is treated exactly like the samples. Therefore, the contamination introduced by the combustion process can be estimated from the deviation of measured values from the nominal values of the standards (Table S3) (Dusek et al., 2014). The contamination inferred in this indirect way is below 1.5 µgC per extraction, which is slightly higher than the directly measured contamination of OC and EC separately but in the range of a TC contamination. It is also relatively small compared to the size of OC (30–445 µgC) and EC samples (30–391 µgC) in this study and thus can be neglected (Supplement S3). The $F^{14}C$ (Eq. 1) of the contamination can also be indirectly inferred and varied between 0.2 and 0.6 for standards measured on the ACS with the last two years. This is broadly within the range of our samples and implies that a correction for $F^{14}C$ will even be considerably smaller than 3%.

2.3.3 ^{14}C measurements by accelerator mass spectrometer (AMS)

AMS measurements were conducted at the Centre for Isotope Research (CIO) at the University of Groningen. The extracted CO_2 is released from the glass ampules and directed to a gas inlet system (Ruff et al., 2007), where the sample is diluted with He to 5 % CO_2 (Salazar et al., 2015). The CO_2/~~H_2~~He mixture is directly fed into the Cs sputter ion sources of the Mini Carbon Dating System (MICADAS) AMS at a constant rate (Synal et al., 2007).

The $^{14}C/^{12}C$ ratio of an aerosol sample is usually reported relative to an oxalic acid standard (OXII) and expressed as fraction modern ($F^{14}C$). The $^{14}C/^{12}C$ ratio of the standard is related to the unperturbed atmosphere in the reference year of 1950 by multiplying it with a factor of 0.7459 (Mook and Van Der Plicht, 1999; Reimer et al., 2004):

$$F^{14}C = \frac{(^{14}C/^{12}C)_{sample,[-25]}}{0.7459 \times (^{14}C/^{12}C)_{OXII,[-25]}}, \tag{1}$$

where the $^{14}C/^{12}C$ ratio of the sample and standard are both corrected for machine background and normalized to $\delta^{13}C$ = -25 ‰. Aerosol carbon from fossil sources has $F^{14}C = 0$ due to the extinction of ^{14}C after long-time decay. Aerosol carbon from contemporary (or non-fossil) sources should have $F^{14}C$ ~1 in an atmosphere undisturbed by human influences. However, the $F^{14}C$ values of contemporary carbon are higher than 1 due to the nuclear bomb tests that nearly doubled the $^{14}CO_2$ in the atmosphere in the 1960s~~ and 1970s~~. The $^{14}CO_2$ produced by the nuclear bomb tests has been taken up by oceans and the biosphere and diluted by the ^{14}C-free CO_2 emitted by the fossil fuel burning. Currently, $F^{14}C$ of the atmosphere CO_2 is ~1.04 (Levin et al., 2010).

The $F^{14}C$ values are corrected for cross contamination (also known as memory effect) (Wacker et al., 2010) using alternate measurements of ~~H~~OxII and ^{14}C-free material as gaseous standards. Correction for instrument background (Salazar et al., 2015) is done by subtracting the memory corrected $F^{14}C$ values of the ^{14}C-free standard. Finally, the values are normalized to the average value of the (memory and background corrected) ~~H~~OxII standards. All standards used for the corrections are measured on the same day as the samples.

2.4 Estimation of source contributions to different carbon fractions

$F^{14}C$ of EC, OC and mvOC (i.e., $F^{14}C_{(EC)}$, $F^{14}C_{(OC)}$ and $F^{14}C_{(mvOC)}$, respectively) ~~are~~ were directly measured. We define 'more refractory organic carbon' (mrOC) as the difference between OC and mvOC. $F^{14}C$ of mrOC ($F^{14}C_{(mrOC)}$) ~~can be~~ was calculated by isotope mass balance:

$$F^{14}C_{(mrOC)} = \frac{F^{14}C_{(OC)} \times OC - F^{14}C_{(mvOC)} \times mvOC}{OC - mvOC}. \tag{2}$$

$F^{14}C_{(EC)}$ ~~can be~~was converted to the fraction of biomass burning (f_{bb}(EC)) by dividing with an $F^{14}C$ value representative of typical biomass burning emissions ($F^{14}C_{bb}$). Analogously, the fraction of non-fossil OC, mvOC and mrOC (i.e., f_{nf}(OC), f_{nf}(mvOC) and f_{nf}(mrOC), respectivly) ~~can be~~were estimated from their corresponding $F^{14}C$ values and $F^{14}C$ of non-fossil sources ($F^{14}C_{nf}$). $F^{14}C_{bb}$ and $F^{14}C_{nf}$ are estimated as 1.10 ± 0.05 and 1.09 ± 0.05 (Lewis et al., 2004; Mohn et al., 2008; Palstra and Meijer, 2014), respectively, based on tree-growth models and the assumption that wood burning dominates biomass burning. $F^{14}C_{bb}$ for EC is slightly bigger than $F^{14}C_{nf}$ for OC, because besides biomass burning, biogenic emissions also contribute to OC, but have a smaller $F^{14}C$ than that of biomass burning. The estimation of $F^{14}C_{bb}$ and $F^{14}C_{nf}$ has been reported in our previous study (Ni et al., 2018).

Then, f_{bb}(EC) ~~can be~~was used to determine EC mass concentrations from non-fossil biomass (EC$_{\mathrm{bb}}$) and fossil fuel combustion (EC$_{\mathrm{fossil}}$):

$$\mathrm{EC_{bb}} = \mathrm{EC} \times f_{\mathrm{bb}}(\mathrm{EC}), \tag{3}$$

$$\mathrm{EC_{fossil}} = \mathrm{EC} - \mathrm{EC_{bb}}. \tag{4}$$

Analogously, mass concentrations of OC, mvOC and mrOC from non-fossil sources (OC$_{\mathrm{nf}}$, mvOC$_{\mathrm{nf}}$ and mrOC$_{\mathrm{nf}}$, respectively) and fossil sources (OC$_{\mathrm{fossil}}$, mvOC$_{\mathrm{fossil}}$ and mrOC$_{\mathrm{fossil}}$, respectively) ~~can be~~were determined.

Secondary OC (SOC) includes SOC from fossil (SOC$_{\mathrm{fossil}}$) and non-fossil sources (SOC$_{\mathrm{nf}}$):

$$\mathrm{SOC} = \mathrm{SOC_{fossil}} + \mathrm{SOC_{nf}}. \tag{5}$$

Fraction fossil in total SOC (f_{fossil}(SOC)) ~~can be~~was formulated as:

$$f_{\mathrm{fossil}}(\mathrm{SOC}) = \frac{\mathrm{SOC_{fossil}}}{\mathrm{SOC_{fossil}} + \mathrm{SOC_{nf}}}. \tag{6}$$

For the following calculations we assume that SOC$_{\mathrm{nf}}$ can be approximated by OC from non-fossil sources excluding primary biomass burning (OC$_{\mathrm{o,nf}}$;OC other non-fossil). In principle, OC$_{\mathrm{o,nf}}$ includes SOC$_{\mathrm{nf}}$ and non-fossil primary OC from vegetative detritus, bioaerosols, resuspended soil organic matter, or cooking. But the contributions from plant detritus, bioaerosols and spores to PM$_{2.5}$ are likely small (Song et al., 2006; Hu et al., 2010; Guo et al., 2012). If cooking sources are significant then this assumption results in an upper limit of SOC$_{\mathrm{nf}}$.

$$\mathrm{SOC_{nf}} \cong \mathrm{OC_{o,nf}} = \mathrm{OC_{nf}} - \mathrm{POC_{bb}}, \tag{7}$$

where OC$_{\mathrm{o.nf}}$ ~~can be~~was calculated by the difference between OC$_{\mathrm{nf}}$ and primary OC from biomass burning (POC$_{\mathrm{bb}}$). POC$_{\mathrm{bb}}$ ~~is~~ was calculated by multiplying EC$_{\mathrm{bb}}$ with the primary OC/EC ratio of biomass burning (r_{bb}):

$$\mathrm{POC_{bb}} = \mathrm{EC_{bb}} \times r_{\mathrm{bb}}. \tag{8}$$

SOC$_{\mathrm{fossil}}$ ~~is~~ was calculated by subtracting primary fossil OC (POC$_{\mathrm{fossil}}$) from OC$_{\mathrm{fossil}}$. POC$_{\mathrm{fossil}}$ ~~is~~ was estimated by multiplying EC$_{\mathrm{fossil}}$ with primary OC/EC ratio of fossil fuel combustion (r_{fossil}):

$$\mathrm{SOC_{fossil}} = \mathrm{OC_{fossil}} - \mathrm{POC_{fossil}}, \tag{9}$$

$$\mathrm{POC_{fossil}} = \mathrm{EC_{fossil}} \times r_{\mathrm{fossil}}. \tag{10}$$

Fossil sources in China are almost exclusively from coal combustion and vehicle emissions, thus r_{fossil} ~~can be~~was estimated as

$$r_{\mathrm{fossil}} = r_{\mathrm{coal}} \times p + r_{\mathrm{vehicle}} \times (1 - p), \tag{11}$$

where r_{coal} and r_{vehicle} are the primary OC/EC ratio of coal combustion and vehicle emissions, respectively. The r_{bb}, r_{coal} and r_{vehicle} varies with the fuel types and properties, combustion conditions, sampling and analysis methods etc. Best estimate of r_{bb} (4 ± 1; average ± standard deviation~~SD~~), r_{coal} (2.38 ± 0.44), and r_{vehicle} (0.85 ± 0.16) is done through a literature search and described in our earlier studies (Ni et al., 2018). p is the fraction of EC from coal combustion (EC$_{\mathrm{coal}}$) in EC$_{\mathrm{fossil}}$.

We used two different methods to estimate p. (1) Since both coal combustion and vehicle emissions do not contain ^{14}C, they can not be distinguished by ^{14}C measurements alone. Therefore, p is randomly chosen from 0–1, that is no constraint on p values. (2) EC from coal combustion is on average more enriched in the stable carbon isotope ^{13}C compared to vehicle emissions. Therefore, complementing ^{14}C results of EC with measurements of the ^{13}C/^{12}C ratios of EC (expressed as δ^{13}C$_{\mathrm{EC}}$ in Eq. S1; Supplement S1) allows separation of EC$_{\mathrm{fossil}}$ into EC$_{\mathrm{coal}}$ and EC from vehicle emissions (EC$_{\mathrm{vehicle}}$). Samples taken from Beijing, Shanghai and Guangzhou using high-volume samplers had enough material for analysis of both F^{14}C$_{\mathrm{EC}}$ and δ^{13}C$_{\mathrm{EC}}$, thus EC$_{\mathrm{coal}}$, and EC$_{\mathrm{vehicle}}$ are separated as described in detail in Supplement S2. In brief, the fraction of coal combustion and vehicle emissions in EC ~~can be~~was calculated from measured F^{14}C$_{\mathrm{EC}}$ and δ^{13}C$_{\mathrm{EC}}$ for ambient EC combined with the source signatures. Bayesian Markov-Chain Monte Carlo (MCMC) calculations were used to account for the uncertainties in the source signatures and the measurement uncertainties (Andersson, 2011; Andersson et al., 2015). The results of the Bayesian calculations are the posterior probability density functions (PDFs) for the relative contributions of each source to EC (f_{coal} and f_{vehicle}; Fig. S3). The p ~~can be~~was formulated as:

$$p = \frac{f_{\mathrm{coal}}}{f_{\mathrm{fossil}}} = \frac{f_{\mathrm{coal}}}{f_{\mathrm{coal}} + f_{\mathrm{vehicle}}} \qquad (12)$$

The PDF of p ~~is~~ was derived from the PDF of f_{coal} and f_{vehicle}, and shown in Fig. S4.

To propagate uncertainties, a Monte Carlo simulation with 10000 individual calculations was conducted. For each individual calculation, F^{14}C$_{\mathrm{(EC)}}$, F^{14}C$_{\mathrm{(OC)}}$, F^{14}C$_{\mathrm{(mvOC)}}$, concentrations of EC, OC and mvOC ~~are~~ were randomly chosen from a normal distribution symmetric around the measured values with the experimental uncertainties as standard deviation (SD; Table S4). For F^{14}C$_{\mathrm{bb}}$, F^{14}C$_{\mathrm{nf}}$, r_{bb}, r_{coal} and r_{vehicle} random values ~~are~~ were chosen from a triangular frequency distribution with its maximum at the central value and is 0 at the lower limit and upper limit. For p ranging from 0 to 1 (no ^{13}C constraints), p ~~is~~ was randomly chosen from a uniform distribution. For p constrained by F^{14}C and δ^{13}C using MCMC (hereafter ^{13}C-constraint p), random values from the respective PDF of p were used (Fig. S4). In this way 10000 different estimation of f_{bb}(EC), f_{nf}(OC), f_{nf}(mvOC), f_{nf}(mrOC), EC$_{\mathrm{bb}}$, EC$_{\mathrm{fossil}}$, OC$_{\mathrm{nf}}$, OC$_{\mathrm{fossil}}$, mvOC$_{\mathrm{nf}}$, mvOC$_{\mathrm{fossil}}$, mrOC$_{\mathrm{nf}}$, mrOC$_{\mathrm{fossil}}$, SOC$_{\mathrm{nf}}$, SOC$_{\mathrm{fossil}}$, SOC and f_{fossil}(SOC) ~~can be~~were calculated (Tables S5, S6, S7, S8). The derived average represents the best estimate, and the SD represents the combined uncertainties.

3 Results

3.1 Method evaluation and quality control for mvOC extraction

The separation of OC and EC for ^{14}C analysis using our aerosol combustion system (ACS) were thoroughly evaluated by Dusek et al. (2014, 2017). It is thus necessary to validate the new extraction method for isolating mvOC. The reproducibility of the extracted mvOC amount was tested for 2 independent test filters with mvOC loadings of 6 and 18 µg cm^{-2}, respectively (Fig. S5). The coefficient of variation was determined as a measure of reproducibility. The reproducibility was found to be ~5% (n = 9).

Since carbon fractions (e.g., OC1) at different desorption temperatures have mostly been measured using the EUSAAR_2 protocol in many previous studies (e.g., Vodička et al., 2015; Keller and Burtscher, 2017), our goal is to define the mvOC fraction as representative of OC1. Therefore, the mvOC is desorbed at 200 °C, the same temperature as used for OC1 in the EUSAAR_2 protocol. However, the extracted amounts on the ACS system might differ due to different heating rates and length of the temperature step. The winter samples from Xi'an as well as the two test filters described above are used to compare mvOC concentrations from the ACS system to OC1. For most samples, excellent agreement was found between mvOC and OC1 (Fig. 1a), and most data points fall close to the 1:1 line. However, there are 3 data points deviating largely from the 1:1 line (red circle and square in Fig. 1). The two red squares represent the mvOC extraction for sample winter-H and winter-M using larger filter pieces (i.e., more mvOC in µgC per extraction). With larger filter pieces, the mvOC (µgC/cm^2 filter area) extracted by the ACS system is significantly lower than that measured by the Sunset analyzer. The recoveries of these two outliers are 0.59 for sample winter-H and 0.74 for winter-M, calculated by dividing mvOC mass by OC1 mass. For winter-H, the low recovery is also repeatable with the same filter area (Fig. S5). The low recoveries for large filter pieces may result from the lower temperature (< 200 °C) towards the ends of the filter boat. At the relatively low temperature of 200 °C only a 3.5 cm long at the centre of a 12 cm combustion tube was maintained at 200 ° C and outside the 3.5 cm the temperature is lower than 200 °C, e.g., ~170 ° C at the end of the combustion tube measured by a thermocouple. When filter pieces are large and placed outside the centred 3.5 cm, the desorption temperature for part of the filter pieces will lower than 200 °C, leading to lower desorbed mvOC amount. Another possibility is saturations of the catalyst (platinum, Pt) in the combustion line of ACS system. Pt works as catalyst by collecting oxygen atoms on the surface as has been demonstrated by direct observation of an ultra-thin oxygen layer on the Pt surface by a microscope (Spronsen et al., 2017). This is used to oxidize CO and hydrocarbons to CO_2 in a reducing atmosphere. Thus, for large sample amounts it is possible that the oxygen on the catalyst could not be sufficient to oxidize all desorbed CO and hydrocarbons to CO_2. However, we observed recoveries near 100% for mvOC amounts up to 120 µg, which was higher than the total amount desorbed for the winter-H sample. Therefore, limited catalyst capacity is not the likely explanation for the low recoveries. For subsequent experiments we consequently placed the filter pieces carefully in the 3.5 cm long 200 °C section of the combustion tube and avoid stacking multiple filter pieces to ensure a desorption temperature of 200 °C and sufficient helium supply.

To examine the effect of the low recoveries of mvOC on the $F^{14}C_{(mvOC)}$, we compare the $F^{14}C_{(mvOC)}$ of winter-M and winter-H samples for both high and low mvOC recoveries. $F^{14}C_{(mvOC)}$ for low recoveries is roughly 0.05 (absolute value, Fig. 1b) higher than for high recoveries, which is non-negligible compared to the measurement uncertainty. In addition, to validate the ~~the~~ measured $F^{14}C_{(mvOC)}$ for the combined sample winter-M, we also extracted mvOC separately from those three filters that were combined for the composite winter-M sample. Figure 2 shows the $F^{14}C_{(mvOC)}$ of combined winter-M and those of the 3 individual filter samples. From the $F^{14}C_{(mvOC)}$ and mvOC mass of the individual filters, we can estimate the expected $F^{14}C_{(mvOC)}$ of the combined winter-M sample using the isotope mass balance equation. The $F^{14}C_{(mvOC)}$ of winter-M calculated from individual filter pieces is 0.524, which is quite similar with the measured $F^{14}C_{(mvOC)}$ of 0.529 ± 0.007 for the combined winter-M with recovery close to 1.

~~Taken together, we~~ We conclude that $F^{14}C_{(mvOC)}$ of samples with mvOC recoveries of ~1 are reliable and used in the following discussion. The mvOC recovery of sample winter-L (red circle in Fig. 1) is also low (0.51), and we could not repeat it due to the limited filter material. For sample winter-L, we take the OC1 concentrations as mvOC and the measured $F^{14}C_{(mvOC)}$ values but assign a bigger absolute uncertainty of 0.05, due to its low mvOC recoveries. This is based on the difference in $F^{14}C_{(mvOC)}$ for winter-H and winter-M with low and high mvOC recoveries which is roughly 0.05 (Fig. 1b).

3.2 mvOC, OC and EC concentrations

Figure 3 shows the concentrations of mvOC, OC and EC and the mvOC contributions to OC (%) for the selected samples in the 6 Chinese megacities. mvOC and OC concentrations averaged 3.3 ± 2.2 μg m^{-3} (range: 0.7–7.4 μg m^{-3}~~; range~~) and 30.0 ± 13.8 μg m^{-3} (8.8–50.4 μg m^{-3}), respectively. EC concentrations ranged from 2.5 μg m^{-3} to 14.8 μg m^{-3}, with an average of 6.9 ± 3.6 μg m^{-3}. High TC concentrations were found in Taiyuan (60 μg m^{-3} for sample Taiyuan-H), Chongqing (59 μg m^{-3} for Chongqing-H), Beijing (57 μg m^{-3} for Beijing-H) and Xi'an (57 μg m^{-3} for winter-H) in descending order. Of these cities, Chongqing is located in southern China, where there is no official heating season using coal in winter. This study nevertheless indicates severe pollution of carbonaceous aerosols in Chongqing. TC concentrations in the other southern Chinese cities (Shanghai and Guangzhou) were much lower than that in Chongqing (Fig. 3).

The fraction of mvOC in total OC (mvOC/OC in Fig. 3) gives an indication of OC volatility. The mvOC contributed on average 10.5 ± 3.3 % to OC, ranging from 3 % to 15 %. The mvOC/OC varies between samples within the same city and between cities, indicating complicate sources and atmospheric processing of OC. The variations might also be partially attributed to the different protocols used for OC quantification. OC in Xi'an is measured with the EUSAAR_2 protocol (up to 650 °C for desorbing OC), whereas the IMPROVE_A protocol (up to 580 °C for OC) was used for the other five cities. However, Han et al. (2016) found that the absolute OC concentrations determined by EUSAAR_2 do not differ much from those determined by IMPROVE_A (22.6 ± 12.0 µg m^{-3} vs. 19.7 ± 10.7 µg m^{-3}) for one-year $PM_{2.5}$ samples in Xi'an during 2012/2013. Because of the small differences of OC between the two protocols, we think the comparison of OC concentrations and mvOC/OC amongst the six cities is justified. The rest of OC (~90 %) was contributed to the mrOC. mrOC concentrations averaged 26.8 ± 12.0 µg m^{-3}, ranging from 7.9 µg m^{-3} for sample Guangzhou-L to 43.1 µg m^{-3} for Beijing-H.

Direct comparison of our results with previous works is somewhat difficult because different thermal/optical protocols were used. The averaged mvOC concentration (3.3 ± 2.2 µg m^{-3}) in winter for the six studied sites in China is higher than winter concentrations at an urban background site (1.6 ± 1.7 µg m^{-3}), a rural background site (0.7 ± 0.6) in Prague (Vodička et al., 2015), where 200 °C in He was also applied to desorb this OC fraction using EUSAAR_2 protocol. The mvOC/OC ratio in our study is smaller than that of ambient samples from various other locations and much smaller than that of fresh source samples. For example, the urban background site in Prague had a mvOC/OC ratio of 28 % and the rural background site of 17 % (Vodička et al., 2015). The contribution of OC1 to total OC was as high as ~60 % for primary biomass burning measured by EUSAAR_2 thermal/optical protocol (Keller and Burtscher, 2017). For vehicle emissions, the OC fractions desorbed at 140 °C and 280 °C are the major OC fractions measured by the IMPROVE_A protocol, contributing ~30 % and ~20 % to total OC in tunnels in Taiwan (Zhu et al., 2014; 2010). Using the same protocol for OC analysis, Tian et al. (2017) found that OC fraction desorbed at 140 °C and 280 °C contributed ~13 % and ~20 % to primary OC from residential coal combustion in China. The mvOC desorbed at 200 °C, fall between 140 °C and 280 °C, thus the mvOC fraction in total OC should be higher than the faction of OC desorbed at 140 °C in total OC and lower than the fraction of OC desorbed up to 280 °C in total OC.

OC from different emission sources has different volatility, and the atmospheric processing can also alter its volatility. Keller and Burtscher (2017) found that aging reduces the volatility of OC from biomass burning, i.e., the contribution of OC1 fraction to total OC decreases from 60 % to 25 % after aging. The photochemical processing of OA can lead to accumulation of carbon in the more refractory organic fraction and also larger organic compounds (Masalaite et al., 2017). The mvOC fraction in OC of our ambient samples is much smaller than that of the primary sources, suggesting that atmospheric aging of OC plays an important role on modifying the volatility of OC.

3.3 Non-fossil and fossil fractions of different carbon fractions

Figure 4a shows the fraction of non-fossil carbon in mvOC, OC and EC (respective f_{nf}(mvOC), f_{nf}(OC) and f_{bb}(EC)). There are no considerable changes in f_{nf}(mvOC), f_{nf}(OC) and f_{bb}(EC) between polluted days ("H" samples) and clean days ("L" samples) within each site (Fig. 4a), despite the very different concentrations of carbonaceous aerosols (Fig. 3). However, f_{nf}(mvOC), f_{nf}(OC) and f_{bb}(EC) varied significantly among different sites: the lowest values are always found in Taiyuan, and highest in Chongqing. This implies that different pollution patterns exist in individual Chinese cities. The smallest f_{nf}(mvOC),

f_{nf}(OC) and f_{bb}(EC) in Taiyuan suggests that fossil sources are the main contributor to mvOC, OC and EC, whereas the largest values in Chongqing shows that the non-fossil contributions to mvOC, OC and EC are evidently higher in Chongqing than in other sites.

Ranging from 22 % to 55 %, f_{nf}(mvOC) (41 ± 11 %) is consistently smaller than f_{nf}(OC) (52 ± 16 %; 29 %–77 %) and larger than f_{bb}(EC) (27 ± 9 %; 10 %–42 %), despite their variations among the cities. The absolute difference in the non-fossil fractions between mvOC and OC is 13% (7 %–25 %), similar to that between mvOC and EC (13%; 4 %–25 %). Consistently smaller f_{nf}(mvOC) than f_{nf}(OC) suggests that mvOC is more fossil (less non-fossil) than the total OC. Liu et al. (2017) also found that F^{14}C of OC desorbed at lower temperature (up to 200 °C) in He was 0.389, smaller than F^{14}C of total OC desorbed in the He phase of EUSAAR_2 protocol (F^{14}C = 0.495, up to 650 °C) for a single test sample collected in winter in Xinjiang, China. Agrios et al. (2016) had the qualitatively similar finding that F^{14}C of OC extracted in O_2 at 200°C was smaller than F^{14}C of OC extracted in O_2 at higher temperature for samples collected from an urban and rural site in the Switzerland and from the Los Angeles Basin, USA. ~~To our best knowledge, these are the first ^{14}C measurements of the more volatile fraction of OC and we~~ We can unambiguously conclude from ^{14}C measurements of mvOC and OC that mvOC is more fossil than OC in six Chinese cites. The fraction of non-fossil carbon in mrOC (f_{nf}(mrOC)) is calculated by the differences between OC and mvOC using the isotope mass balance. Since mvOC is only a small fraction of OC, f_{nf}(mrOC) is very similar to f_{nf}(OC).

Primary OC from vehicular emissions is generally more volatile (i.e., less refractory) than OC from biomass burning, which is in line with the ambient results presented. For example, Grieshop et al. (2009c) constrains the volatility distribution of primary OA from a diesel engine and wood burning using measurements of TD coupled to aerosol mass spectrometer and found that OA from wood burning is less volatile than from diesel exhaust. Chen et al. (2007) measured OC/EC from fresh biomass burning emissions and found that high-temperature OC fractions (desorbed from 450 °C to 550 °C) is the major fraction of OC, in contrast to gasoline and diesel exhausts where OC fractions desorbed at temperature lower than 250 °C are more abundant (Watson et al., 1994; Chow et al., 2004). Zhu et al. (2010, 2014) also found that OC desorbed at 140 °C is the major fraction of OC in fresh vehicle emissions in tunnel experiments. A more recent study of Masalaite et al. (2017) found that OC desorbed at 200 °C in He has higher contributions from vehicular emissions than OC desorbed at higher temperature (250–350 °C) at three sites (urban, coastal and forest) in Lithuania, based on δ^{13}C of OC desorbed at different temperature step. However, the conclusions of this study remained qualitative, because δ^{13}C of organic carbon can be changed significantly by isotopic fractionation during atmospheric processing, whereas the ^{14}C source apportionment used in our study is independent of atmospheric processing.

By comparing $(mvOC/OC)_{fossil}$ (i.e., the fraction of $mvOC_{fossil}$ in OC_{fossil}) and $(mvOC/OC)_{nf}$, we can get a measure of the volatility of OC from fossil and non-fossil sources, respectively:

$$\frac{(\mathrm{mvOC/OC})_{\mathrm{fossil}}}{(\mathrm{mvOC/OC})_{\mathrm{nf}}} = \frac{\mathrm{mvOC_{fossil}}/\mathrm{mvOC_{nf}}}{\mathrm{OC_{fossil}}/\mathrm{OC_{nf}}} = \frac{\frac{1}{f_{nf}\,(mvOC)} - 1}{\frac{1}{f_{nf}\,(OC)} - 1}. \tag{13}$$

As f_{nf}(mvOC) is smaller than f_{nf}(OC), this is equivalent to (mvOC/OC)$_{\mathrm{fossil}}$ > (mvOC/OC)$_{\mathrm{nf}}$ (Eq. 13). That is, OC from fossil sources contains a larger more volatile fraction than OC from non-fossil sources. This is true for all studied cities, despite the variation of f_{nf}(mvOC) and f_{nf}(OC) in different cities. (mvOC/OC)$_{\mathrm{fossil}}$ (14 ± 6.6 %; 3.7 %–28 %) is consistently higher and more variable than (mvOC/OC)$_{\mathrm{nf}}$ (7.5 ± 2.9 %; 2.6 %–11.6 %; Fig. 4b). (mvOC/OC)$_{\mathrm{fossil}}$ and (mvOC/OC)$_{\mathrm{nf}}$ in general tracks the variation of mvOC/OC, except that (mvOC/OC)$_{\mathrm{fossil}}$ for Chongqing (28% for Chongqing-H and 21% for Chongqing-L) is much higher than the other sites (averaged 12 %). When comparing the mvOC/OC within each city, it is found that (mvOC/OC)$_{\mathrm{fossil}}$ changes more strongly between H and L samples than (mvOC/OC)$_{\mathrm{nf}}$, indicated by the bigger absolute differences of (mvOC/OC)$_{\mathrm{fossil}}$ between H and L samples than that of (mvOC/OC)$_{\mathrm{nf}}$ ~~(Fig. 4b)~~. Correlations between f_{nf}(mvOC) and f_{nf}(OC), and between f_{nf}(mvOC) and f_{bb}(EC) are examined. f_{nf}(mvOC) correlates more closely with f_{nf}(OC) (r^2 = 0.89) than with f_{bb}(EC) (r^2 = 0.62) (Fig. 5). ~~This suggests that primary combustion sources including biomass burning and fossil fuel combustion (i.e., EC sources) can not fully explain the variation of f_{nf}(mvOC), and indicates the importance of secondary formation of mvOC and/or other non-fossil contribution to mvOC besides primary biomass burning.~~

It is likely that some of mvOC are of secondary origin, since SOC is formed in the atmosphere and subsequently condenses onto the aerosol particles (Hallquist et al., 2009; Jimenez et al., 2009). It has been shown that SOC formed in chambers initially desorbed at relatively low temperatures (e.g., 200 °C) (Holzinger et al., 2010; Salo et al., 2011; Meusinger et al., 2017; Gkatzelis et al., 2018). However, there is also evidence that the formation of highly oxidized low-volatile compounds can occur in SOA formation (Ehn et al., 2014). We thus compared concentrations and sources of SOC to those of mvOC. SOC concentrations and f_{fossil}(SOC) are estimated based on the ^{14}C-apportioned OC and EC in combination with p values of 0–1 (Sect. 2.4). Where δ^{13}C measurements were available for high-volume filter samples (Beijing, Shanghai and Guangzhou), we compare the SOC concentrations and f_{fossil}(SOC) derived from p values of 0–1 with p values constrained by δ^{13}C. In these three cities, SOC concentrations and f_{fossil}(SOC) without constraints of p value (0–1) is very similar to that with constraints of p value using δ^{13}C, only with relatively larger uncertainties (Fig. 6). This indicates that the unconstrained p-values does not lead to significant bias in SOC concentrations and f_{fossil}(SOC) and the main gain in using δ^{13}C is currently a decrease in uncertainty.

When choosing p randomly from 0 to 1, the calculated median f_{fossil}(SOC) is smaller than 0 for samples in Chongqing, reflecting negative SOC$_{\mathrm{fossil}}$ values. Since SOC$_{\mathrm{fossil}}$ is calculated by subtracting POC$_{\mathrm{fossil}}$ from OC$_{\mathrm{fossil}}$, this indicates POC$_{\mathrm{fossil}}$ is overestimated in Chongqing. Because the primary OC/EC ratio is higher for coal (r_{coal}) than vehicle (r_{vehicle}) emissions, an overestimate of POC$_{\mathrm{fossil}}$ is the direct result of overestimated p values, i.e. a too high fraction of coal burning in EC$_{\mathrm{fossil}}$ (Eq.

11). Chongqing is in southern China, where there is no official heating using coal in winter and smaller contribution of coal combustion is expected than in northern China. Further, earlier studies found that vehicle emissions contribute more to EC than coal combustion in Chongqing (Chen et al., 2017). We thus tried to lower p values to 0–0.5. Lower p values lead to higher f_{fossil}(SOC) (Fig. 6c) and to a lesser extent higher SOC concentrations (Fig. 6b). For Chongqing, we took p from 0–0.5 as a conservative estimate. For other cities except Chongqing, we kept p values of 0–1 due to the very similar f_{fossil}(SOC) and SOC concentrations derived from p values with and without constrains by δ^{13}C, especially for the two southern cities in China, e.g., Shanghai and Guangzhou.

f_{fossil}(mvOC) ranged from 45 % to 78 %, with an average of 59 %, whereas f_{fossil}(SOC) ranged from 10 % to 70 %, averaged 43 %. f_{fossil}(mvOC) is always larger than f_{fossil}(SOC) (Fig. 6c), showing that mvOC is more fossil than SOC. However, both SOC and mvOC have a larger contribution of fossil sources than the total OC. The smallest differences between f_{fossil}(SOC) and f_{fossil}(mvOC) are found in Beijing for both samples Beijing-H and Beijing-L with the absolute difference of 3 % and 2 %, respectively, within the uncertainty of the measurements. Much higher differences are found in other cities, with the absolute differences ranging from 13 % to 35 %, well outside the measurement uncertainties.

Median values for SOC, $\mathrm{SOC_{fossil}}$ and $\mathrm{SOC_{nf}}$ are very close to their mean values (Fig. S6, Tables S7, S8). To compare with mvOC, here we use mean (± SD) as well for SOC, $\mathrm{SOC_{fossil}}$ and $\mathrm{SOC_{nf}}$. Lowest SOC concentrations are found to be 2.95 μg m^{-3} for Guangzhou-L and highest to be 35.9 μg m^{-3} for Beijing-H. SOC concentrations (15.4 ± 9.0 μg m^{-3}) are consistently higher than that of mvOC (3.3 ± 2.2 μg m^{-3}, Fig. 6a), showing that the contribution of SOC to total OC is considerably larger than that of mvOC. The major fraction of SOC has desorption temperatures above 200 °C and falls into our operationally defined more refractory OC. $\mathrm{SOC_{fossil}}$ ranged from 0.90 to 25.3 μg m^{-3}, with an average of 6.8 ± 6.4 μg m^{-3}, which is consistently higher than $\mathrm{mvOC_{fossil}}$ ranging from 0.5 to 5.4 μg m^{-3} with an average of 2.1 ± 1.4 μg m^{-3} (Table S6). $\mathrm{mvOC_{nf}}$ is smaller than $\mathrm{SOC_{nf}}$ as well (Fig. S7), averaged $\mathrm{mvOC_{nf}}$ concentrations (1.5 ± 1.1 μg m^{-3}) is only 1/5 of that $\mathrm{SOC_{nf}}$ (8.5 ± 5 μg m^{-3}).

We examined the correlation between mvOC and SOC from non-fossil sources ($\mathrm{mvOC_{nf}}$ vs. $\mathrm{SOC_{nf}}$) and from fossil sources ($\mathrm{mvOC_{fossil}}$ vs. $\mathrm{SOC_{fossil}}$). Comparing absolute concentrations between different cities and pollution levels is expected to result in reasonably positive correlations for all species, because it can be expected that all carbon fractions are higher in polluted cities than in clean cities. However, it is still interesting to compare the correlation coefficients relative to one another. $\mathrm{mvOC_{nf}}$ includes primary and secondary mvOC from non-fossil sources. Good correlation was found between $\mathrm{mvOC_{nf}}$ and $\mathrm{SOC_{nf}}$ (r^2 = 0.87, bootstrapped 95% confidence interval: (0.21, 0.94); Fig. 7), which is not significantly different ~~larger than~~ from the correlation between $\mathrm{mvOC_{nf}}$ and $\mathrm{POC_{bb}}$ (r^2 = 0.71, bootstrapped 95% confidence interval: (0.0.60, 0.99)). ~~This indicates that secondary formation of OC from non-fossil sources explains more of the variation of $\mathrm{mvOC_{nf}}$ than primary biomass burning. However,~~ $\mathrm{SOC_{nf}}$ is estimated by subtracting primary OC from biomass burning ($\mathrm{POC_{bb}}$) from $\mathrm{OC_{nf}}$, where $\mathrm{POC_{bb}}$ is estimated by multiplying $\mathrm{EC_{bb}}$ with the OC/EC ratio of fresh biomass burning plumes

(r_{bb}) (Eq. 7). Due to the large uncertainty in r_{bb}, separation between POC_{bb} and SOC_{nf} is rather uncertain, and ~~The~~ the r^2 for a correlation of $mvOC_{nf}$ and SOC_{nf} is therefore affected by r_{bb}. For example, with lower r_{bb} of 3 (mean), the correlation between SOC_{nf} and $mvOC_{nf}$ is stronger ($r^2 = 0.92$) than for our best estimate of r_{bb} (4) ($r^2 = 0.87$). For r_{bb} of 5, it is slightly weaker ($r^2 = 0.76$, Fig S8).~~, but overall r^2 is not very sensitive to reasonable variations in r_{bb}. Thus, our choice of r_{bb} will not change our conclusion that SOC_{nf} correlates well with $mvOC_{nf}$., and the correlation is stronger than that between POC_{bb} and $mvOC_{nf}$.~~ OC_{nf}, the sum of POC_{bb} and SOC_{nf}, is well-constrained by $F^{14}C_{OC}$ and not affected by r_{bb}. $mvOC_{nf}$ correlates ~~more~~ strongly with OC_{nf} ($r^2 = 0.91$)~~ than with SOC_{nf} ($r^2 = 0.87$) or POC_{bb} ($r^2 = 0.71$)~~, suggesting strong impacts on the variability of $mvOC_{nf}$ from non-fossil emissions including ~~on the variability of $mvOC_{nf}$, where~~ the secondary formation from non-fossil sources ~~VOCs explains more of the variation than~~ and primary biomass burning emissions.

SOC_{fossil} is produced by the oxidation of VOCs from fossil origins, including coal combustion and vehicle emissions, whereas $mvOC_{fossil}$ can have both primary and secondary sources. No correlation is found between $mvOC_{fossil}$ and SOC_{fossil} ($r^2 = 0.01$, Fig. 7c), implying that in cities or pollution conditions characterized by high concentrations of fossil SOC, $mvOC_{fossil}$ is not concurrently elevated. However, demonstrated by the good correlation between POC_{fossil} and $mvOC_{fossil}$ ($r^2 = 0.69$; Fig. 7c) we ~~can~~ conclude that primary fossil sources may play an important role on the variation of $mvOC_{fossil}$. Larger f_{fossil}(mvOC) than f_{fossil}(SOC) also indicate that fossil sources are associated more with mvOC than SOC. In Fig. 7c there are two outli~~n~~er data points ~~of~~ from sample Beijing-H with strongly elevated SOC_{fossil} and lower POC_{fossil} (shown in red circle and diamond, respectively). The highest $SOC_{fossil}/POC_{fossil}$ ratio (3.1) is found in Beijing-H, suggesting the largest fossil SOC formation during polluted days in Beijing compared to clean days in Beijing (Beijing-L with $SOC_{fossil}/POC_{fossil}$ ratio of 1.4) and samples in other cities (average $SOC_{fossil}/POC_{fossil}$ ratio of 0.7). This is also found in an early study that during winter 2013, $SOC_{fossil}/POC_{fossil}$ ratios in Beijing (with an average of 4.2) were much higher than those in Xi'an, Shanghai and Guangzhou (average $SOC_{fossil}/POC_{fossil}$ ratio of 1.3) (Zhang et al., 2015). This pollution event of Beijing-H is thus not included in the regression.

4 Discussion

In this study, samples are collected on a single bare-quartz (BQ) filters. mvOC may be influenced by absorption of organic vapors to the quartz fibers (positive sampling artifact). In ~~an~~other words, the measured mvOC in the earlier discussion include particulate mvOC and gaseous carbon adsorbed to the quartz filters that can also be desorbed from the filters up to 200 °C. This artifact can be estimated by using a backup quartz filter behind the BQ filter (quartz behind quartz, QBQ). The QBQ filter is assumed to be exposed to the same organic vapor concentrations as the front BQ filter and the carbon measured on the QBQ filter is mainly due to adsorbed organic vapor and can serve as an estimate of the positive artifact (Chow et al., 2010; Zhu et al., 2012).

Without the QBQ back filters in this study, we estimate the particulate fraction of mvOC ($X_{\mathrm{p\_mvOC}}$) on the BQ filters using the OC fractions measured by the thermal/optical carbon analyzer in combination with an empirical volatility basis set (VBS) model, following the method of Ma et al. (2016) (Supplement ~~S3~~S4). The VBS bins the organic aerosol (OA) compounds according to the effective saturation concentrations (C^*). For example, if C^* is equal to the concentrations of organic aerosols (C_{OA}), then 50 % of OA mass will be in the particle phase (Donahue et al., 2006). Ma et al. (2016) provide an empirical C^* values for each desorption temperature corresponding to the measured particulate fraction on the filter, determined by the comparison of BQ and QBQ filters. They show that these empirical C^* values ($10^{1.6}$ for $\mathrm{OC_{140°C}}$, $10^{1.1}$ for $\mathrm{OC_{280°C}}$, $10^{0.6}$ for $\mathrm{OC_{480°C}}$, $10^{0.1}$ for $\mathrm{OC_{580°C}}$, where the subscript refers to the desorption temperature of the IMPROVE_A protocol) are useful to predict particulate fractions for various OC loadings and sampling environments. Assuming OA/OC mass ratio is of 1.8 for urban environment (Xing et al., 2013), the particulate fraction of the collected OC for each of the four IMPROVE_A temperature steps i ($X_{\mathrm{p}i}$) can be estimated as a function of OC concentration, as shown in Fig. 8a. The particulate fraction of OC increases considerably from $\mathrm{OC_{140°C}}$ to $\mathrm{OC_{580°C}}$ and with increasing OC concentration. The desorption temperature for mvOC is 200 °C, falling within the 140 °C for $\mathrm{OC_{140°C}}$ and 280 °C for $\mathrm{OC_{280°C}}$. We thus estimated the $X_{\mathrm{p\_mvOC}}$ will fall within the X_{p1} for $\mathrm{OC_{140°C}}$ and X_{p2} for $\mathrm{OC_{280°C}}$. Particulate fraction of mvOC is estimated by interpolating the particulate fraction of $\mathrm{OC_{140°C}}$, $\mathrm{OC_{280°C}}$ (Fig. 8a). $X_{\mathrm{p\_mvOC}}$ ranged from 0.54 for sample winter-L with the lowest OC concentration of 15 μg $\mathrm{m^{-3}}$ to 0.79 for sample Beijing-H with the highest OC concentration of 50 μg $\mathrm{m^{-3}}$ (Fig. 8b). However, for our study we consider this is a lower estimate of particulate fraction of mvOC (i.e., higher limits of the positive artifact):

i. Our sampling duration (24 h) is much longer than that of Ma et al (2016) which is 45 min or 1 h. With longer sampling duration, the loading on the quartz filter of both particulate OC and adsorbed organic vapors increase initially, however, the latter will reach a saturation point and level out. Thus, the percent bias by the adsorbed organics is smaller for longer sampling duration (Turpin et al., 2000). For example, Turpin et al. (1994) found that the loading of adsorbed organics reached to around 1.7 μg/ $\mathrm{cm^2}$ and remained constant after 200 min of sampling time, but the aerosol loading increased linearly with the sampling time.

ii. The empirically determined C^* is affected by the sampling conditions, for example, temperature. The C_i^* are defined at 300 K, higher than the average temperature in winter in China. The lower temperature drives the semi-volatile OC into the particle phase and leads to higher particulate fraction of each OC fraction (Donahue et al., 2006).

iii. The adsorption of organic vapors is also influenced by the face velocity (the volumetric flow rate divided by the exposed filter area). As the face velocity decreases, the adsorption of organic gaseous species increases (McDow and Huntzicker, 1990; Turpin et al., 2000; Viana et al., 2006). In this study, most of samples were collected using high-volume samplers (HiVol) with a flow rate of 1 $\mathrm{m^3\ min^{-1}}$, including samples collected in Xi'an, Beijing, Guangzhou and Shanghai. Only samples in Taiyuan and Chongqing were collected using mini-volume samplers (MiniVol) at a flow rate of 5 L $\mathrm{min^{-1}}$. The face velocities for HiVol and MiniVol sampler were 42 cm $\mathrm{s^{-1}}$ and 7 cm $\mathrm{s^{-1}}$, respectively. Turpin et al. (1994) found that the apparent OC concentrations on the front quartz filter were 22%

greater with a face velocity of 20 cm s^{-1} than those with a face velocity of 40 cm s^{-1}. A more recent study of Kim et al. (2016) found the positive artifacts for OC using sampler with the face velocity of 42 cm s^{-1} is 7.2 %, which is smaller than 12.2% using sampler of a face velocity of 24 cm s^{-1} in spring and fall of 2014 in Korea. We do not take this into consideration and apply the same C_i^* for HiVol and MiniVol samples, due to the lake of C_i^* for different face velocities.

Due to the lack of information on how sampling duration, temperature, and face velocity affect the C^* for each carbon fraction, we treat the particulate fraction in Fig. 8b as a rough estimate. But with long sampling duration, low temperature and high face velocities for most of samples as well as high OC concentrations in winter in this study, the particulate fraction of mvOC on the collected filters should be considerably higher than the estimate derived from VBS. For example, Cheng and He (2015) found that the positive artifacts to OC was lowest (~10 %) in winter, much lower than that in summer (~23 %) in Beijing, China. With the same face velocity of ~10 cm s^{-1}, the smaller positive artifacts in winter than that in summer can be attributed to higher OC concentrations (35 µg m^{-3} in winter vs. 12 µg m^{-3} in summer) and lower temperatures in winter. We consider the positive sampling artifact in this study is small and the collected mvOC on the bare quartz filter is dominated by the particulate mvOC.

Even thought the positive artifact introduced by the adsorbed organic vapors is likely small, it is worth to investigate its potential effect on the ^{14}C results. The measured $F^{14}C_{(mvOC)}$ on the BQ filter can be explained by the $F^{14}C$ of particulate mvOC ($F^{14}C_{(p\_mvOC)}$) and adsorbed organic vapors ($F^{14}C_{(g\_mvOC)}$). The $F^{14}C_{(p\_mvOC)}$ can be calculated as:

$$F^{14}C_{(p\_mvOC)} = \frac{F^{14}C_{(mvOC)} - (1 - X_{p\_mvOC}) \times F^{14}C_{(g\_mvOC)}}{X_{p\_mvOC}}, \tag{14}$$

where X_{p_mvOC} is the estimated particulate fraction of mvOC as shown in Fig. 8b, which is a very much lower limit as discussed earlier. ($1 - X_{p\_mvOC}$) is thus an estimate of positive artifact. How close the measured $F^{14}C_{(mvOC)}$ to the $F^{14}C_{(p\_mvOC)}$ depends on the $F^{14}C_{(g\_mvOC)}$.

Therefore, we conducted a sensitivity study based on the following assumption: the positive artifact is dominated by semi-volatile gases that actively partition between gas and particle phase. As the base case, we assume that $F^{14}C_{(g\_mvOC)} = F^{14}C_{(mvOC)}$ and consider extreme cases of $F^{14}C_{(g\_mvOC)} = 1.5 \times F^{14}C_{(mvOC)}$ and $F^{14}C_{(g\_mvOC)} = 0.5 \times F^{14}C_{(mvOC)}$, i.e. a variation of ± 50 %. This allows $F^{14}C$ values for the adsorbed gas phase as low as for EC and higher than for OC in most cases. When the lower limit of $F^{14}C_{(g\_mvOC)}$ is used (50% lower than $F^{14}C_{(mvOC)}$), the f_{nf}(p_mvOC), calculated by dividing $F^{14}C_{(p\_mvOC)}$ with $F^{14}C_{nf}$, ~~are~~ is ~~from~~ 0.04 to 0.19 (absolute value)~~,~~ higher than f_{nf}(mvOC) (Fig. 8), but still lower than f_{nf}(OC) and f_{nf}(SOC) for most of samples, at least for highly-polluted (H) samples with higher particulate fraction of mvOC. ~~That is~~Consequently, our conclusion that mvOC is more fossil than OC and SOC is still valid for most of samples, especially since this sensitivity study assumes (i) an upper limit of the positive artifact as well as (ii) a very large maximum difference between the $F^{14}C$ of the adsorbed gas phase and the semi-volatile particle phase. The upper limit of f_{nf}(p_mvOC) corresponds to a semi-volatile gas phase with F^{14}C values in the range of EC, which is probably not realistic.

5 Conclusions

Radiocarbon measurements are conducted for EC and~~,~~ OC ~~and mvOC~~ of PM$_{2.5}$ samples collected in six Chinese megacities at wintertime. In addition, ~~To our best knowledge, this is the first time that~~ the sources of ~~more volatile OC~~mvOC are measured unambiguously using ^{14}C.~~–~~ mvOC is isolated by desorbing organics in He at 200 °C using our custom-made aerosol combustion system with reproducibility of ~5%. This new isolation method is evaluated by comparing with the OC1 fraction of the EUSAAR_2 protocol using a thermal/optical analyzer. The mvOC amount agrees very well with the OC1, despite the different heating rate and length of temperature step, showing the representativeness of the isolated mvOC. The measured F^{14}C$_{(\mathrm{mvOC})}$ for a combined sample (0.529 ± 0.007), which consists of 3 individual daily filters, is quite similar to the weighted average of the individual filters. This further validates our isolation method for mvOC that the F^{14}C$_{(\mathrm{mvOC})}$ is representative of the combined samples. With long sampling duration, low temperature and high face velocities as well as high OC concentrations in winter in this study, the positive artifacts to mvOC should be relatively small and play a limited role on the F^{14}C$_{(\mathrm{mvOC})}$.

mvOC/OC ranges from 3 % to 15 %, with an average of 10.5 ± 3.3 %. The ambient samples in this study have a smaller mvOC/OC than ambient samples from other places, and have a much smaller mvOC fraction than fresh source samples, likely due to the effects from atmospheric aging processes. mvOC/OC from fossil sources averages 14 ± 6.6 %, consistently higher and more variable than that from non-fossil sources (7.5 ± 2.9 %). ~~-~~That is, OC from fossil sources contains a larger more volatile fraction than that from non-fossil sources.

The non-fossil contribution to mvOC, OC and EC (f_{nf}(mvOC), f_{nf}(OC), f_{bb}(EC)) varies significantly among samples in different sites: the lowest values are always found in Taiyuan, and the highest values in Chongqing. This implies that different pollution patterns exist in individual Chinese cities. Despite the variations of f_{nf}(mvOC), f_{nf}(OC), f_{bb}(EC) in different cities, mvOC is more fossil than OC and less fossil than EC in all locations. The fossil contribution to mvOC, OC and EC are on average 59 ± 11 %, 48 ± 16 % and 73 ± 9 %, respectively. Higher fossil contribution to mvOC than to OC is consistent with conclusions from δ^{13}C of OC desorbed at different temperatures for ambient samples in other locations ~~(Masalaite et al., 2017, 2018)~~. f_{nf}(mvOC) correlates better with f_{nf}(OC) (r^2 = 0.89) than f_{bb}(EC) (r^2 = 0.62) ~~(Fig. 5)~~. ~~This suggests that primary combustion sources including biomass burning and fossil fuel combustion (i.e., EC sources) can not fully explain the variation of f_{nf}(mvOC), and indicates the importance of secondary formation of mvOC and/or other non-fossil contribution to mvOC besides primary biomass burning.~~

SOC concentrations and sources are modeled based on the ^{14}C-apportioned OC and EC. SOC concentrations (15.4 ± 9.0 µg m^{-3}) are consistently higher than that of mvOC (3.3 ± 2.2 µg m^{-3}), showing that the contribution of SOC to total OC is considerably larger than that of mvOC. A major fraction of SOC has desorption temperatures above 200 °C and falls into our operationally defined mrOC. mvOC is more fossil than SOC. The relative contribution of fossil sources to mvOC is on average 59 % (range: 45 %–78 %~~; range~~), which is higher than that to SOC (43 %; 10 %–70 %).

Good correlation is found between $mvOC_{nf}$ and OC_{nf} (r^2 = 0.91). ~~SOC_{nf} (r^2 = 0.87, Fig. 7), which is stronger than the correlation between $mvOC_{nf}$ and POC_{bb} (r^2 = 0.71).~~ This indicates strong impacts on the variability of $mvOC_{nf}$ from non-fossil emissions, including the ~~that~~ secondary formation of OC from non-fossil sources ~~has a higher contribution than~~and primary biomass burning ~~to the variation of $mvOC_{nf}$~~. The variation of $mvOC_{fossil}$ is mainly explained by a good correlation with POC_{fossil} (r^2 = 0.69) and no correlation is found between $mvOC_{fossil}$ and SOC_{fossil} (r^2 = 0.01). This indicates that primary mvOC from fossil sources may play an important role in the variation of $mvOC_{fossil}$.

Author contributions

UD, RJH, HN, and JC conducted the study design. HN, HD, WD, and JZ carried out the experimental work. HN, UD, AAB, and HAJM analysed data. HN wrote the manuscript. HN, UD, and RJH interpreted data and edited the manuscript. HN prepared display items. All authors commented on and discussed the manuscript.

Competing interests

The authors declare that they have no conflict of interest.

Acknowledgments

This work was supported by the National Key Research and Development Program of China (no. 2017YFC0212701), the National Natural Science Foundation of China (NSFC; no. 91644219 and 41877408), and a KNAW project (no. 530-5CDP30). The authors acknowledge the financial support from the Gratama Foundation. Special thanks are given to Dipayan Paul, Marc Bleeker and Henk Been for their help with the AMS measurements at CIO, and to Dicky van Zonneveld for her help with ^{14}C data correction at CIO.

References

Agrios, K., Salazar, G., and Szidat, S.: A continuous-flow gas interface of a thermal/optical analyzer With ^{14}C AMS for source apportionment of atmospheric aerosols, Radiocarbon, 59, 921-932, 10.1017/RDC.2016.88, 2016.

Andersson, A.: A systematic examination of a random sampling strategy for source apportionment calculations, Sci. Total Environ., 412, 232–238, 2011.

Andersson, A., Deng, J., Du, K., Zheng, M., Yan, C., Sköld, M., and Gustafsson, Ö.: Regionally-varying combustion sources of the January 2013 severe haze events over eastern China, Environ. Sci. Technol., 49, 2038–2043, 2015.

Bond, T.C., Doherty, S.J., Fahey, D.W., Forster, P.M., Berntsen, T., DeAngelo, B.J., Flanner, M.G., Ghan, S., Kärcher, B., Koch, D., Kinne, S., Kondo, Y., Quinn, P. K., Sarofim, M. C., Schultz, M. G., Schulz, M., Venkataraman, C., Zhang, H., Zhang, S., Bellouin, N., Guttikunda, S. K., Hopke, P. K., Jacobson, M. Z., Kaiser, J. W., Klimont, Z., Lohmann, U., Schwarz, J. P., Shindell, D., Storelvmo, T., Warren, S. G., and Zender, C. S.:Bounding the role of black carbon in the climate system: a scientific assessment. J. Geophys. Res.-Atmos., 118, 5380-5552, https://doi.org/10.1002/jgrd.50171, 2013

Burtscher, H., Baltensperger, U., Bukowiecki, N., Cohn, P., Hüglin, C., Mohr, M., Matter, U., Nyeki, S., Schmatloch, V., Streit, N., and Weingartner, E.: Separation of volatile and non-volatile aerosol fractions by thermodesorption: instrumental development and applications, J. Aerosol Sci., 32, 427-442, 2001.

Cao, J. J., Lee, S. C., Chow, J. C., Watson, J. G., Ho, K. F., Zhang, R. J., Jin, Z. D., Shen, Z. X., Chen, G. C., Kang, Y. M., Zou, S. C., Zhang, L. Z., Qi, S. H., Dai, M. H., Cheng, Y., and Hu, K.: Spatial and seasonal distributions of carbonaceous aerosols over China, J. Geophys. Res.-Atmos., 112, 2007.

Cao, J.-J., Zhu, C.-S., Tie, X.-X., Geng, F.-H., Xu, H.-M., Ho, S. S. H., Wang, G.-H., Han, Y.-M., and Ho, K.-F.: Characteristics and sources of carbonaceous aerosols from Shanghai, China, Atmos. Chem. Phys., 13, 803-817, https://doi.org/10.5194/acp-13-803-2013, 2013.

Cao, L.-M., Huang, X.-F., Li, Y.-Y., Hu, M., and He, L.-Y.: Volatility measurement of atmospheric submicron aerosols in an urban atmosphere in southern China, Atmos. Chem. Phys., 18, 1729-1743, https://doi.org/10.5194/acp-18-1729-2018, 2018.

Cavalli, F., Viana, M., Yttri, K. E., Genberg, J., and Putaud, J.-P.: Toward a standardised thermal-optical protocol for measuring atmospheric organic and elemental carbon: the EUSAAR protocol, Atmos. Meas. Tech., 3, 79-89, https://doi.org/10.5194/amt-3-79-2010, 2010.

Chen, L.-W. A., Moosmüller, H., Arnott, W. P., Chow, J. C., Watson, J. G., Susott, R. A., Babbitt, R. E., Wold, C. E., Lincoln, E. N., and Hao, W. M.: Emissions from laboratory combustion of wildland fuels: emission factors and source profiles, Environ. Sci. Technol., 41, 4317-4325, 2007.

Chen, Y., Xie, S.-D., Luo, B., and Zhai, C.-Z.: Particulate pollution in urban Chongqing of southwest China: historical trends of variation, chemical characteristics and source apportionment, Sci. Total Environ., 584-585, 523-534, https://doi.org/10.1016/j.scitotenv.2017.01.060, 2017.

Chow, J. C., Watson, J. G., Kuhns, H., Etyemezian, V., Lowenthal, D. H., Crow, D., Kohl, S. D., Engelbrecht, J. P., and Green, M. C.: Source profiles for industrial, mobile, and area sources in the Big Bend Regional Aerosol Visibility and Observational study, Chemosphere, 54, 185-208, 10.1016/j.chemosphere.2003.07.004, 2004.

Chow, J. C., Watson, J. G., Chen, L.-W. A., Chang, M. O., Robinson, N. F., Trimble, D., and Kohl, S.: The IMPROVE_A temperature protocol for thermal/optical carbon analysis: maintaining consistency with a long-term database, J. Air Waste Manage., 57, 1014–1023, 2007.

Chow, J. C., Watson, J. G., Chen, L.-W. A., Rice, J., and Frank, N. H.: Quantification of $PM_{2.5}$ organic carbon sampling artifacts in US networks, Atmos. Chem. Phys., 10, 5223-5239, https://doi.org/10.5194/acp-10-5223-2010, 2010.

Donahue, N. M., Robinson, A. L., Stanier, C. O., and Pandis, S. N.: Coupled partitioning, dilution, and chemical aging of semivolatile organics, Environ. Sci. Technol., 40, 2635-2643, 2006.

Donahue, N. M., Robinson, A. L., and Pandis, S. N.: Atmospheric organic particulate matter: from smoke to secondary organic aerosol, Atmos. Environ., 43, 94-106, http://dx.doi.org/10.1016/j.atmosenv.2008.09.055, 2009.

Donahue, N. M., Epstein, S. A., Pandis, S. N., and Robinson, A. L.: A two-dimensional volatility basis set: 1. organic-aerosol mixing thermodynamics, Atmos. Chem. Phys., 11, 3303-3318, https://doi.org/10.5194/acp-11-3303-2011, 2011.

Dusek, U., Ten Brink, H., Meijer, H., Kos, G., Mrozek, D., Röckmann, T., Holzinger, R., and Weijers, E.: The contribution of fossil sources to the organic aerosol in the Netherlands, Atmos. Environ., 74, 169-176, 2013.

Dusek, U., Monaco, M., Prokopiou, M., Gongriep, F., Hitzenberger, R., Meijer, H. A. J., and Röckmann, T.: Evaluation of a two-step thermal method for separating organic and elemental carbon for radiocarbon analysis, Atmos. Meas. Tech., 7, 1943-1955, https://doi.org/10.5194/amt-7-1943-2014, 2014.

Dusek, U., Hitzenberger, R., Kasper-Giebl, A., Kistler, M., Meijer, H. A. J., Szidat, S., Wacker, L., Holzinger, R., and Röckmann, T.: Sources and formation mechanisms of carbonaceous aerosol at a regional background site in the Netherlands: insights from a year-long radiocarbon study, Atmos. Chem. Phys., 17, 3233-3251, https://doi.org/10.5194/acp-17-3233-2017, 2017.

Ehn, M., Thornton, J. A., Kleist, E., Sipilä, M., Junninen, H., Pullinen, I., Springer, M., Rubach, F., Tillmann, R., Lee, B., Lopez-Hilfiker, F., Andres, S., Acir, I.-H., Rissanen, M., Jokinen, T., Schobesberger, S., Kangasluoma, J., Kontkanen, J., Nieminen, T., Kurtén, T., Nielsen, L. B., Jørgensen, S., Kjaergaard, H. G., Canagaratna, M., Maso, M. D., Berndt, T., Petäjä, T., Wahner, A., Kerminen, V.-M., Kulmala, M., Worsnop, D. R., Wildt, J., and Mentel, T. F.: A large source of low-volatility secondary organic aerosol, Nature, 506, 476-479, 2014.

Fang, W., Andersson, A., Zheng, M., Lee, M., Holmstrand, H., Kim, S.-W., Du, K., and Gustafsson, Ö.: Divergent evolution of carbonaceous aerosols during dispersal of East Asian haze, Sci. Rep., 7, 10422, 2017.

Fuzzi, S., Baltensperger, U., Carslaw, K., Decesari, S., Denier van der Gon, H., Facchini, M. C., Fowler, D., Koren, I., Langford, B., Lohmann, U., Nemitz, E., Pandis, S., Riipinen, I., Rudich, Y., Schaap, M., Slowik, J. G., Spracklen, D. V., Vignati, E., Wild, M., Williams, M., and Gilardoni, S.: Particulate matter, air quality and climate: lessons learned and future needs, Atmos. Chem. Phys., 15, 8217-8299, https://doi.org/10.5194/acp-15-8217-2015, 2015.

Gaston, C. J., Lopez-Hilfiker, F. D., Whybrew, L. E., Hadley, O., McNair, F., Gao, H., Jaffe, D. A., and Thornton, J. A.: Online molecular characterization of fine particulate matter in Port Angeles, WA: Evidence for a major impact from residential wood smoke, Atmos. Environ., 138, 99-107, https://doi.org/10.1016/j.atmosenv.2016.05.013, 2016.

Gkatzelis, G. I., Tillmann, R., Hohaus, T., Müller, M., Eichler, P., Xu, K.-M., Schlag, P., Schmitt, S. H., Wegener, R., Kaminski, M., Holzinger, R., Wisthaler, A., and Kiendler-Scharr, A.: Comparison of three aerosol chemical characterization techniques utilizing PTR-ToF-MS: a study on freshly formed and aged biogenic SOA, Atmos. Meas. Tech., 11, 1481-1500, https://doi.org/10.5194/amt-11-1481-2018, 2018.

Grieshop, A. P., Donahue, N. M., and Robinson, A. L.: Laboratory investigation of photochemical oxidation of organic aerosol from wood fires 2: analysis of aerosol mass spectrometer data, Atmos. Chem. Phys., 9, 2227-2240, https://doi.org/10.5194/acp-9-2227-2009, 2009a.

Grieshop, A. P., Logue, J. M., Donahue, N. M., and Robinson, A. L.: Laboratory investigation of photochemical oxidation of organic aerosol from wood fires 1: measurement and simulation of organic aerosol evolution, Atmos. Chem. Phys., 9, 1263-1277, https://doi.org/10.5194/acp-9-1263-2009, 2009b.

Grieshop, A. P., Miracolo, M. A., Donahue, N. M., and Robinson, A. L.: Constraining the volatility distribution and gas-particle partitioning of combustion aerosols using isothermal dilution and thermodenuder measurements, Environ. Sci. Technol., 43, 4750-4756, 2009c.

Guo, S., Hu, M., Guo, Q., Zhang, X., Zheng, M., Zheng, J., Chang, C. C., Schauer, J. J., and Zhang, R.: Primary sources and secondary formation of organic aerosols in Beijing, China, Environ. Sci. Technol., 46, 9846–9853, 2012.

Guo, S., Hu, M., Zamora, M. L., Peng, J., Shang, D., Zheng, J., Du, Z., Wu, Z., Shao, M., Zeng, L., Molina, M. J., and Zhang, R: Elucidating severe urban haze formation in China, P. Natl. Acad. Sci. USA, 111, 17373-17378, https://doi.org/10.1073/pnas.1419604111, 2014.

Hallquist, M., Wenger, J. C., Baltensperger, U., Rudich, Y., Simpson, D., Claeys, M., Dommen, J., Donahue, N. M., George, C., Goldstein, A. H., Hamilton, J. F., Herrmann, H., Hoffmann, T., Iinuma, Y., Jang, M., Jenkin, M. E., Jimenez, J. L., Kiendler-Scharr, A., Maenhaut, W., McFiggans, G., Mentel, Th. F., Monod, A., Prévôt, A. S. H., Seinfeld, J. H., Surratt, J.

D., Szmigielski, R., and Wildt, J.: The formation, properties and impact of secondary organic aerosol: current and emerging issues, Atmos. Chem. Phys., 9, 5155-5236, https://doi.org/10.5194/acp-9-5155-2009, 2009.

Han, Y. M., Chen, L.W., Huang, R.J., Chow, J. C., Watson, J. G., Ni, H. Y., Liu, S. X., Fung, K. K., Shen, Z. X, Wei, C., Wang, Q. Y., Tian, J., Zhao, Z. Z., Prévôt, A. S. H., and Cao, J. J.: Carbonaceous aerosols in megacity Xi'an, China: implications of thermal/optical protocols comparison, Atmos. Environ., 132, 58–68, 2016.

Heal, M. R.: The application of carbon-14 analyses to the source apportionment of atmospheric carbonaceous particulate matter: a review, Anal. Bioanal. Chem., 406, 81-98, 2014.

Holzinger, R., Williams, J., Herrmann, F., Lelieveld, J., Donahue, N. M., and Röckmann, T.: Aerosol analysis using a Thermal-Desorption Proton-Transfer-Reaction Mass Spectrometer (TD-PTR-MS): a new approach to study processing of organic aerosols, Atmos. Chem. Phys., 10, 2257-2267, https://doi.org/10.5194/acp-10-2257-2010, 2010.

Holzinger, R., Goldstein, A. H., Hayes, P. L., Jimenez, J. L., and Timkovsky, J.: Chemical evolution of organic aerosol in Los Angeles during the CalNex 2010 study, Atmos. Chem. Phys., 13, 10125-10141, https://doi.org/10.5194/acp-13-10125-2013, 2013.

Huang, R. J., Zhang, Y., Bozzeti, C., Ho, K. F., Cao, J. J., Han, Y., Daellenbach, K. R., Slowik, J.G., Platt, S. M., Canonaco, F., Zotter, P., Wolf, R., Pieber, S. M., Bruns, E. A., Crippa, M., Ciarelli, G., Piazzalunga, A., Schwikowski, M., Abbaszade, G., SchnelleKreis, J., Zimmermann, R., An, Z., Szidat, S., Baltensperger, U., El Haddad, I., and Prévôt, A. S. H.: High secondary aerosol contribution to particulate pollution during haze events in China, Nature, 514, 218–222, doi:10.1038/nature13774, 2014.

Hu, D., Bian, Q., Lau, A. K. H., and Yu, J. Z.: Source apportioning of primary and secondary organic carbon in summer $PM_{2.5}$ in Hong Kong using positive matrix factorization of secondary and primary organic tracer data, J. Geophys. Res.-Atmos., 115, 10.1029/2009jd012498, 2010.

Huffman, J. A., Docherty, K. S., Aiken, A. C., Cubison, M. J., Ulbrich, I. M., DeCarlo, P. F., Sueper, D., Jayne, J. T., Worsnop, D. R., Ziemann, P. J., and Jimenez, J. L.: Chemically-resolved aerosol volatility measurements from two megacity field studies, Atmos. Chem. Phys., 9, 7161-7182, https://doi.org/10.5194/acp-9-7161-2009, 2009a.

Huffman, J., Docherty, K., Mohr, C., Cubison, M., Ulbrich, I., Ziemann, P., Onasch, T., and Jimenez, J.: Chemically-resolved volatility measurements of organic aerosol from different sources, Environ. Sci. Technol., 43, 5351-5357, 2009b.

Jacobson, M. C., Hansson, H. C., Noone, K. J., and Charlson, R. J.: Organic atmospheric aerosols: review and state of the science, Rev. Geophys., 38, 267–294, 2000.

Jayne, J. T., Leard, D. C., Zhang, X., Davidovits, P., Smith, K. A., Kolb, C. E., and Worsnop, D. R.: Development of an aerosol mass spectrometer for size and composition analysis of submicron particles, Aerosol Sci. Technol., 33, 49-70, https://doi.org/10.1080/027868200410840, 2000.

Jimenez, J. L., Canagaratna, M. R., Donahue, N. M., Prevot, A. S. H., Zhang, Q., Kroll, J. H., DeCarlo, P. F., Allan, J. D., Coe, H., Ng, N. L., Aiken, A. C., Docherty, K. S., Ulbrich, I. M., Grieshop, A. P., Robinson, A. L., Duplissy, J., Smith, J. D., Wilson, K. R., Lanz, V. A., Hueglin, C., Sun, Y. L., Tian, J., Laaksonen, A., Raatikainen, T., Rautiainen, J., Vaattovaara, P., Ehn, M., Kulmala, M., Tomlinson, J. M., Collins, D. R., Cubison, M. J., Dunlea, J., Huffman, J. A., Onasch, T. B., Alfarra, M. R., Williams, P. I., Bower, K., Kondo, Y., Schneider, J., Drewnick, F., Borrmann, S., Weimer, S., Demerjian, K., Salcedo, D., Cottrell, L., Griffin, R., Takami, A., Miyoshi, T., Hatakeyama, S., Shimono, A., Sun, J. Y., Zhang, Y. M., Dzepina, K., Kimmel, J. R., Sueper, D., Jayne, J. T., Herndon, S. C., Trimborn, A. M., Williams, L. R., Wood, E. C., Middlebrook, A. M., Kolb, C. E., Baltensperger, U., and Worsnop, D. R.: Evolution of organic aerosols in the atmosphere, Science, 326, 1525-1529, 2009.

Keller, A., and Burtscher, H.: Characterizing particulate emissions from wood burning appliances including secondary organic aerosol formation potential, J. Aerosol Sci., 114, 21-30, https://doi.org/10.1016/j.jaerosci.2017.08.014, 2017.

Kim, D., Jung, J., Lee, H., Choi, S.-H., Lee, S., and Oh, S.: Characterization of sampling artifacts in the measurement of carbonaceous particles using high- and low-volume samplers in Daejeon, Korea, Atmos. Environ., 139, 157-166, https://doi.org/10.1016/j.atmosenv.2016.05.029, 2016.

Levin, I., Naegler, T., Kromer, B., Diehl, M., Francey, R. J., Gomez-Pelaez, A. J., Steele, L., Wagenbach, D., Weller, R., and Worthy, D. E.: Observations and modelling of the global distribution and long-term trend of atmospheric $^{14}CO_2$, Tellus B, 62, 26–46, 2010.

Lewis, C. W., Klouda, G. A., and Ellenson, W. D.: Radiocarbon measurement of the biogenic contribution to summertime $PM_{2.5}$ ambient aerosol in Nashville, TN, Atmos. Environ., 38, 6053–6061, 2004.

Lipsky, E. M., and Robinson, A. L.: Effects of dilution on fine particle mass and partitioning of semivolatile organics in diesel exhaust and wood smoke, Environ. Sci. Technol., 40, 155-162, 2006.

Liu, J., Li, J., Ding, P., Zhang, Y., Liu, D., Shen, C., and Zhang, G.: Optimizing isolation protocol of organic carbon and elemental carbon for ^{14}C analysis using fine particulate samples, Atmos. Environ., 154, 9-19, https://doi.org/10.1016/j.atmosenv.2017.01.027, 2017.

Lopez-Hilfiker, F. D., Mohr, C., Ehn, M., Rubach, F., Kleist, E., Wildt, J., Mentel, Th. F., Lutz, A., Hallquist, M., Worsnop, D., and Thornton, J. A.: A novel method for online analysis of gas and particle composition: description and evaluation of a Filter Inlet for Gases and AEROsols (FIGAERO), Atmos. Meas. Tech., 7, 983-1001, https://doi.org/10.5194/amt-7-983-2014, 2014.

Lopez-Hilfiker, F. D., Mohr, C., Ehn, M., Rubach, F., Kleist, E., Wildt, J., Mentel, Th. F., Carrasquillo, A. J., Daumit, K. E., Hunter, J. F., Kroll, J. H., Worsnop, D. R., and Thornton, J. A.: Phase partitioning and volatility of secondary organic aerosol components formed from α-pinene ozonolysis and OH oxidation: the importance of accretion products and other low volatility compounds, Atmos. Chem. Phys., 15, 7765-7776, https://doi.org/10.5194/acp-15-7765-2015, 2015.

Ma, J., Li, X., Gu, P., Dallmann, T. R., Presto, A. A., and Donahue, N. M.: Estimating ambient particulate organic carbon concentrations and partitioning using thermal optical measurements and the volatility basis set, Aerosol Sci. Technol., 50, 638-651, 2016.

Masalaite, A., Holzinger, R., Remeikis, V., Roeckmann, T., and Dusek, U.: Characteristics, sources and evolution of fine aerosol (PM_1) at urban, coastal and forest background sites in Lithuania, Atmos. Environ., 148, 62-76, 2017.

Masalaite, A., Holzinger, R., Ceburnis, D., Remeikis, V., Ulevičius, V., Röckmann, T., and Dusek, U.: Sources and atmospheric processing of size segregated aerosol particles revealed by stable carbon isotope ratios and chemical speciation, Environm. Pollut., 240, 286-296, https://doi.org/10.1016/j.envpol.2018.04.073, 2018.

May, A. A., Presto, A. A., Hennigan, C. J., Nguyen, N. T., Gordon, T. D., and Robinson, A. L.: Gas-particle partitioning of primary organic aerosol emissions: (1) gasoline vehicle exhaust, Atmos. Environ., 77, 128-139, https://doi.org/10.1016/j.atmosenv.2013.04.060, 2013a.

May, A. A., Presto, A. A., Hennigan, C. J., Nguyen, N. T., Gordon, T. D., and Robinson, A. L.: Gas-particle partitioning of primary organic aerosol emissions:(2) diesel vehicles, Environ. Sci. Technol., 47, 8288-8296, 2013b.

McDow, S. R., and Huntzicker, J. J.: Vapor adsorption artifact in the sampling of organic aerosol: Face velocity effects, Atmos. Environ. A.-Gen., 24, 2563-2571, https://doi.org/10.1016/0960-1686(90)90134-9, 1990.

Meusinger, C., Dusek, U., King, S. M., Holzinger, R., Rosenørn, T., Sperlich, P., Julien, M., Remaud, G. S., Bilde, M., Röckmann, T., and Johnson, M. S.: Chemical and isotopic composition of secondary organic aerosol generated by α-pinene ozonolysis, Atmos. Chem. Phys., 17, 6373-6391, https://doi.org/10.5194/acp-17-6373-2017, 2017.

Mohn, J., Szidat, S., Fellner, J., Rechberger, H., Quartier, R., Buchmann, B., and Emmenegger, L.: Determination of biogenic and fossil CO_2 emitted by waste incineration based on $^{14}CO_2$ and mass balances, Bioresource Technol., 99, 6471–6479, 2008.

Mook, W. G. and van der Plicht, J.: Reporting ^{14}C activities and concentrations, Radiocarbon, 41, 227–239, 1999.

Ni, H., Huang, R.-J., Cao, J., Liu, W., Zhang, T., Wang, M., Meijer, H. A. J., and Dusek, U.: Source apportionment of carbonaceous aerosols in Xi'an, China: insights from a full year of measurements of radiocarbon and the stable isotope ^{13}C, Atmos. Chem. Phys., 18, 16363-16383, https://doi.org/10.5194/acp-18-16363-2018, 2018.

Paciga, A., Karnezi, E., Kostenidou, E., Hildebrandt, L., Psichoudaki, M., Engelhart, G. J., Lee, B.-H., Crippa, M., Prévôt, A. S. H., Baltensperger, U., and Pandis, S. N.: Volatility of organic aerosol and its components in the megacity of Paris, Atmos. Chem. Phys., 16, 2013-2023, https://doi.org/10.5194/acp-16-2013-2016, 2016.

Palstra, S. W. and Meijer, H. A.: Biogenic carbon fraction of biogas and natural gas fuel mixtures determined with ^{14}C, Radiocarbon, 56, 7-28, 2014.

Petzold, A., Ogren, J. A., Fiebig, M., Laj, P., Li, S.-M., Baltensperger, U., Holzer-Popp, T., Kinne, S., Pappalardo, G., Sugimoto, N., Wehrli, C., Wiedensohler, A., and Zhang, X.-Y.: Recommendations for reporting "black carbon" measurements, Atmos. Chem. Phys., 13, 8365-8379, https://doi.org/10.5194/acp-13-8365-2013, 2013.

Pöschl, U.: Aerosol particle analysis: challenges and progress, Anal. Bioanal. Chem., 375, 30-32, 2003.

Pöschl, U.: Atmospheric aerosols: composition, transformation, climate and health effects, Angew. Chem. Int. Ed. Engl., 44, 7520-7540, 2005.

Presto, A. A., Gordon, T. D., and Robinson, A. L.: Primary to secondary organic aerosol: evolution of organic emissions from mobile combustion sources, Atmos. Chem. Phys., 14, 5015-5036, https://doi.org/10.5194/acp-14-5015-2014, 2014.

Reimer, P. J., Brown, T. A., and Reimer, R. W.: Discussion: reporting and calibration of post-bomb ^{14}C data, Radiocarbon, 46, 1299–1304, 2004.

Robinson, A. L., Donahue, N. M., Shrivastava, M. K., Weitkamp, E. A., Sage, A. M., Grieshop, A. P., Lane, T. E., Pierce, J. R., and Pandis, S. N.: Rethinking organic aerosols: semivolatile emissions and photochemical aging, Science, 315, 1259-1262, 2007.

Ruff, M., Wacker, L., Gäggeler, H., Suter, M., Synal, H.-A., and Szidat, S.: A gas ion source for radiocarbon measurements at 200 kV, Radiocarbon, 49, 307-314, 2007.

Salazar, G., Zhang, Y. L., Agrios, K., and Szidat, S.: Development of a method for fast and automatic radiocarbon measurement of aerosol samples by online coupling of an elemental analyzer with a MICADAS AMS, Nucl. Instrum. Meth. B, 361, 163-167, https://doi.org/10.1016/j.nimb.2015.03.051, 2015.

Salo, K., Hallquist, M., Jonsson, Å. M., Saathoff, H., Naumann, K.-H., Spindler, C., Tillmann, R., Fuchs, H., Bohn, B., Rubach, F., Mentel, Th. F., Müller, L., Reinnig, M., Hoffmann, T., and Donahue, N. M.: Volatility of secondary organic aerosol during OH radical induced ageing, Atmos. Chem. Phys., 11, 11055-11067, https://doi.org/10.5194/acp-11-11055-2011, 2011.

Shrivastava, M. K., Lipsky, E. M., Stanier, C. O., and Robinson, A. L.: Modeling semivolatile organic aerosol mass emissions from combustion systems, Environ. Sci. Technol., 40, 2671-2677, 2006.

Song, Y., Zhang, Y., Xie, S., Zeng, L., Zheng, M., Salmon, L. G., Shao, M., and Slanina, S.: Source apportionment of $PM_{2.5}$ in Beijing by positive matrix factorization, Atmos. Environ., 40, 1526-1537, https://doi.org/10.1016/j.atmosenv.2005.10.039, 2006.

Spronsen, M. A., Frenken, J. W., and Groot, I. M.: Observing the oxidation of platinum, Nat. Commun., 8, 429, 2017.

Synal, H.-A., Stocker, M., and Suter, M.: MICADAS: A new compact radiocarbon AMS system, Nucl. Instrum. Meth. B, 259, 7-13, https://doi.org/10.1016/j.nimb.2007.01.138, 2007.

Szidat, S., Jenk, T. M., Gäggeler, H. W., Synal, H.-A., Fisseha, R., Baltensperger, U., Kalberer, M., Samburova, V., Reimann, S., Kasper-Giebl, A., and Hajdas, I.: Radiocarbon (^{14}C)-deduced biogenic and anthropogenic contributions to organic carbon (OC) of urban aerosols from Zürich, Switzerland, Atmos. Environ., 38, 4035-4044, 2004.

Szidat, S., Jenk, T. M., Synal, H. A., Kalberer, M., Wacker, L., Hajdas, I., Kasper-Giebl, A., and Baltensperger, U.: Contributions of fossil fuel, biomass-burning, and biogenic emissions to carbonaceous aerosols in Zurich as traced by ^{14}C, J. Geophys. Res.-Atmos., 111, 2006.

Tao, J., Zhang, L., Cao, J., and Zhang, R.: A review of current knowledge concerning $PM_{2.5}$ chemical composition, aerosol optical properties and their relationships across China, Atmos. Chem. Phys., 17, 9485-9518, https://doi.org/10.5194/acp-17-9485-2017, 2017.

Tian, J., Ni, H., Cao, J., Han, Y., Wang, Q., Wang, X., Chen, L. W. A., Chow, J. C., Watson, J. G., Wei, C., Sun, J., Zhang, T., and Huang, R.: Characteristics of carbonaceous particles from residential coal combustion and agricultural biomass burning in China, Atmos. Pollut. Res., 8, 521-527, https://doi.org/10.1016/j.apr.2016.12.006, 2017.

Timkovsky, J., Dusek, U., Henzing, J. S., Kuipers, T. L., Röckmann, T., and Holzinger, R.: Offline thermal-desorption proton-transfer-reaction mass spectrometry to study composition of organic aerosol, J. Aerosol Sci., 79, 1-14, https://doi.org/10.1016/j.jaerosci.2014.08.010, 2015.

Turpin, B. J., Huntzicker, J. J., and Hering, S. V.: Investigation of organic aerosol sampling artifacts in the Los Angeles Basin, Atmos. Environ., 28, 3061-3071, 1994.

Turpin, B. J., Saxena, P., and Andrews, E.: Measuring and simulating particulate organics in the atmosphere: problems and prospects, Atmos. Environ., 34, 2983-3013, https://doi.org/10.1016/S1352-2310(99)00501-4, 2000.

Viana, M., Chi, X., Maenhaut, W., Cafmeyer, J., Querol, X., Alastuey, A., Mikuška, P., and Večeřa, Z.: Influence of sampling artefacts on measured PM, OC, and EC levels in carbonaceous aerosols in an urban area, Aerosol Sci. Technol., 40, 107-117, 2006.

Vodička, P., Schwarz, J., Cusack, M., and Ždímal, V.: Detailed comparison of OC/EC aerosol at an urban and a rural Czech background site during summer and winter, Sci. Total Environ., 518-519, 424-433, https://doi.org/10.1016/j.scitotenv.2015.03.029, 2015.

Wacker, L., Christl, M., and Synal, H. A.: Bats: A new tool for AMS data reduction, Nucl. Instrum. Meth. B, 268, 976-979, https://doi.org/10.1016/j.nimb.2009.10.078, 2010.

Wang, Y. C., Huang, R. J., Ni, H. Y., Chen, Y., Wang, Q. Y., Li, G. H., Tie, X. X., Shen, Z. X., Huang, Y., Liu, S. X., Dong, W. M., Xue, P., Fröhlich, R., Canonaco, F., Elser, M., Daellenbach, K. R., El Haddad, I., Prevot, A. S. H., Canagaratna, M. R., Worsnop, D. R., Cao, J. J.: Chemical composition, sources and secondary processes of aerosols in Baoji city of north China, Atmos. Environ., 158, 128-137, 2017.

Watson, J. G., Chow, J. C., Lowenthal, D. H., Pritchett, L. C., Frazier, C. A., Neuroth, G. R., and Robbins, R.: Differences in the carbon composition of source profiles for diesel- and gasoline-powered vehicles, Atmos. Environ., 28, 2493-2505, http://dx.doi.org/10.1016/1352-2310(94)90400-6, 1994.

Wehner, B., Philippin, S., and Wiedensohler, A.: Design and calibration of a thermodenuder with an improved heating unit to measure the size-dependent volatile fraction of aerosol particles, J. Aerosol Sci., 33, 1087-1093, 2002.

Xing, L., Fu, T.-M., Cao, J. J., Lee, S. C., Wang, G. H., Ho, K. F., Cheng, M.-C., You, C.-F., and Wang, T. J.: Seasonal and spatial variability of the OM/OC mass ratios and high regional correlation between oxalic acid and zinc in Chinese urban organic aerosols, Atmos. Chem. Phys., 13, 4307-4318, https://doi.org/10.5194/acp-13-4307-2013, 2013.

Yu, J. Z., Xu, J., and Yang, H.: Charring characteristics of atmospheric organic particulate matter in thermal analysis, Environ. Sci. Technol., 36, 754–761, 2002.

Zenker, K., Vonwiller, M., Szidat, S., Calzolai, G., Giannoni, M., Bernardoni, V., Jedynska, A. D., Henzing, B., Meijer, H. A., and Dusek, U.: Evaluation and inter-comparison of oxygen-based OC-EC separation methods for radiocarbon analysis of ambient aerosol particle samples, Atmosphere, 8, 226, 2017.

Zhang, Y. L., Perron, N., Ciobanu, V. G., Zotter, P., Minguillón, M. C., Wacker, L., Prévôt, A. S. H., Baltensperger, U., and Szidat, S.: On the isolation of OC and EC and the optimal strategy of radiocarbon-based source apportionment of carbonaceous aerosols, Atmos. Chem. Phys., 12, 10841-10856, https://doi.org/10.5194/acp-12-10841-2012, 2012.

Zhang, Y. L., Li, J., Zhang, G., Zotter, P., Huang, R.-J., Tang, J.-H., Wacker, L., Prévôt, A. S. H., and Szidat, S.: Radiocarbon-based source apportionment of carbonaceous aerosols at a regional background site on Hainan Island, South China, Environ. Sci. Technol., 48, 2651–2659, https://doi.org/10.1021/es4050852, 2014.

Zhang, Y.-L., Huang, R.-J., El Haddad, I., Ho, K.-F., Cao, J.-J., Han, Y., Zotter, P., Bozzetti, C., Daellenbach, K. R., Canonaco, F., Slowik, J. G., Salazar, G., Schwikowski, M., Schnelle-Kreis, J., Abbaszade, G., Zimmermann, R., Baltensperger, U., Prévôt, A. S. H., and Szidat, S.: Fossil vs. non-fossil sources of fine carbonaceous aerosols in four Chinese cities during the extreme winter haze episode of 2013, Atmos. Chem. Phys., 15, 1299-1312, https://doi.org/10.5194/acp-15-1299-2015, 2015.

Zhu, C.-S., Chen, C.-C., Cao, J.-J., Tsai, C.-J., Chou, C. C.-K., Liu, S.-C., and Roam, G.-D.: Characterization of carbon fractions for atmospheric fine particles and nanoparticles in a highway tunnel, Atmos. Environ., 44, 2668-2673, 2010.

Zhu, C.-S., Tsai, C.-J., Chen, S.-C., Cao, J.-J., and Roam, G.-D.: Positive sampling artifacts of organic carbon fractions for fine particles and nanoparticles in a tunnel environment, Atmos. Environ., 54, 225-230, 2012.

Zhu, C.-S., Cao, J.-J., Tsai, C.-J., Shen, Z.-X., Han, Y.-M., Liu, S.-X., and Zhao, Z.-Z.: Comparison and implications of $PM_{2.5}$ carbon fractions in different environments, Sci. Total Environ., 466-467, 203-209, https://doi.org/10.1016/j.scitotenv.2013.07.029, 2014.

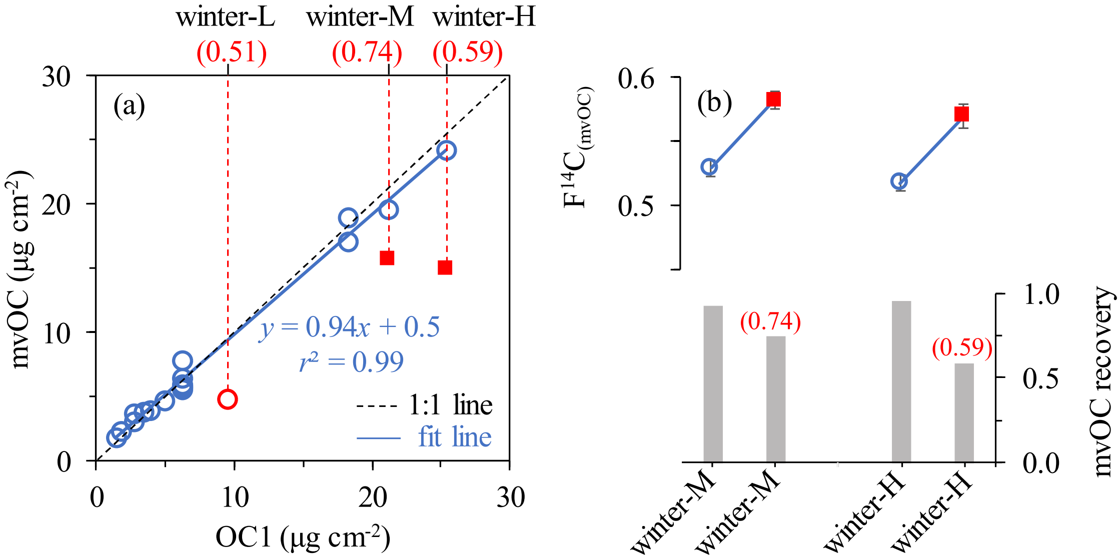

Figure 1. (a) OC1 loading (µg cm^{-2}) measured with a thermo-optical method (EUSAAR_2 protocol using a Sunset Analyzer) and mvOC loading measured using our custom-made aerosol combustion system. The outliers are shown in red circle and square with their sample name on the top *x*-axis. **(b)** F^{14}C$_{(mvOC)}$ of winter-M and winter-H with high and low recoveries with respect to OC1. The red numbers in brackets in panel a and b give the respective outliers' mvOC recoveries to OC1.

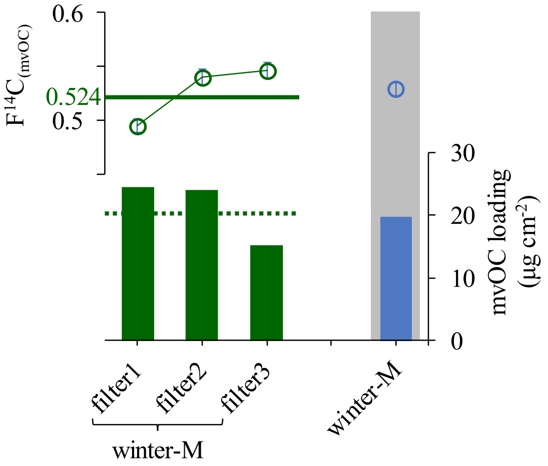

Figure 2. F^{14}C$_{(\mathrm{mvOC})}$ (shown in circle) and mvOC loading (vertical bar) of the the 3 daily filters (“filter1”, “filter2” and “filter3” shown in dark green) that comprise winter-M and the composite winter-M (shown in blue in the dashed area) with mvOC recovery of ~1. The dashed line in dark green indicates the expected mvOC loading and the horizontal in solid green the F^{14}C$_{(\mathrm{mvOC})}$ for the combined winter-M (weighted mean ± standard deviation; 0.524 ± 0.028). The latter is calculated from the mvOC loading (µg cm^{-2}) and F^{14}C$_{(\mathrm{mvOC})}$ of the 3 daily filters using the isotope mass balance equation. F^{14}C$_{(\mathrm{mvOC})}$ uncertainties are indicated but are too small to be visible.

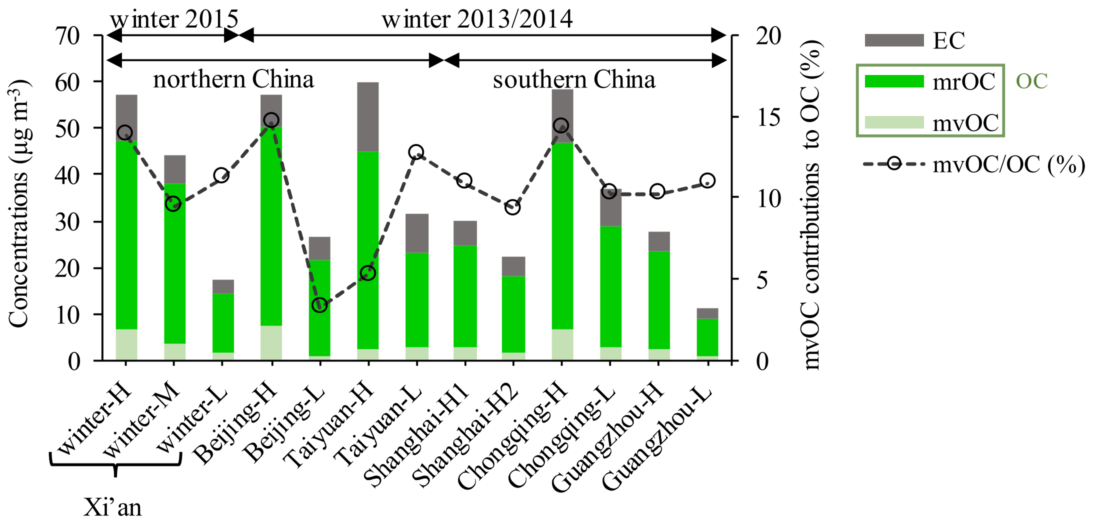

Figure 3. Concentrations of mvOC, mrOC and EC (μg m^{-3}) and contribution of mvOC to total OC (%) in 3 cities in northern China (Xi'an, Beijing and Taiyuan) and 3 in southern China (Shanghai, Chongqing, Guangzhou). mrOC concentrations are 5 calculated by the difference between OC and mvOC. For details see Table S4.

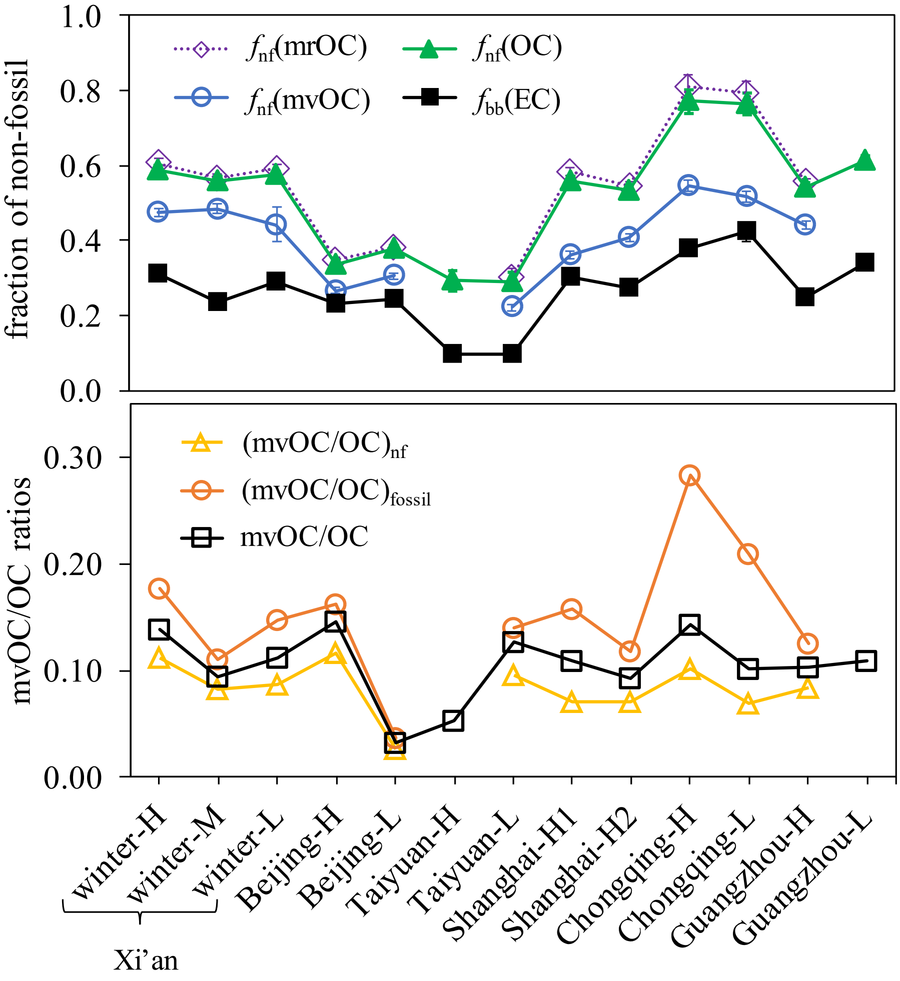

Figure 4. (a) Fraction of non-fossil (f_{nf}) in mvOC, OC and EC. f_{nf}(mrOC) is calculated by the differences between OC and
5 mvOC using isotope mass balance equation. **(b)** mvOC/OC ratios for non-fossil, fossil and total OC.

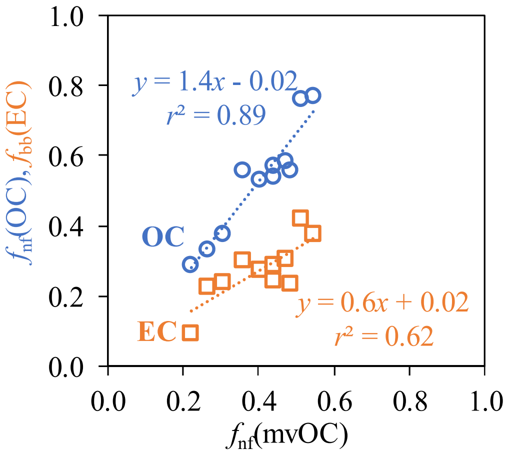

Figure 5. Correlation between f_{nf}(mvOC) and f_{nf}(OC), f_{nf}(mvOC) and f_{bb}(EC) for Xi'an, Beijing, Taiyuan, Shanghai, Chongqing and Guangzhou at wintertime.

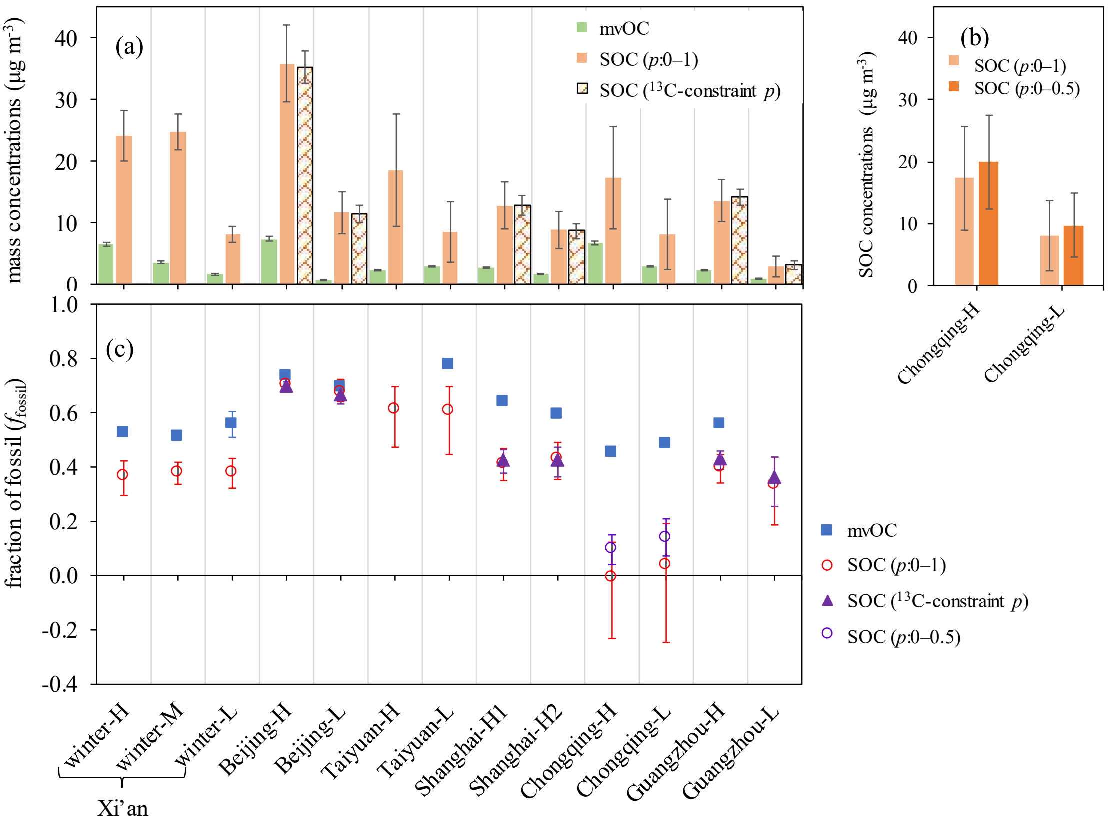

Figure 6. (a) Observed mvOC concentrations (show as green bar) and estimated SOC concentrations by apportioned OC and EC in combination with *p* values without (*p*=0–1) and with constraints by δ^{13}C (^{13}C-constraint *p*), shown as bars filled in orange and pattern fill with stripes. Error bars indicate the uncertainties of mvOC and SOC concentrations calculated by Monte Carlo error propagation. **(b)** For Chongqing, lower *p* values of 0–0.5 are used to estimate SOC concentrations, and compared with *p* values of 0–1. **(c)** Fraction of fossil (f_{fossil}) in mvOC (blue square) and SOC. f_{fossil} of SOC is estimated using *p* values without constraints (*p*=0–1) are shown as red circles and with constraints by δ^{13}C (^{13}C-constraint *p*) as purple triangles, respectively. For Chongqing, lower *p* values of 0–0.5 are used (purple circle). Interquartile range (25th-75th percentile) of the median f_{fossil} (SOC) are shown as vertical bars, uncertainties of f_{fossil}(mvOC) are indicated but are too small to be visible.

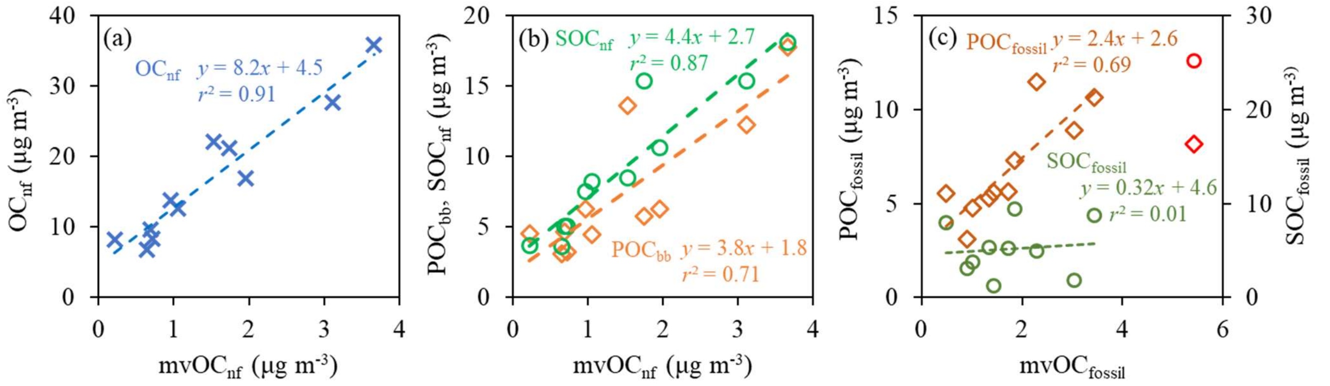

Figure 7. Correlation between **(a)** OC$_{nf}$ and mvOC$_{nf}$ (blue cross), **(b)** POC$_{bb}$ and mvOC$_{nf}$ (orange diamond), SOC$_{nf}$ and mvOC$_{nf}$ (green circle), **(c)** POC$_{fossil}$ and mvOC$_{fossil}$ (diamond in dark orange), SOC$_{fossil}$ and mvOC$_{fossil}$ (circle in dark green) for Xi'an, Beijing, Taiyuan, Shanghai, Chongqing and Guangzhou at wintertime. In panel c, the data points marked in red are from sample Beijing-H with the considerably higher SOC$_{fossil}$/POC$_{fossil}$ ratio (3.1) than other samples (an average of 0.8) and are not included in the regression.

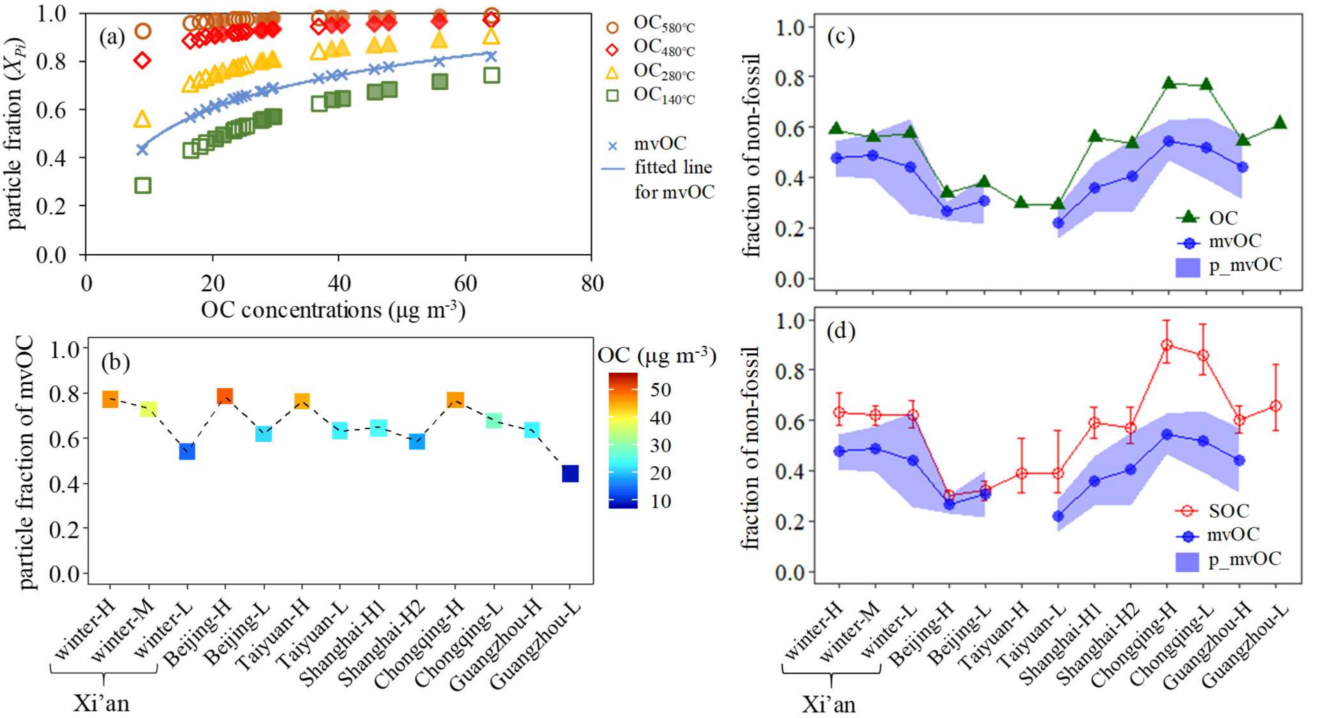

Figure 8. (a) The predicted particulate fraction of OC fractions (i.e., $OC_{140^{\circ}C}$, $OC_{280^{\circ}C}$, $OC_{480^{\circ}C}$, $OC_{580^{\circ}C}$, where the subscript refers to the desorption temperature of the IMPROVE_A protocol) as function of OC concentrations (Supplement ~~S3~~S4). Hollow shapes are used to indicated samples collected by high-volume samplers (HiVol) at a flow rate of 1.0 m^3 min^{-1} and filled shapes by mini-volume samplers (MiniVol) at a flow rate of 5 L min^{-1}. Particulate fraction of mvOC (X_{p_mvOC}, blue cross) is estimated by interpolating the particulate fraction of $OC_{140^{\circ}C}$ and $OC_{280^{\circ}C}$. The blue solid line is the fitted line for the X_{p_mvOC}. **(b)** The X_{p_mvOC} for each sample corresponding to the fitted line in panel a for each sample; **(c, d)** fraction of non-fossil in mvOC collected on the single bare quartz (BQ) filter (f_{nf}(mvOC), blue line and solid circle). The dashed area in blue indicates the possible range of the non-fossil fraction of particulate carbon after correction for the positive artifact (f_{nf}(p_mvOC)), using an upper limit estimate for the positive artifact. The upper and lower limits of the range correspond to the extreme assumption that the F^{14}C of the adsorbed organic vapor is 50 % lower and 50 % higher than measured F^{14}C$_{(mvOC)}$, respectively. f_{nf}(p_mvOC) are compared with f_{nf}(OC) (green solid triangle) in panel c and f_{nf}(SOC) (red circle) in panel d. Interquartile range (25th-75th percentile) of the median f_{fossil} (SOC) are shown as vertical bars.

Supplement of

High contributions of fossil sources to more volatile organic ~~carbon~~ aerosol

Haiyan Ni[1,2,3], Ru-Jin Huang[2*], Junji Cao[2], Wenting Dai[2], Jiamao Zhou[2], Haoyue Deng[1], Anita Aerts-Bijma[1], Harro A.J. Meijer[1], Ulrike Dusek[1]

[1]Centre for Isotope Research (CIO), Energy and Sustainability Research Institute Groningen (ESRIG), University of Groningen, Groningen, 9747 AG, the Netherlands
[2]State Key Laboratory of Loess and Quaternary Geology, Key Laboratory of Aerosol Chemistry and Physics, Institute of Earth Environment, Chinese Academy of Sciences, Xi'an, 710061, China
[3]University of Chinese Academy of Sciences, Beijing, 100049, China

Correspondence to: Ru-Jin Huang (rujin.huang@ieecas.cn)

S1. Stable carbon isotopic composition of EC

The stable carbon isotopic composition of EC was determined using a Finnigan MAT 251 mass spectrometer with a dual inlet system (Bremen, Germany) at the Stable Isotope Laboratory at the Institute of Earth Environment, Chinese Academy of Sciences. OC is removed by heating the filter pieces at 375 °C for 3 h in a vacuum-sealed quartz tube in the presence of CuO catalyst grains. Extraction of EC was done by heating the carbon that remained on the filters at 850 °C for 5 h. The evolved CO_2 from EC was isolated by a series of cold traps and quantified manometrically. The stable carbon isotopic composition of the purified CO_2 of EC was measured and determined as $\delta^{13}C_{EC}$. A routine laboratory working standard with a known $\delta^{13}C$ value was measured every day. The quantitative levels of ^{13}C and ^{12}C isotopes were characterized using a ratio of peak intensities of m/z 45 ($^{13}C^{16}O_2$) and 44 ($^{12}C^{16}O_2$) in the mass spectrum of CO_2. Samples were analyzed at least in duplicate, and all replicates showed differences less than 0.3 ‰. $\delta^{13}C$ values are reported in the delta notation with respect to the international standard Vienna Pee Dee Belemnite (V-PDB):

$$\delta^{13}\mathrm{C}\ (‰) = \left[\frac{\left(^{13}\mathrm{C}/^{12}\mathrm{C}\right)_{\mathrm{sample}}}{\left(^{13}\mathrm{C}/^{12}\mathrm{C}\right)_{\mathrm{V-PDB}}} - 1\right] \times 1000. \tag{S1}$$

Details of stable carbon isotope measurements are described by our previous studies (Cao et al., 2011; Ni et al., 2018).

S2. Separation of fossil sources into coal and vehicle for EC using Bayesian statistics

Contributions from biomass burning and fossil sources to EC is separated by $F^{14}C_{EC}$ (Sect. 2.4). The relative contribution of fossil fuel combustion to EC (f_{fossil}(EC)) and biomass burning to EC (f_{bb}(EC)) constrained by $F^{14}C_{EC}$ is shown in Table S5. f_{fossil}(EC) can be further separated into the fraction of EC contributed by coal combustion(f_{coal}) and vehicle emissions (f_{vehicle}) using $\delta^{13}C$ of EC in a Bayesian Markov chain Monte Carlo (MCMC) scheme:

$$\delta^{13}\mathrm{C}_{\mathrm{EC}} = \delta^{13}\mathrm{C}_{\mathrm{bb}} \times f_{\mathrm{bb}}(\mathrm{EC}) + \delta^{13}\mathrm{C}_{\mathrm{coal}} \times f_{\mathrm{coal}} + \delta^{13}\mathrm{C}_{\mathrm{vehicle}} \times f_{\mathrm{vehicle}}\,, \tag{S2}$$

$$f_{\mathrm{coal}} + f_{\mathrm{vehicle}} = f_{\mathrm{fossil}}\,(\mathrm{EC}), \tag{S3}$$

where $\delta^{13}C_{bb}$, $\delta^{13}C_{vehicle}$ and $\delta^{13}C_{coal}$ are the $\delta^{13}C$ signature of EC emitted from biomass burning, vehicle emissions and coal combustion, respectively. The means and the standard deviations for $\delta^{13}C_{bb}$ (-26.7 ± 1.8 ‰ for C3 plants), $\delta^{13}C_{vehicle}$ (-25.5 ± 1.3 ‰) and $\delta^{13}C_{coal}$ (-23.4 ± 1.3 ‰) are established in Andersson et al. (2015) by a thorough literature search and full compilation of $\delta^{13}C$ source signatures for EC. In brief, the mean and standard deviation for $\delta^{13}C$ endmembers for the different sources are estimated as the average and standard deviation of the different data sets, respectively.

The source endmembers for δ^{13}C are less well-constrained than f_{bb}(EC) and f_{fossil}(EC), as δ^{13}C varies with fuel types and combustion conditions. For example, the range of possible δ^{13}C values for vehicle emission overlaps to a small extent with the range for coal combustion, although EC from vehicle emissions are usually more depleted than from coal combustion. Uncertainties of source signatures of δ^{13}C (i.e., $\delta^{13}C_{bb}$, $\delta^{13}C_{vehicle}$, $\delta^{13}C_{coal}$), the calculated f_{fossil}(EC) derived from $F^{14}C_{EC}$, and the measured $\delta^{13}C_{EC}$ are propagated by the MCMC technique, where source signatures of δ^{13}C introduces a larger uncertainty than f_{fossil}(EC) constrained by $F^{14}C$.

MCMC was implemented in the freely available R software (https://cran.r-project.org/), using the *simmr* package (https://CRAN.R-project.org/package=simmr). Convergence diagnostics were created to make sure the model has converged properly. The simulation for each sample was run with 10,000 iterations, using a burn-in of 1000 steps, and a data thinning of 100. The results of the MCMC are the posterior probability density functions (PDF) for the relative contributions from the sources (Fig. S3).

S3. Blank corrections for $F^{14}C$ of carbon fractions

The ^{14}C values of carbon fractions (i.e., mvOC, OC and EC) can be blank corrected accordioning to the mass balance equation:

$$F^{14}C_S = \frac{F^{14}C_m \times M_m - F^{14}C_b \times M_b}{M_m - M_b} \tag{S4}$$

where $F^{14}C_S$ is $F^{14}C$ of the aerosol carbon collected on the filter, which is blank corrected, $F^{14}C_m$ and M_m are the measured $F^{14}C$ and the measured mass of the respective carbon fraction (mvOC, OC or EC), and $F^{14}C_b$ and M_b the fraction modern and the mass of the respective carbon fraction of blanks.

Since the directly determined system blank (i.e. the amount of CO_2 measured, when no sample is introduced into the aerosol combustion system) is 0.52 ± 0.31 μgC mvOC per extraction (i.e., M_b for mvOC), it is much too small to be analyzed for $F^{14}C_b$ of mvOC. To do blank corrections for mvOC, we need to estimate its $F^{14}C_b$. We assume that $F^{14}C_b$ for mvOC ranges from 0 to 1 with a continuous uniform distribution as the reviewer suggested. To propagate uncertainties, a Monte Carlo simulation with 10,000 individual calculations of $F^{14}C_S$ for mvOC was conducted according to Eq. (S4). For calculation inputs, $F^{14}C_b$ of mvOC. was randomly chosen from a continuous uniform distribution between 0 and 1. $F^{14}C_m$ for mvOC was randomly chosen from a normal distribution symmetric around the measured values with uncertainties as standard deviation (Table S4). The random values for M_m and M_b were taken from a triangular distribution, which has its maximum at the central value and 0 at the upper and lower limits. Then 10,000 different estimations of $F^{14}C_S$ for mvOC were calculated. The derived average represents the best estimate, and the standard deviation represents the combined uncertainties.

Figure S9 shows the $F^{14}C$ of mvOC before and after blank corrections ($F^{14}C_m$ and $F^{14}C_s$, respectively) for the contamination introduced by the isolation procedure.

As shown in Figure S9, the differences in $F^{14}C$ values of mvOC before and after blank corrections are really small, with the biggest absolute difference of 0.009 for sample Taiyuan-L. The small correction of $F^{14}C$ for mvOC will not affect any conclusion from this study. Thus, in this study, the contamination is assessed but not used for further data correction.

For OC and EC, the contamination introduced by the isolation procedure yields 0.72 ± 0.44 µgC EC and 0.85 ± 0.49 µgC OC per extraction, respectively, which are the directly determined system blank (i.e. the amount of CO_2 measured, when no sample is introduced into the aerosol combustion system). The blanks are less than 3% of the sample amount and thus can be neglected, compared with our sample size of 30–391 µgC EC per extraction and 30–445 µgC OC per extraction. Therefore, the blank correction will not introduce large uncertainties to the data. In this study, the contamination is assessed but not used for further data correction for $F^{14}C$ of OC and EC.

~~S3~~S4. Gas-particle partitioning of OC fractions

Ambient OC has a large range of volatility and contains low to high volatility compounds. The low-volatility OC is in the particle phase, and high volatility OC is mostly in the gas phase. OC with intermediate volatility are semi-volatile (SVOC) and can either be in the particle or the gas phase depending on temperature, concentrations of OC etc. (Donahue et al., 2006, 2009).

In this study, particulate OC is collected on a single bare-quartz filter. mvOC (desorbed at 200 °C in He) on the quartz filters is influenced by evaporation of SVOC from collected particles and adsorption of organic vapors to the quartz fibers. To estimate the particulate fraction of mvOC, we estimate the gas-particle partitioning of individual OC fractions using the thermal/optical OC/EC analysis and a volatility basis set (VBS) model. The VBS bins the organic aerosol (OA) compounds according to the effective saturation concentrations (*C**). If we project concentrations of organic aerosol (OA) onto the basis set of saturation concentrations, we can estimate the volatility distribution of the organic material. The concentrations of OA (C_{OA}) and the equilibrium partitioning fractions (f_i) at equilibrium can be described by (Donahue et al., 2006, 2011):

$$f_i = \left(1 + \frac{C_i^*}{C_{OA}}\right)^{-1} \quad (\text{~~S4~~S5})$$

where C_i^* is the C^* for OC fraction i. If C_i^* is equal to C_{OA}, then 50 % of OA mass will be in the particle phase, that is $f_i = 0.5$; if $C_i^* = 4 \times C_{OA}$, then the OA is more volatile, and only 20 % OA mass in the particle phase ($f_i = 0.2$).

Thermal-optical OC/EC analysis measures OC, not the OA. We use the OA/OC mass ratio to estimate OA concentrations from the OC concentrations. Then Eq. ~~S4~~ S5 can be reformulated as:

$$X_{Pi} = \left(1 + \frac{C_i^*}{\frac{OA}{OC} \times C_{OC}}\right)^{-1} \quad (\text{~~S5~~S6})$$

where X_{Pi} is the particulate fraction in OC fraction i; C_{OC} can be quantified by the thermal-optical OC/EC analysis, and is the sum of particulate OC fractions;

The C^* value for each OC fraction are taken from Ma et al. (2016), where OC fractions are measured using the IMPROVE_A protocol, and are derived so that X_{Pi} stands for the particulate fraction of the total carbon found on the filter for each temperature step i. The IMPROVE_A temperature plateaus in the pure He phase are 140 °C, 280 °C, 480 °C, 580 °C, and the corresponding thermal carbon fractions are called $OC_{140°C}$, $OC_{280°C}$, $OC_{480°C}$ and $OC_{580°C}$, where the subscript refers to the desorption temperature of the IMPROVE_A protocol, respectively. The empirical VBS consisting of bins separated by 0.5 of an order of magnitude in volatility at 300 K: the C^* for $OC_{140°C}$ to $OC_{580°C}$ are $10^{1.6}$, $10^{1.1}$, $10^{0.6}$ and $10^{0.1}$ μg m^{-3}, respectively. The OA/OC is assumed to be 1.8 for urban environment (Turpin and Lim, 2001; Xing et al., 2013). In this study, samples in Beijing, Guangzhou, Shanghai, Taiyuan and Chongqing are measured using the IMPROVE_A protocol, thus X_{pi} for samples of these five cities are estimated using the empirical C^*, as shown in Fig. 8a in the main text.

The particulate fraction (X_{pi}) of OC fractions increases considerably from $OC_{140°C}$ to $OC_{580°C}$, consistent with the temperature steps. The temperature of the OC/EC analysis is the desorption temperature rather than evaporation, but it is still reasonable to assume that the desorption temperature is closely related to the volatility. OC desorbed at higher temperature tends to have a low volatility and more likely to exist in the particle phase.

Increasing the particulate OC concentrations (C_{OC} in Eq. ~~S5~~S6) increase the particulate fraction for each OC fraction (X_{p1}, X_{p2}, X_{p3} and X_{p4}). For example, when C_{OC} increases from 8.8 μg m^{-3} to 64 μg m^{-3}, particulate fraction of OC$_{140°\mathrm{C}}$ increases from 0.28 (i.e., 28 % OC$_{140°\mathrm{C}}$ in the particle phase) to 0.74 and particulate fraction of OC$_{280°\mathrm{C}}$ increases from 0.56 to 0.90. The desorption temperature for mvOC is 200 °C, falling within the 140 °C for OC$_{140°\mathrm{C}}$ and 280 °C for OC$_{28}$~~$_{0}$~~$_{0°\mathrm{C}}$. We thus estimated the particulate fraction for mvOC will fall within the X_{p1} for OC$_{140°\mathrm{C}}$ and X_{p2} for OC$_{280°\mathrm{C}}$.

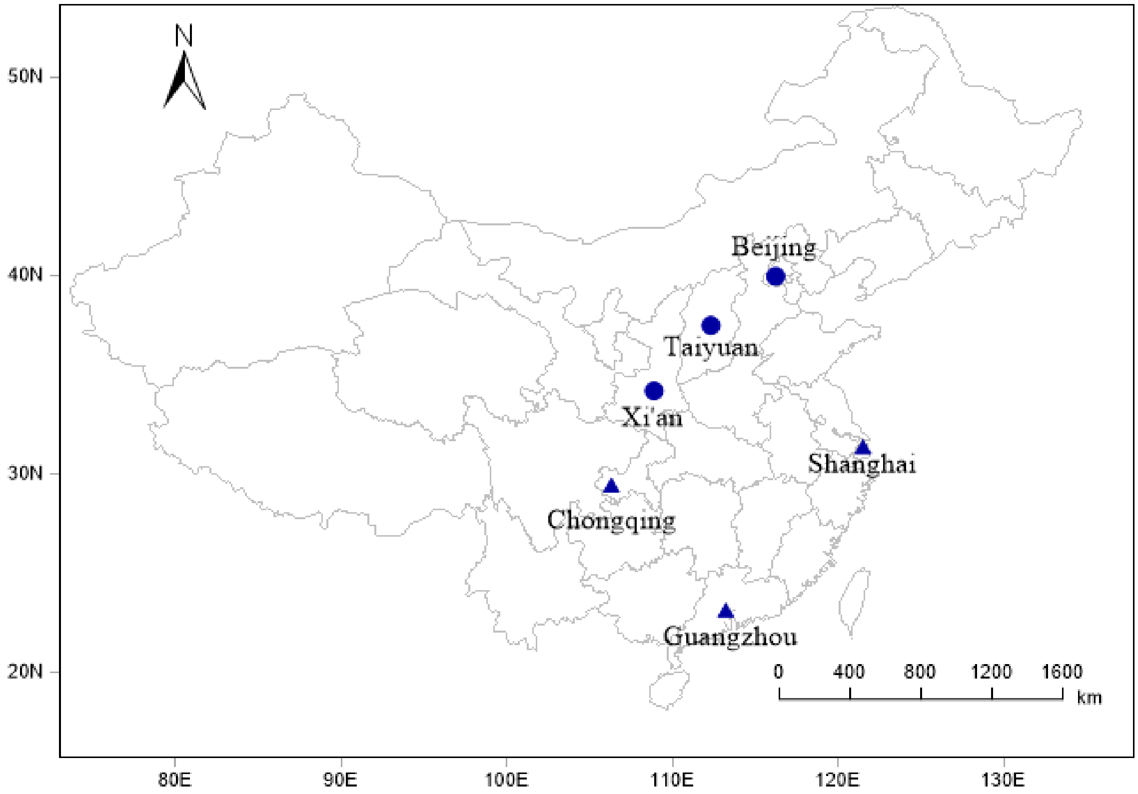

Figure S1. Geographic locations of the six Chinese sampling sites. Cities in northern China are shown as blue circle, cities in southern China as blue triangle. In northern China, large quantities of coal are used for heating during a formal residential "heating season" (15 November to 15 March next year) in winter.

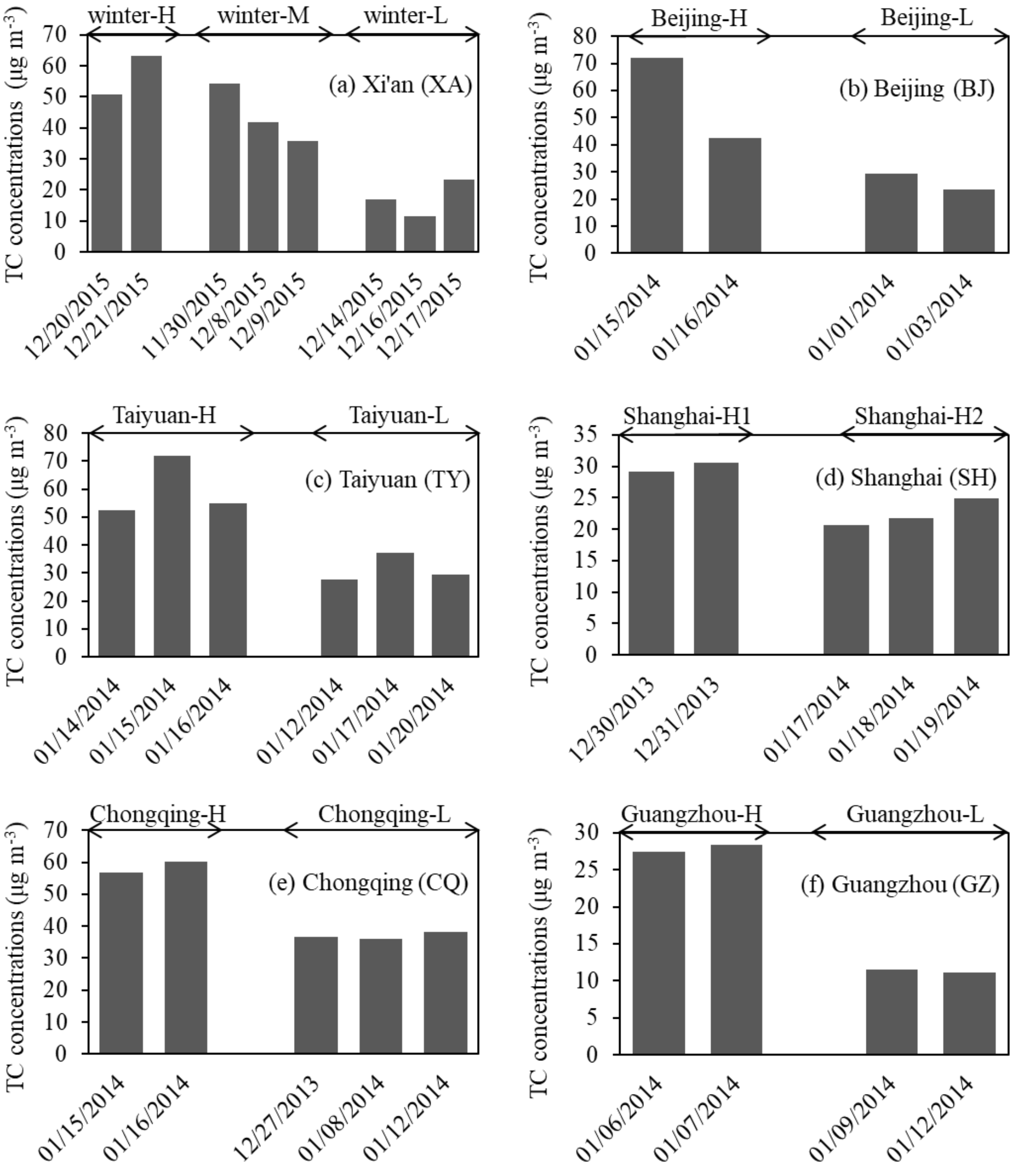

Figure S2. Selected samples for ^{14}C analysis. 2-3 composite samples that represent high (H), medium (M) and low (L) TC concentrations are combined from several individual filter samples for each city (a. Xi'an; b. Beijing; c. Taiyuan; d. Shanghai; e. Chongqing; f. Guangzhou). Each sample is consisting of 2 to 3 24-hr filter pieces with similar TC loadings and air mass backward trajectories (Table S1).

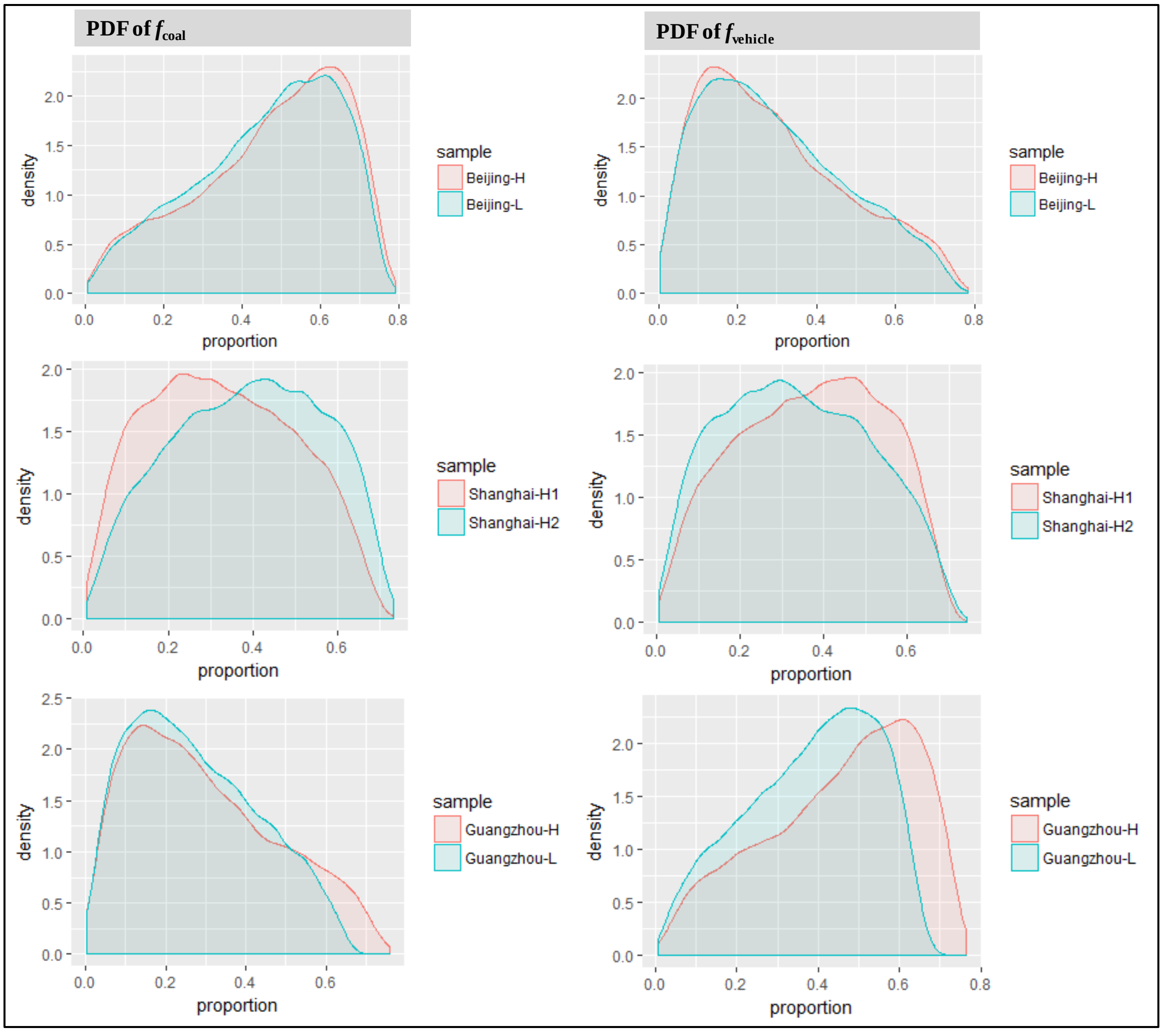

Figure S3. Probability density function (PDF) of the relative source contributions of coal and vehicle to EC (f_{coal}, $f_{vehicle}$) constrained by δ^{13}C, calculated using the Bayesian Markov chain Monte Carlo approach (Supplement S2). Samples collected from other cities including Xi'an, Taiyuan, Chongqing were not measured for $\delta^{13}C_{EC}$.

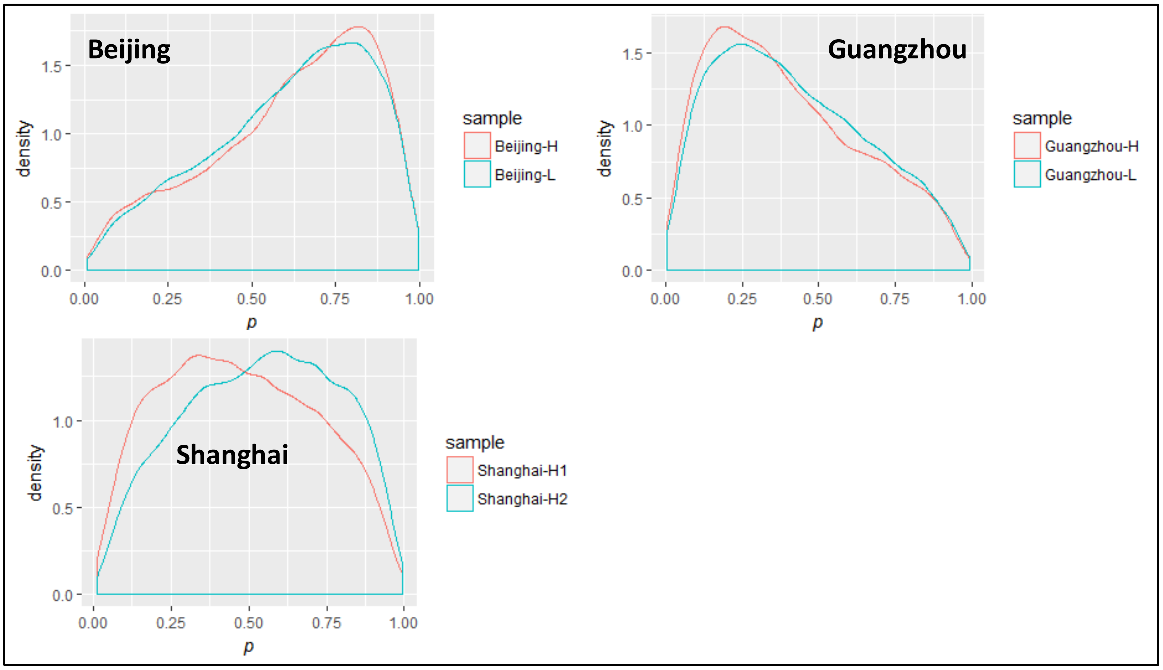

Figure S4. The PDF of *p* values (*p* is the fraction of EC from coal combustion in that from total fossil sources) for each sample, which is constrained by $\delta^{13}C_{EC}$. Calculation of *p* is present in Sect. 2.4. Other cities including Xi'an, Taiyuan, Chongqing were not measured for $\delta^{13}C$.

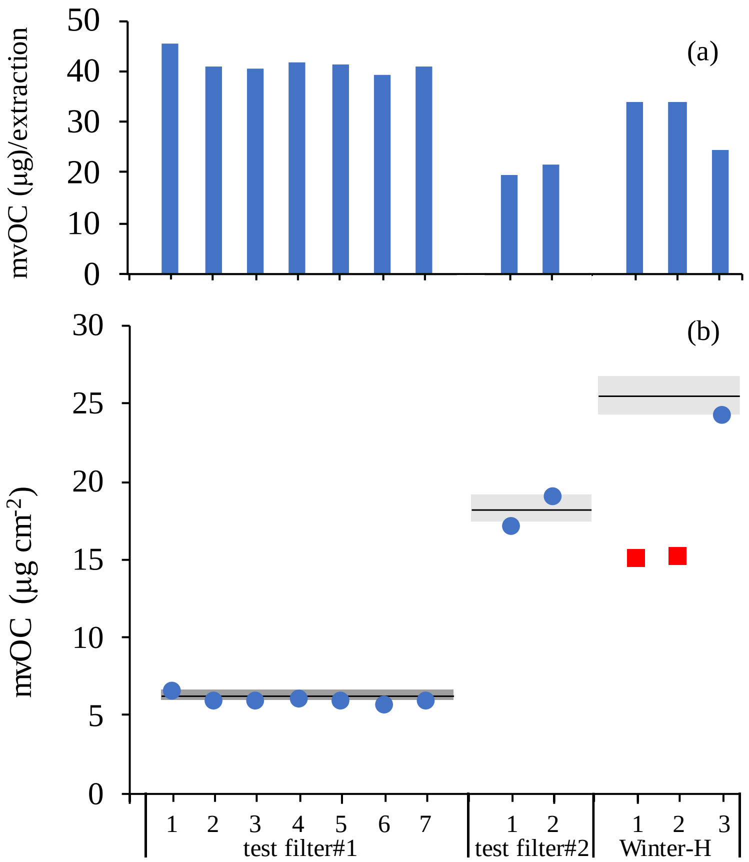

Figure S5. Reproducibility of desorption performed for test filter#1, test filter#2 and winter-H. The number on the *x*-axis represent the times of mvOC desorption. **(a)** the desorbed mvOC amount in µgC per extraction; **(b)** the desorbed mvOC in µg cm^{-2} calculated by dividing the desorbed mvOC amount (µgC) by the filter area (cm^{-2}). The horizontal black line indicates the OC1 (µg cm^{-2}) measured by EUSAAR_2 protocol and the shaded area denotes its uncertainties. The two red squares represent the repeated mvOC extraction for sample winter-H using larger filter pieces. The panel (a) and (b) ~~has~~ have the same *x*-axis.

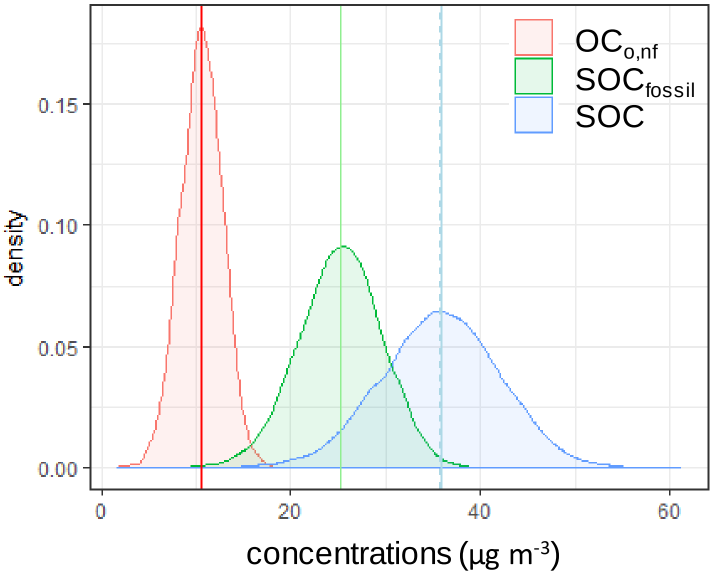

Figure S6. An example PDF of SOC concentrations (in light blue), SOC$_{fossil}$ (light green) and OC$_{o.nf}$ (approximately SOC$_{nf}$, orange) for sample Beijing-H. The estimated SOC and SOC$_{fossil}$ concentrations are estimated by ^{14}C-apportioned OC and EC in combination with *p* values randomly chosen from 0–1 (Sect. 2.4). The mean and median are indicated by the dashed and solid vertical lines. The mean and median are very close to each other due to the symmetric PDF. The median (interquartile range) and mean (± SD) values are given in Table S7 and Table S8, respectively.

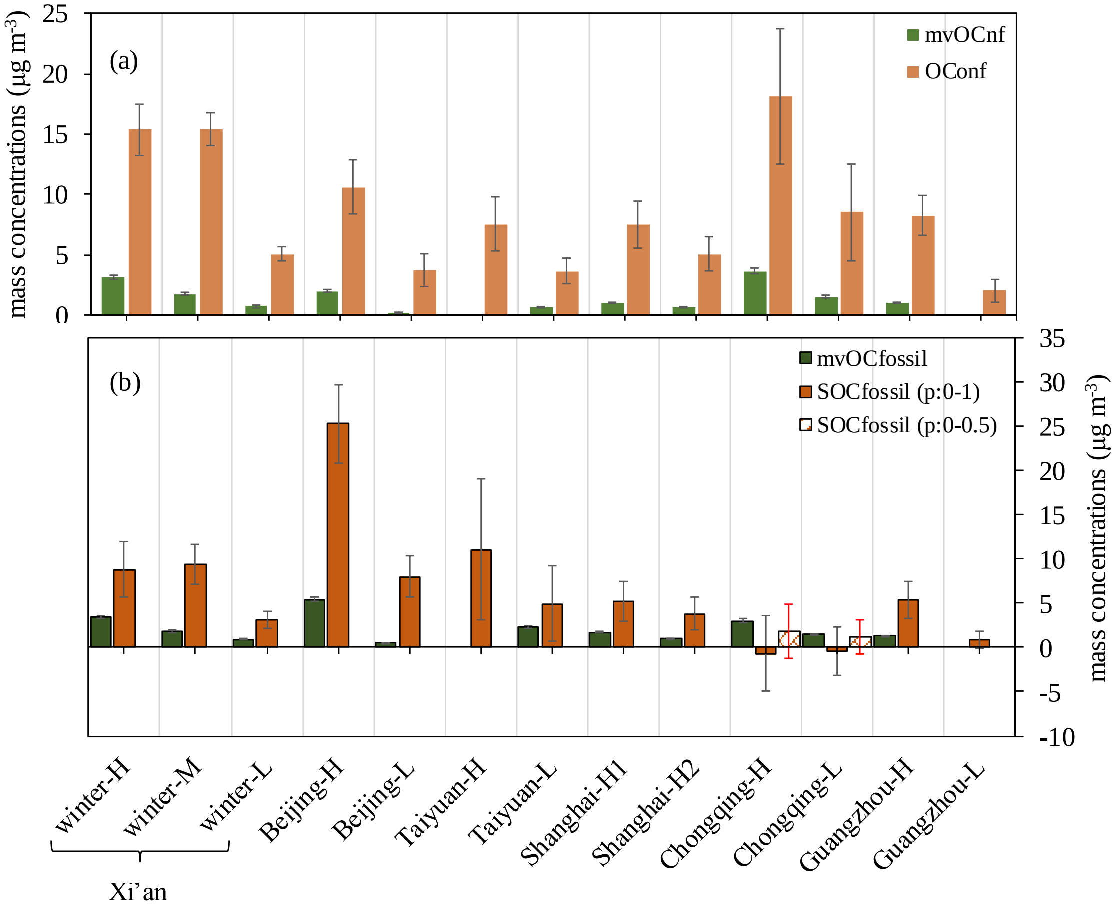

Figure S7. (a) Concentrations of mvOC$_{nf}$ (green bar) and OC$_{o,nf}$ (approximately SOC$_{nf}$, orange bar); **(b)** Concentrations of mvOC$_{fossil}$ (dark green bar), and SOC$_{fossil}$. SOC$_{fossil}$ is estimated based on ^{14}C-apportioned OC and EC, combined with primary OC/EC ratios of coal combustion and vehicle exhaust, and *p* values. SOC$_{fossil}$ estimated using using *p* values of 0–1 are shown in dark orange. For Chongqing, lower *p* values of 0–0.5 are used to estimate SOC$_{fossil}$, shown as bars filled with stripes. The panel (a) and (b) has the same *x*-axis.

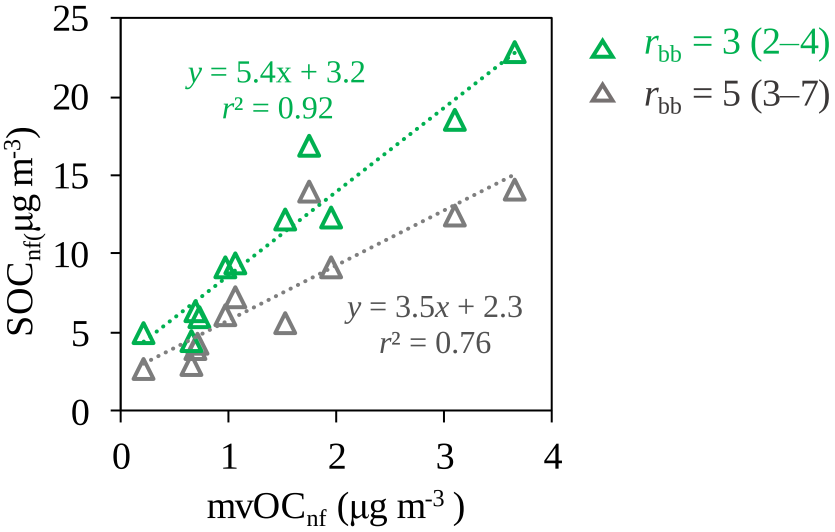

Figure S8. Correlation between mvOC$_{nf}$ and SOC$_{nf}$. SOC$_{nf}$ is estimated by subtracting primary OC from biomass burning (POC$_{bb}$) from OC$_{nf}$, where POC$_{bb}$ is estimated by multiplying EC$_{bb}$ with the OC/EC ratio of fresh biomass burning plumes(r_{bb}). Here we take r_{bb}= 5 (3–7; mean; minimum-maximum) and r_{bb}= 3 (2–4), higher and lower than our best estimate of r_{bb} (4, 3–5), respectively.

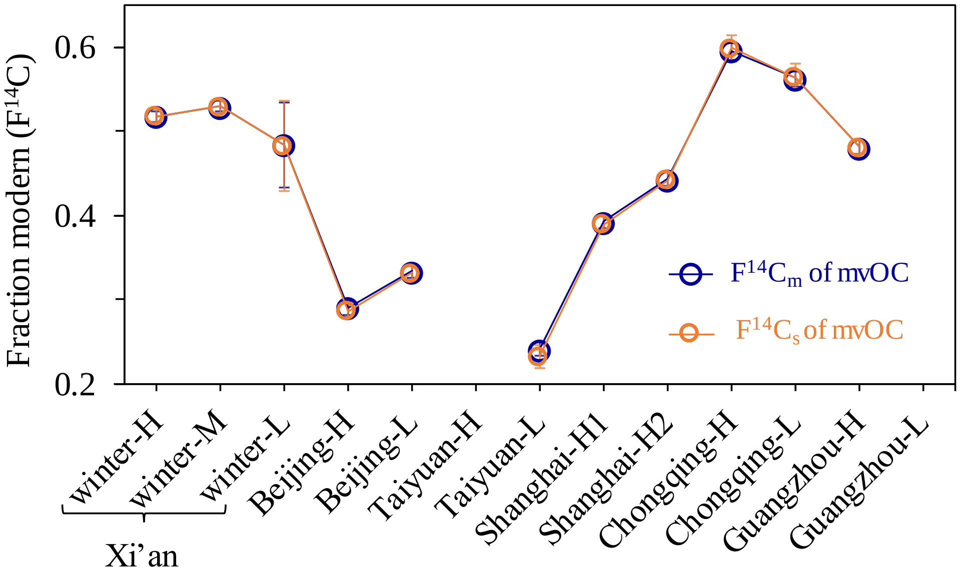

Figure S9. Fraction modern ($F^{14}C$) of mvOC before and after blank corrections ($F^{14}C_m$ and $F^{14}C_s$, respectively) for the contamination introduced by the isolation procedure. Detailed method to do the blank corrections is described in Supplement S3.

Table S1. Details of sampling information.

	City	Sampling sites	Longitude, latitude	Sample name*	Sampling date	RH (%)**	Temperature (°C)**	Wind speed (m s^{-1})**
Northern China	Xi'an (XA)	Institute of Earth Environment, Chinese Academy of Sciences	34.2° N, 108.9° E	winter-H	12/20/2015 12/21/2015	73 79	-3~6 -1~5	1.0 0.6
				winter-M	11/30/2015 12/8/2015 12/9/2015	 85 85	3~11 2~8 2~6	1.1 1.1 1.0
				winter-L	12/14/2015 12/16/2015 12/17/2015	67 50 65	-2~8 -5~4 -4~3	1.9 1.3 1.2
	Beijing (BJ)	Institute of Remote Sensing Applications, Chinese Academy of Sciences	39.9° N, 116.4° E	Beijing-H	1/15/2014 1/16/2014	56 67	-4~13 -3~5	1.5 1.9
				Beijing-L	1/1/2014 1/3/2014	37 50	-2~13 -4~8	1.6 2.2
	Taiyuan (TY)	Taiyuan University of Technology	37.9° N, 112.5° E	Taiyuan-H	1/14/2014 1/15/2014 1/16/2014	37 37 37	-14~3 -11~4 -13~5	1.3 1.2 1.2
				Taiyuan-L	1/12/2014 1/17/2014 1/20/2014	36 37 30	-15~2 -14~3 -14~3	1.2 1.6 2.5
Southern China	Shanghai (SH)	Fudan University	31.2° N, 121.4° E	Shanghai-H1	12/30/2013 12/31/2013	55 49	-3~10 -1~14	1.8 2.0
				Shanghai-H2	1/17/2014 1/18/2014 1/19/2014	70 76 67	5~11 -2~7 3~10	2.4 1.8 2.5
	Chongqing (CQ)	Super Monitoring Station of Chongqing	29.9° N, 106.5° E	Chongqing-H	1/15/2014 1/16/2014	86 91	7~9 7~10	0.5 0.2
				Chongqing-L	12/27/2013 1/8/2014 1/12/2014	92 90 89	6~9 6~8 4~10	0.4 0.3 0.5
	Guangzhou (GZ)	South China Institute of Environmental Sciences, Ministry of Environment Protection	23.1° N, 113.2° E	Guangzhou-H	1/6/2014 1/7/2014	73 84	11~20 16~21	1.6 1.7
				Guangzhou-L	1/9/2014 1/12/2014	62 67	11~15 8~18	2.8 4.9

*Composite samples that represent high (H), medium(M) and low (L) TC concentrations are combined from several individual 24-hr samples for ^{14}C analysis.

**The meteorological data is obtained from the Meteorological Institute of Shaanxi Province, Xi'an, China. Daily average relative humidity (RH), daily average wind speed (m s-1) and ambient temperature (minimum~maximum; °C). There was no precipitation in all cities during all sampling dates.

Table S2. Pilot tests to determine the flushing time using He before heating the filter pieces at 200 °C in He to desorb mvOC, using a test filter. The results show that the flushing time (10 min, 15 min or 60 min) does not affect the desorption amount of mvOC.

Test	Flushing time	Desorbed amount of mvOC
1	10 min	5.8 μg cm^{-2}
2	15 min	5.9 μg cm^{-2}
3	15 min	5.8 μg cm^{-2}
4	60 min	5.7 μg cm^{-2}
5	60 min	5.7 μg cm^{-2}

Table S3. Measured $F^{14}C$ values and masses of the standards with their nominal $F^{14}C$ values.

Standards		nominal $F^{14}C$	measured $F^{14}C$ ($F^{14}C_m$)	measured mass (M_m, μgC)
Combustion processes[a]	OXII	1.3406	1.327 ± 0.022	65
	OXII	1.3406	1.321 ± 0.012	117
	anthracite	0	0.020 ± 0.001	51
	anthracite	0	0.002 ± 0.001	75
	anthracite	0	0.008 ± 0.001	217
	anthracite	0	0.004 ± 0.001	219
	anthracite	0	0.005 ± 0.001	254

[a] For combustion processes, two sets of standard material: the oxalic acid HOxII and anthracite with known ^{14}C contents ($F^{14}C = 1.3406$ and $F^{14}C = 0$, respectively) were combusted using the aerosol combustion system (ACS) and used for quality control.

Table S4. Concentrations of mvOC, OC and EC (μg m^{-3}), the contribution of mvOC to the total OC (mvOC/OC, %), fraction modern of mvOC, OC and EC ($F^{14}C_{(mvOC)}$, $F^{14}C_{(OC)}$, $F^{14}C_{(EC)}$) and stable carbon isotopic composition of EC ($\delta^{13}C_{EC}$).

City	Sample Name	mvOC* (μg m^{-3})	OC (μg m^{-3})	EC (μg m^{-3})	mvOC/OC (%)	$F^{14}C_{(mvOC)}$	$F^{14}C_{(OC)}$	$F^{14}C_{(EC)}$	$\delta^{13}C_{EC}$ (‰)
Xi'an (XA)	winter-H	6.5	47.1	9.9	13.9	0.517 ± 0.006	0.640 ± 0.009	0.340 ± 0.005	
	winter-M	3.6	37.9	6.1	9.5	0.529 ± 0.007	0.609 ± 0.007	0.258 ± 0.005	
	winter-L	1.6	14.5	2.8	11.2	0.483 ± 0.050**	0.626 ± 0.007	0.320 ± 0.005	
Beijing (BJ)	Beijing-H	7.4	50.4	6.9	14.6	0.290 ± 0.008	0.366 ± 0.003	0.253 ± 0.002	-23.96 ± 0.02
	Beijing-L	0.7	21.8	4.7	3.3	0.334 ± 0.008	0.413 ± 0.004	0.266 ± 0.003	-24.06 ± 0.02
Taiyuan (TY)	Taiyuan-H	2.4	45.1	14.8	5.3	NA***	0.320 ± 0.030	0.106 ± 0.002	
	Taiyuan-L	2.9	23.2	8.2	12.7	0.241 ± 0.008	0.318 ± 0.023	0.105 ± 0.003	
Shanghai (SH)	Shanghai-H1	2.7	24.7	5.2	10.9	0.392 ± 0.008	0.609 ± 0.004	0.332 ± 0.003	-25.45 ± 0.03
	Shanghai-H2	1.7	18.2	4.2	9.3	0.443 ± 0.008	0.580 ± 0.004	0.303 ± 0.003	-24.72 ± 0.02
Chongqing (CQ)	Chongqing-H	6.7	46.7	11.8	14.3	0.595 ± 0.011	0.839 ± 0.029	0.414 ± 0.010	
	Chongqing-L	3	29	8.1	10.2	0.562 ± 0.010	0.833 ± 0.028	0.466 ± 0.026	
Guangzhou (GZ)	Guangzhou-H	2.4	23.4	4.5	10.3	0.481 ± 0.008	0.592 ± 0.004	0.271 ± 0.002	-26.01 ± 0.02
	Guangzhou-L	1	8.8	2.5	10.9	NA***	0.667 ± 0.005	0.375 ± 0.004	-26.15 ± 0.02

* Excellent agreement was found between mvOC amount measured using ACS system and OC1 following EUSAAR_2 using a Sunset carbon analyzer, except for sample winter-L. Here we took the OC1 by EUSAAR_2 as mvOC concentrations (both desorbed at 200 °C in He) for samples at Xi'an. Blank corrections were performed for OC1 mass, the mvOC concentrations in Xi'an were therefore blank corrected. ** For sample winter-L, we take the measured $F^{14}C_{(mvOC)}$ values but assign a bigger absolute uncertainty of 0.05, due to their low mvOC recoveries. *** Samples get lost during the ^{14}C measurements.

Table S5. Relative non-fossil sources contribution to mvOC, OC, EC and mrOC (f_{nf}(mvOC), f_{nf}(OC), f_{bb}(EC), f_{nf}(mrOC)), and relative fossil sources contribution to mvOC, OC, EC and mrOC(f_{fossil}(mvOC), f_{fossil}(OC), f_{fossil}(EC), f_{fossil}(mrOC)).

City	Sample Name	f_{nf}(mvOC)	f_{nf}(OC)	f_{bb}(EC)	f_{nf}(mrOC)*	f_{fossil}(mvOC)	f_{fossil}(OC)	f_{fossil}(EC)	f_{fossil}(mrOC)*
Xi'an	winter-H	0.475 ± 0.011	0.587 ± 0.014	0.309 ± 0.008	0.606 ± 0.015	0.525 ± 0.011	0.413 ± 0.014	0.691 ± 0.008	0.394 ± 0.015
(XA)	winter-M	0.485 ± 0.011	0.558 ± 0.012	0.235 ± 0.006	0.566 ± 0.013	0.515 ± 0.011	0.442 ± 0.012	0.765 ± 0.006	0.434 ± 0.013
	winter-L	0.443 ± 0.047	0.574 ± 0.012	0.291 ± 0.007	0.591 ± 0.014	0.557 ± 0.047	0.426 ± 0.012	0.709 ± 0.007	0.409 ± 0.014
Beijing	Beijing-H	0.266 ± 0.009	0.336 ± 0.007	0.230 ± 0.005	0.348 ± 0.008	0.734 ± 0.009	0.664 ± 0.007	0.770 ± 0.005	0.652 ± 0.008
(BJ)	Beijing-L	0.306 ± 0.009	0.379 ± 0.008	0.242 ± 0.005	0.382 ± 0.008	0.694 ± 0.009	0.621 ± 0.008	0.758 ± 0.005	0.618 ± 0.008
Taiyuan	Taiyuan-H	NA**	0.293 ± 0.028	0.096 ± 0.003	NA	NA	0.707 ± 0.028	0.904 ± 0.003	NA
(TY)	Taiyuan-L	0.221 ± 0.009	0.292 ± 0.022	0.095 ± 0.003	0.302 ± 0.025	0.779 ± 0.009	0.708 ± 0.022	0.905 ± 0.003	0.698 ± 0.025
Shanghai	Shanghai-H1	0.360 ± 0.010	0.559 ± 0.011	0.302 ± 0.006	0.584 ± 0.012	0.640 ± 0.010	0.441 ± 0.011	0.698 ± 0.006	0.416 ± 0.012
(SH)	Shanghai-H2	0.406 ± 0.011	0.532 ± 0.011	0.275 ± 0.006	0.545 ± 0.011	0.594 ± 0.011	0.468 ± 0.011	0.725 ± 0.006	0.455 ± 0.011
Chongqing	Chongqing-H	0.546 ± 0.014	0.771 ± 0.030	0.377 ± 0.011	0.809 ± 0.035	0.454 ± 0.014	0.229 ± 0.030	0.623 ± 0.011	0.191 ± 0.035
(CQ)	Chongqing-L	0.516 ± 0.014	0.764 ± 0.030	0.423 ± 0.025	0.794 ± 0.033	0.484 ± 0.014	0.236 ± 0.030	0.577 ± 0.025	0.206 ± 0.033
Guangzhou	Guangzhou-H	0.441 ± 0.011	0.543 ± 0.011	0.246 ± 0.005	0.555 ± 0.011	0.559 ± 0.011	0.457 ± 0.011	0.754 ± 0.005	0.445 ± 0.011
(GZ)	Guangzhou-L	NA**	0.612 ± 0.012	0.341 ± 0.007	NA	NA	0.388 ± 0.012	0.659 ± 0.007	NA

* f_{nf}(mrOC) is calculated by the differences between OC and mvOC (Sect. 2.4); ** Samples get lost during the ^{14}C measurements.

Table S6. Concentrations of mvOC, OC and EC from non-fossil sources ($mvOC_{nf}$, OC_{nf} and EC_{bb}) and fossil sources ($mvOC_{fossil}$, OC_{fossil} and EC_{fossil}) in units of µg m^{-3}.

City	Sample Name	$mvOC_{nf}$	$mvOC_{fossil}$	OC_{nf}	OC_{fossil}	EC_{bb}	EC_{fossil}
Xi'an	winter-H	3.11 ± 0.19	3.44 ± 0.21	27.69 ± 1.53	19.46 ± 1.17	3.08 ± 0.18	6.86 ± 0.37
(XA)	winter-M	1.74 ± 0.11	1.85 ± 0.12	21.15 ± 1.17	16.73 ± 0.97	1.44 ± 0.09	4.70 ± 0.26
	winter-L	0.72 ± 0.09	0.91 ± 0.10	8.32 ± 0.47	6.17 ± 0.37	0.82 ± 0.05	1.99 ± 0.12
Beijing	Beijing-H	1.96 ± 0.12	5.41 ± 0.28	16.91 ± 1.73	33.47 ± 3.37	1.58 ± 0.32	5.29 ± 1.06
(BJ)	Beijing-L	0.22 ± 0.01	0.49 ± 0.03	8.25 ± 0.84	13.49 ± 1.36	1.13 ± 0.23	3.55 ± 0.73
Taiyuan	Taiyuan-H	NA	NA	13.22 ± 1.85	31.86 ± 3.42	1.42 ± 0.29	13.38 ± 2.69
(TY)	Taiyuan-L	0.65 ± 0.04	2.29 ± 0.12	6.76 ± 0.84	16.42 ± 1.72	0.78 ± 0.16	7.40 ± 1.48
Shanghai	Shanghai-H1	0.97 ± 0.06	1.72 ± 0.09	13.79 ± 1.40	10.88 ± 1.13	1.58 ± 0.32	3.64 ± 0.73
(SH)	Shanghai-H2	0.69 ± 0.04	1.01 ± 0.05	9.71 ± 0.99	8.54 ± 0.87	1.16 ± 0.23	3.05 ± 0.61
Chongqing	Chongqing-H	3.66 ± 0.21	3.04 ± 0.18	35.97 ± 3.89	10.73 ± 1.76	4.44 ± 0.90	7.34 ± 1.47
(CQ)	Chongqing-L	1.53 ± 0.09	1.43 ± 0.08	22.14 ± 2.39	6.81 ± 1.11	3.39 ± 0.70	4.62 ± 0.94
Guangzhou	Guangzhou-H	1.06 ± 0.06	1.34 ± 0.07	12.70 ± 1.29	10.66 ± 1.09	1.11 ± 0.22	3.40 ± 0.68
(GZ)	Guangzhou-L	NA	NA	5.39 ± 0.54	3.43 ± 0.36	0.84 ± 0.17	1.62 ± 0.32

Table S7. Concentrations of SOC, SOC from fossil sources ($\mathrm{SOC_{fossil}}$) and OC from non-fossil sources excluding primary biomass burning ($\mathrm{OC_{o,nf}}$) and fraction of fossil in SOC (f_{fossil}(SOC)) (median and interquartile range).

City	Sample Name	f_{fossil}(SOC)			SOC concentrations (μg $\mathrm{m^{-3}}$)		
		p (0–1)[a]	^{13}C-constrained p[b]	p (0–0.5)[c]	p (0–1)	^{13}C-constrained p	p (0–0.5)
Xi'an (XA)	winter-H	0.37 (0.29–0.42)			24.25 (21.41–27.10)		
	winter-M	0.38 (0.34–0.42)			24.83 (22.79–26.84)		
	winter-L	0.38 (0.32–0.43)			8.15 (7.28–8.99)		
Beijing (BJ)	Beijing-H	0.70 (0.68–0.72)	0.70 (0.68–0.71)		36.01 (31.67–40.13)	35.20 (32.75–37.82)	
	Beijing-L	0.68 (0.64–0.72)	0.67 (0.63–0.70)		11.80 (9.48–14.06)	11.49 (9.99–12.78)	
Taiyuan (TY)	Taiyuan-H	0.61 (0.47–0.69)			19.13 (12.56–24.90)		
	Taiyuan-L	0.61 (0.44–0.69)			8.88 (5.30–12.04)		
Shanghai (SH)	Shanghai-H1	0.41 (0.35–0.47)	0.43 (0.38–0.46)		12.87 (10.22–15.36)	12.85 (11.28–14.38)	
	Shanghai-H2	0.43 (0.35–0.49)	0.42 (0.36–0.47)		8.96 (6.87–10.87)	8.74 (7.44–9.90)	
Chongqing (CQ)	Chongqing-H	-0.01 (-0.23–0.12)		0.10 (0–0.17)	17.70 (12.03–23.06)		20.20 (15.05–25.20)
	Chongqing-L	0.04 (-0.25–0.19)		0.14 (0.02–0.22)	8.34 (4.50–12.06)		9.84 (6.25–13.31)
Guangzhou (GZ)	Guangzhou-H	0.40 (0.34–0.45)	0.43 (0.39–0.46)		13.69 (11.37–15.96)	14.30 (12.93–15.50)	
	Guangzhou-L	0.34 (0.18–0.44)	0.36 (0.25–0.44)		2.99 (1.84–4.06)	3.15 (2.49–3.79)	

Table S7. Continued

City	Sample Name	SOC_{fossil}			$OC_{o,nf}$ (approximately SOC_{nf})
		p (0–1)	^{13}C-constrained *p*	*p* (0–0.5)	
Xi'an (XA)	winter-H	8.86 (6.49–11.28)			15.42 (13.98–16.82)
	winter-M	9.46 (7.77–11.13)			15.38 (14.46–16.31)
	winter-L	3.10 (2.37–3.80)			5.05 (4.64–5.48)
Beijing (BJ)	Beijing-H	25.41 (22.33–28.29)	24.55 (22.69–26.58)		10.60 (9.13–12.15)
	Beijing-L	8.09 (6.45–9.66)	7.63 (6.60–8.82)		3.74 (2.82–4.63)
Taiyuan (TY)	Taiyuan-H	11.63 (5.74–16.78)			7.49 (6.02–9.01)
	Taiyuan-L	5.27 (2.05–8.07)			3.64 (2.90–4.39)
Shanghai (SH)	Shanghai-H1	5.36 (3.78–6.85)	5.39 (4.23–6.45)		7.54 (6.19–8.88)
	Shanghai-H2	3.92 (2.60–5.11)	3.62 (2.72–4.55)		5.07 (4.12–6.05)
Chongqing (CQ)	Chongqing-H	-0.37 (-3.58–2.38)		2.00 (-0.10–3.91)	18.24 (14.51–21.93)
	Chongqing-L	-0.16 (-2.14–1.58)		1.27 (0.03–2.52)	8.65 (5.94–11.27)
Guangzhou (GZ)	Guangzhou-H	5.52 (3.99–6.87)	6.12 (5.10–6.95)		8.26 (7.16–9.37)
	Guangzhou-L	0.99 (0.28–1.57)	1.19 (0.68–1.56)		2.06 (1.41–2.67)

[a] *p* is the contribution of coal combustion to fossil EC (Eq. 12), *p* was randomly chosen from 0–1, that is no constrains on *p* values.
[b] Samples taken from Beijing, Shanghai and Guangzhou were measured for both $F^{14}C_{(EC)}$ and $\delta^{13}C_{EC}$, and *p* in these three cities is further constrained by $\delta^{13}C_{EC}$ (Supplement S2).
[c] For Chongqing, we did a sensitive analysis for *p* and tried a smaller *p* of 0–0.5.

Table S8. Concentrations of SOC, SOC from fossil sources (SOC_{fossil}) and non-fossil sources ($OC_{o,nf}$) and fraction of fossil in SOC (f_{fossil}(SOC)) (μg m^{-3}; mean ± standard deviation).

City	Sample Name	SOC concentrations		SOC_{fossil}		$OC_{o,nf}$ (approximately SOC_{nf})
		p (0–1)[a]	*p* (0–0.5)[b]	*p* (0–1)	*p* (0–0.5)	
Xi'an (XA)	winter-H	24.17 ± 4.12		8.79 ± 3.17		15.38 ± 2.13
	winter-M	24.79 ± 2.91		9.41 ± 2.25		15.38 ± 1.36
	winter-L	8.13 ± 1.24		3.08 ± 0.94		5.05 ± 0.61
Beijing (BJ)	Beijing-H	35.87 ± 6.29		25.26 ± 4.40		10.61 ± 2.24
	Beijing-L	11.67 ± 3.36		7.96 ± 2.33		3.71 ± 1.32
Taiyuan (TY)	Taiyuan-H	18.56 ± 9.12		11.02 ± 7.96		7.54 ± 2.26
	Taiyuan-L	8.60 ± 4.90		4.94 ± 4.27		3.65 ± 1.11
Shanghai (SH)	Shanghai-H1	12.75 ± 3.80		5.24 ± 2.22		7.51 ± 1.98
	Shanghai-H2	8.84 ± 2.97		3.78 ± 1.85		5.05 ± 1.44
Chongqing (CQ)	Chongqing-H	17.40 ± 8.33	20.0 ± 7.6	-0.72 ± 4.28	1.80 ± 3.04	18.12 ± 5.59
	Chongqing-L	8.13 ± 5.65	9.8 ± 5.1	-0.38 ± 2.71	1.23± 1.90	8.51 ± 3.97
Guangzhou (GZ)	Guangzhou-H	13.62 ± 3.39		5.38 ± 2.10		8.25 ± 1.64
	Guangzhou-L	2.95 ± 1.67		0.90 ± 0.93		2.04 ± 0.94

[a] *p* is the contribution of coal combustion to fossil EC (Eq. 12), *p* was randomly chosen from 0–1, that is no constrains on *p* values.

[b] For Chongqing, we did a sensitive analysis for *p* and tried a smaller *p* of 0–0.5.

References

Andersson, A., Deng, J., Du, K., Zheng, M., Yan, C., Sköld, M., and Gustafsson, Ö.: Regionally-varying combustion sources of the January 2013 severe haze events over eastern China, Environ. Sci. Technol., 49, 2038–2043, 2015.

Cao, J.-j., Chow, J. C., Tao, J., Lee, S.-c., Watson, J. G., Ho, K.-f., Wang, G.-h., Zhu, C.-s., and Han, Y.-m.: Stable carbon isotopes in aerosols from Chinese cities: Influence of fossil fuels, Atmos. Environ., 45, 1359-1363, http://dx.doi.org/10.1016/j.atmosenv.2010.10.056, 2011.

Donahue, N. M., Robinson, A. L., Stanier, C. O., and Pandis, S. N.: Coupled Partitioning, Dilution, and Chemical Aging of Semivolatile Organics, Environ. Sci. Technol., 40, 2635-2643, 2006.

Donahue, N. M., Robinson, A. L., and Pandis, S. N.: Atmospheric organic particulate matter: From smoke to secondary organic aerosol, Atmos. Environ., 43, 94-106, http://dx.doi.org/10.1016/j.atmosenv.2008.09.055, 2009.

Donahue, N. M., Epstein, S. A., Pandis, S. N., and Robinson, A. L.: A two-dimensional volatility basis set: 1. organic-aerosol mixing thermodynamics, Atmos. Chem. Phys., 11, 3303-3318, https://doi.org/10.5194/acp-11-3303-2011, 2011.

Ma, J., Li, X., Gu, P., Dallmann, T. R., Presto, A. A., and Donahue, N. M.: Estimating ambient particulate organic carbon concentrations and partitioning using thermal optical measurements and the volatility basis set, Aerosol Sci. Technol., 50, 638-651, 2016.

Ni, H., Huang, R.-J., Cao, J., Liu, W., Zhang, T., Wang, M., Meijer, H. A. J., and Dusek, U.: Source apportionment of carbonaceous aerosols in Xi'an, China: insights from a full year of measurements of radiocarbon and the stable isotope ^{13}C, Atmos. Chem. Phys., 18, 16363-16383, https://doi.org/10.5194/acp-18-16363-2018, 2018.

Turpin, B. J., and Lim, H.-J.: Species contributions to $PM_{2.5}$ mass concentrations: revisiting common assumptions for estimating organic mass, Aerosol Sci. Technol., 35, 602-610, 2001.

Xing, L., Fu, T.-M., Cao, J. J., Lee, S. C., Wang, G. H., Ho, K. F., Cheng, M.-C., You, C.-F., and Wang, T. J.: Seasonal and spatial variability of the OM/OC mass ratios and high regional correlation between oxalic acid and zinc in Chinese urban organic aerosols, Atmos. Chem. Phys., 13, 4307-4318, https://doi.org/10.5194/acp-13-4307-2013, 2013.